

# **PIKK-dependent activation of the DNA damage response by long wavelength ultraviolet radiation**

**James Copley**

**Division of Biomedicine and Life Sciences**

**Faculty of Health and Medicine**

**Lancaster University**

**Thesis submitted for the degree of Master of Science in Biomedicine (by research)**

**February 2018**

## **Declaration**

I declare that this thesis is my own work and has not been submitted in part, or as a whole, for the award of a higher degree of qualification at this university or elsewhere.

James Copley

## **Acknowledgements**

I would like to thank Dr. Sarah Allinson for the opportunity to be a part of this research project, as well as her valuable guidance and insight throughout the entire year. Dr. Sarah Allinson's patience and understanding, even when things do not go according to plan, and her feedback when writing up has been essential to the success of this project, and for that I am incredibly grateful.

I would also like to thank the other members of lab A27, for their help throughout this project, particularly in the early stages, teaching me valuable skills and providing information and feedback on how techniques may be improved and optimised for better results. Lab meetings provided a great method of presenting my findings, and receiving suggestions and feedback, and I thank everyone who participated throughout the year for listening and providing input.

I would also like to thank all my friends and family, for their support throughout this project. I would particularly like to thank my parents and Emma for their continuous backing and motivation.

I would also like to thank Sarah and Max for allowing me to stay at their house while I write up my thesis.

## Abbreviations

53BP1	53 Binding Protein 1
6-4 PP	6-4 Photoproducts
8-oxoG	8-Oxoguanine
UV	Ultraviolet Light
9-1-1	RAD9-RAD1-HUS1
ATM	Ataxia Telangiectasia Mutated
ATR	Ataxia Telangiectasia and Rad3-related protein
BCC	Basal Cell Carcinoma
BRCT	BRCA1 C-terminus domain
CDK	Cyclin Dependant Kinase
CHK2	Checkpoint Kinase 2
CPD	Cyclobutane Pyrimidine Dimers
CTD	C terminus domain
DBD	DNA Binding Domain
DDR	DNA Damage Response
DISCs	Death Inducing Signalling Complexes
DMEM	Dulbecco's Modified Eagle's Medium
DNA-PKcs	DNA-Protein Kinase catalytic subunit
DSB	Double Strand Break
EDTA	Ethylenediamine
EGFR	Epidermal Growth Factor Receptor
FCS	Foetal Calf Serum
FHA	Fork-head association
GG-NER	Global-genomic NER
H2AX	Histone 2AX
HR	Homologous Recombination
KD	Kinase Domain
KO	Knockout
L-Glut	L-Glutamine
MAPK	Mitogen Activated Protein Kinase
MDM2	Mouse Double Minute 2 homolog

MMEJ	Microhomology-mediated end joining
MRN	Mre11-Rad50-Nbs1
NER	Nucleotide Excision Repair
NHEJ	Non homologous end joining
NMSC	Non Melanoma Skin Cancer
PBS	Phosphate Buffered Saline
PCNA	Proliferating Cell Nuclear Antigen
PFA	Paraformaldehyde
PI3K	Phosphoinositide 3-Kinase
PIKK	Phosphatidylinositol 3-Kinase-related Kinase
PNKP	Polynucleotide kinase 3'-phosphatase
Pol $\eta$	Polymerase $\eta$
PRR	Protein Rich Regions
ROS	Reactive Oxygen Species
RPA	Replication Protein A
SCC	Squamous Cell Carcinoma
SDS-PAGE	Sodium Dodecyl Sulphate Polyacrylamide Gel Electrophoresis
ssDNA	single stranded DNA
TAD	Transcription activation domain
TC-NER	Transcription-coupled NER
TLS	Translesion Synthesis
TNF-R	Tumour Necrosis Factor Receptor
TSG	Tumour Suppressor Gene
UVI	UV index
XP	Xeroderma Pigmentosa

## Contents

Abstract .....	6
1. Introduction .....	7
I.    Ultraviolet Radiation .....	8
II.   Skin cancer .....	9
III.  Skin cancer factors .....	12
IV.   UVA and skin cancer .....	16
V.    DNA damage .....	19
VI.   Mutations seen in skin cancer .....	24
VII.  DNA Damage Response .....	27
VIII. DNA Repair .....	42
IX.   Experimental aims .....	50
2. Materials and Methods .....	52
I.    Media and Buffers .....	52
II.   Cell Culture .....	52
III.  Treatment – UVA irradiation .....	53
IV.   Comet Assay .....	54
V.    Western Blotting Analysis .....	56
VI.   Immunofluorescence .....	58
VII.  EdU Assay .....	60
3. Results .....	62
I.    UVA induces DNA damage in HaCaT cells, but is repaired quickly.....	64
II.   Inhibition of ATM via 200 nM KU-60019 alters the phosphorylation of H2AX and other components of the DDR post UVA irradiation .....	69
III.  200 nM KU-60019 is not enough to fully inhibit ATM phosphorylation .....	75
IV.   2 $\mu$ M KU-60019 is enough to inhibit the immediate phosphorylation of ATM following UVA irradiation .....	77
V.    ATM inhibition with 2 $\mu$ M KU-60019 reduces the intensity of $\gamma$ H2AX formation and DDR activation .....	78
VI.   The influence of UVA and cell cycle status on 53BP1 foci formation in HaCaT cells .....	83
4. Discussion .....	89
I.    UVA induces double strand breaks in HaCaT cells, but is rapidly repaired .....	90
II.   UVA causes an increase in $\gamma$ H2AX accumulation, which peaks at 1 and 2 hours post irradiation .....	92
III.  The ATM inhibitor KU-60019 prevents the accumulation of $\gamma$ H2AX in the early response to UVA irradiation.....	93
IV.   ATM inhibition causes significant decreases in the activation of the UVA induced DDR .....	97
V.    53BP1 foci formation increase following UVA irradiation .....	100
VI.   Future Work .....	104
VII.  Conclusion .....	106
5. References .....	108

## Abstract

Ultraviolet radiation (UV) is one of the main risk factors that increase a person's chance of developing skin cancer. UV is divided into three subtypes, called UVA, UVB and UVC. UVA and UVB both have the ability to cause different types of DNA damage. Our understanding of UVA and its mechanism of carcinogenesis is poorly understood due to UVB being the focus of research. The DNA damage response (DDR) detects DNA damage, and triggers a signalling pathway which results in cell cycle arrest, DNA repair or apoptosis. The DDR is important for preventing the persistence of UV-induced DNA damage in skin cells. This project used HaCaT cells to investigate UVA and its ability to generate double strand breaks, and how the DDR is activated as a result. Cells exposed to 100 KJ m<sup>-2</sup> UVA displayed significant amounts of DSBs, which were largely repaired within 1 hour of irradiation.  $\gamma$ H2AX was used as a biomarker of DNA damage, and investigated using Western blotting and immunofluorescence. UVA-induced  $\gamma$ H2AX accumulation peaked between 1 and 2 hours, which was seen in the Western blotting. ATM was inhibited using KU-60019, which caused a delay in the accumulation of UVA-induced  $\gamma$ H2AX following. UVA-induced CHK2 and p53 activation followed similar patterns in both ATM inhibited and uninhibited samples, and suggested that both components are linked to an ATM independent pathway. UVA-induced PNKP activation was delayed with the addition of an ATM inhibitor, and increased slightly 1 hour post irradiation, suggesting a greater dependence on ATM activity. 53BP1 foci formation was used to investigate NHEJ activation. There was a significant increase in the number of UVA-induced 53BP1 foci, while the addition of an ATM inhibitor prevented this increase, suggesting an ATM dependence for NHEJ activation. This data suggests that UVA generates double strand breaks, which result in the activation of the DDR which peaks within the first 2 hours following UVA irradiation. Furthermore, ATM is essential for the activation of NHEJ, but is not the only kinase responsible for the activation the DDR.

## 1. Introduction

Cancer is a disease involving the uncontrolled proliferation of cells. There are a variety of factors that can increase the chances of cells becoming cancerous. Some of these factors are lifestyle based, such as diet or smoking, while others are less controllable, for example genetics or aging. For a cell to be classed as cancerous, it must acquire several traits that are common to all cancer cells. These traits are known as the hallmarks of cancer, and were first described by Hanahan and Weinberg in 2000 (Hanahan and Weinberg, 2000, Hanahan and Weinberg, 2011). There are some types of cancer which are associated to certain hallmarks more than others. Skin cancer is mainly associated with (1) genomic instability, (2) tumour-promoting inflammation and (3) metastasis.

An increase in genomic instability leads to an increased rate of mutation. Mutation is often the first step that occurs within a cell and can lead to the development of other hallmarks of cancer.

Genomic instability in skin cancer most commonly results from solar ultraviolet radiation (UVR), which has the ability to cause DNA damage, leading to mutation. Inflammation of the skin following exposure to UVR (sunburn) allows for immune cells to reach the site of exposure to prevent infection. However, the inflammatory response causes the secretion of signalling molecules, free radicals and enzymes, which can drive proliferation and stimulate angiogenesis, contributing to the development of cancer. Metastasis is often one of the final hallmarks to occur in cells, and represents a significant stage in tumour development. Metastasis occurs when cells from the primary tumour break away and invade surrounding tissue, and eventually distant body parts. In skin cancer, as layers of the skin become compromised (such as the basal membrane), cancer cells are able to break away from the tumour and enter the bloodstream, where they are carried to other organs and form secondary tumours (Broertjes, 2015).

Lifestyle and environment are two of the largest factors that contribute to the development of cancer. Unlike smoking, drinking and obesity, exposure to ultraviolet radiation is difficult to avoid

completely, and can be a factor that increases the chance of developing skin cancer (Anand et al, 2008). There are lifestyle choices that can increase a person's exposure time to UV, but to receive zero ultraviolet radiation is almost impossible while still leading a regular life. It is difficult to state the number of new cases of skin cancer that occurs worldwide per year due to the large rate of incidence, and differences in reporting of some types of cancer between countries. The American Cancer Society estimate that there are at least 5.4 million cases of skin cancer diagnosed in the United States alone per year (American Cancer Society, 2017). Cancer Research UK state there are around 150 000 new cases of skin cancer every year in the UK, but also suggest that the number may be inaccurate due to how common and easily treated some types are (Cancer Research UK, 2017).

This literature review will discuss the detrimental effect of UVA on DNA, and how this may lead to tumorigenesis. The repair of UV-induced DNA damage, as well as the documented mutations found in skin cancers will be discussed. The activation, mechanism and cellular result of the DNA damage response induced by UVA will also be covered.

## **I - Ultraviolet Radiation**

Ultraviolet radiation (UV) is type of electromagnetic radiation emitted from the sun. The sun emits three types of UV radiation, which are: UVA, UVB and UVC. UVC (wavelength 100-280nm) is completely absorbed by the Earth's atmosphere, so plays no role in affecting people's health. UVB (280 – 315nm) is partially absorbed by the ozone layer and Earth's atmosphere, with rays that are towards the larger wavelength range being able to reach the Earth's surface. UVA (315-400nm) can completely penetrate the ozone layer, and is responsible for 95% of the UV radiation that reaches the Earth's surface (figure 1.1). UVA is the lowest in energy of the three sub-types of UV, and as a result was initially deemed harmless. However, studies revealed that UVA (and UVB) are both carcinogenic, with both being assigned as class one carcinogens (IARC, 1992). Being ranked as a class one carcinogen means that exposure to UV poses a risk of causing cancer in humans. In the case of UV, skin cancer is the type of cancer that may arise.

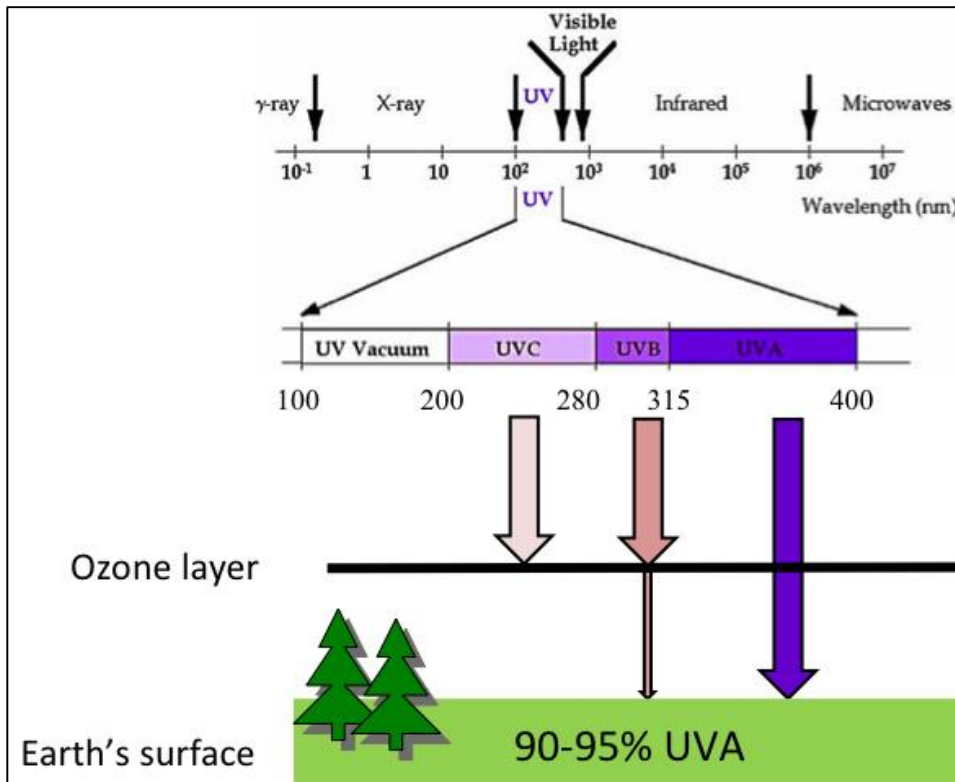


**Figure 1.1 – Biologically relevant wavelengths of UV radiation.**

*A large proportion of solar UV is prevented from reaching the Earth's surface by the atmosphere. Only around 5 – 10% of UV radiation reaching the surface of the planet is UVB, with UVA accounting for 90-95%.*

*This UVA is able to penetrate the epidermis of the skin, and can lead to damage of skin cells.*

## II. Skin cancer

Skin cancers arise from skin cells, and are triggered due to overexposure to UV radiation. There are two main groups of skin cancers, non-melanoma skin cancers (NMSCs) and Cutaneous Malignant Melanomas. The two main types of NMSCs are Basal-Cell Carcinoma (BCC) and Squamous-Cell Carcinoma (SCC). BCC arises from the basal keratinocyte cells at the base of the epidermis, which is the outer layer of the skin (figure 1.2). The precise origin of SCC is not fully understood, but it is thought to start in the stem cells at the base of the epidermis or in the hair follicle bulb. NMSCs are far more common than melanoma, accounting for 90% of all registered skin cancers in the UK (NCIN Data briefing, 2013). These NMSCs are rarely fatal, but can cause disfigurement of the skin as they are often removed via surgery, leaving a permanent scar. NMSCs can also cause a burden on health

care services, particularly due to their higher rate incidence. Cutaneous Malignant Melanomas result from melanocytes, which are a type of cell that sits between the epidermis and the dermis layer of the skin. Melanocytes are responsible for producing the pigment melanin. Melanogenesis occurs when the skin is exposed to UV radiation. The function of melanin is to absorb UV light, and it is able to dissipate >99.9% of absorbed UV (Meredith and Riesz, 2004). By absorbing UV radiation, melanin protects skin cells, reducing the risk of cancer developing.

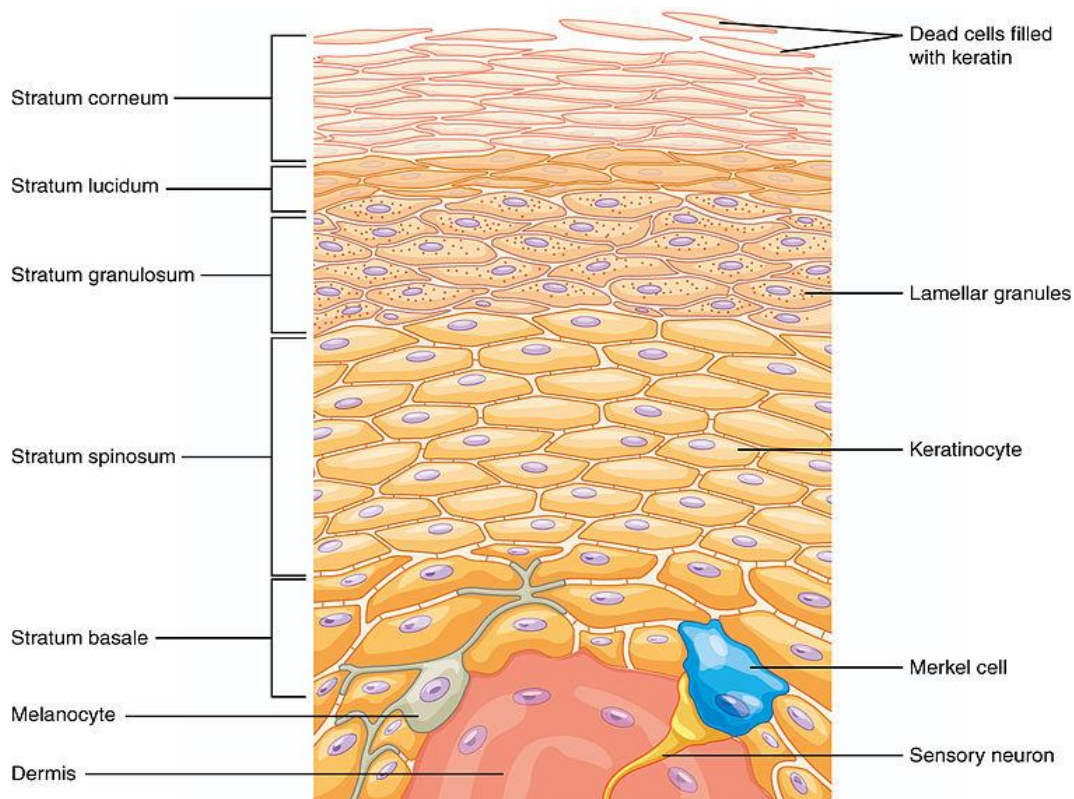


**Figure 1.2 – The structure of the epidermis (OpenStax College, 2013).**

*The various layers of the epidermis. Keratinocytes originate at the Stratum basale layer, which consists of proliferating and non-proliferating keratinocytes. Melanocytes are also present in this layer. The spinous layer contains mostly keratinocytes, and in the granulosum layer, these cells begin to lose their nuclei, with lamellar granules forming in the cytoplasm and being released into the extracellular space. Only thick skin has the lucidium layer (found in palms and soles). The corneum layer consists of mainly dead keratinocytes, which is the final differentiation step (corneocytes). These cells are filled with keratin.*

### **2.1 - Incidence of skin cancer**

Over the last 40 years, our knowledge on the mechanisms behind the cause and development of skin cancer has grown massively; the incidence rate in the UK has increased dramatically over the same time period. Malignant melanoma has seen an overall rate of incidence increase of 360% since the late 1970s. The rate of increase is much higher in males than females, with men showing a 544% increase in incidence rate, while women show a 263% increase from 1979-2013 (Cancer Research UK, 2016). In the past decade (2003 – 2013), the incidence rate of malignant melanoma has

increased by 46%, with the male incidence rate increasing more than females – 59% and 36% respectively.

### **III. Skin cancer factors**

In light of these statistics, the question must be asked as to why the incidence of skin cancer has increased over the past 40 years, and is still continuing to rise. The answer is that people are exposing themselves to more UV radiation than ever before. Overexposure to sunlight without appropriate protection is one of the main causes of skin cancer, and the increase in incidence of melanoma can be associated with this (Leiter and Garbe, 2008). A study by Parkin and colleagues estimate that 86% of malignant melanoma cases in the UK can be linked to solar UV radiation (Parkin et al, 2011).

Over-exposure to sunlight can be linked with lifestyle. In the UK, between 2010 and 2015, the number of residents traveling abroad has increased from 55.6 million to 65.7 million, with the top three destinations being Spain, France and Italy (Office for National Statistics). These three countries all have an average UV index (UVI) of three, while the UK has a UVI of two (WHO). This suggests that increases in the number of people going abroad to countries of a higher UV index could be linked to the increase in melanoma cases in the UK.

There are various other reasons for the increase in melanoma incidence. The use of sunbeds or sunlamps is estimated to be responsible for 5.4% (3438) of malignant melanoma causes in Europe, and 440 cases in the UK per year (Boniol et al, 2012). The International Agency for Research on Cancer (IARC) also state that the use of sunbeds or other UV emitting tanning devices are a cause of melanoma (IARC, 2009). The risk posed by the use of a sunbed varies with age. The risk of developing malignant melanoma increases from 11% to 35% if tanning beds are used before the age of 25, compared to those who start after turning 25 years old (Diffey, 2003, Colantonio et al, 2014). An American study showed that the use of sunbeds, especially by younger women, has increased

over the past 20-30 years, which suggests a correlation between the increased incidence of melanoma and the increased use of sunbeds over the same timespan (Coelho and Hearing, 2010).

### **3.1 - Genetic factors**

Genetics also plays a role in a person's risk in developing skin cancer. Familial melanoma (FM) is an inherited condition, in which a person receives a genetic trait from a parent which results in an increased chance of developing melanoma. Two genes have been identified to be associated with FM, which are called *CDKN2A* and *CDK4*. In people with FM, one of these has mutated. The *CDKN2A* gene encodes the proteins p16 and ARF. The *CDKN2A* gene has three exons, and is able to produce the two different proteins via alternate splicing (Foulkes et al, 1997). The p16 protein is a tumour suppressor gene (TSG), and is involved in negatively regulating the cell cycle by inhibiting cyclin dependant kinases (CDK) 4 and 6. CDK4 and 6 activity is required for the transition from G1 to S phase by phosphorylating pRb (Reznikoff et al, 1996). Hyperphosphorylated pRB is in an inactive state, and as a result cannot prevent cell cycle progression. Mutation in *CDKN2A* results in the inactivation of *p16*, and results in unregulated cell cycle progression (Ai et al, 2003). *P16* inactivation has been observed in an estimated 68% of primary tumours (Rocco and Sidransky, 2001).

The ARF protein is a part of the p53 regulatory mechanism in which cell proliferation is controlled. ARF upregulates the activity of p53 by inhibiting Mdm2 (figure 1.3). When *CDKN2A* is mutated, the structure of the ARF protein is disrupted, and cannot function as a result. This allows Mdm2 to freely inhibit p53, meaning that damaged cells are free to progress through the cell cycle and proliferate uncontrollably, resulting in tumour formation (Sherr, 2006).

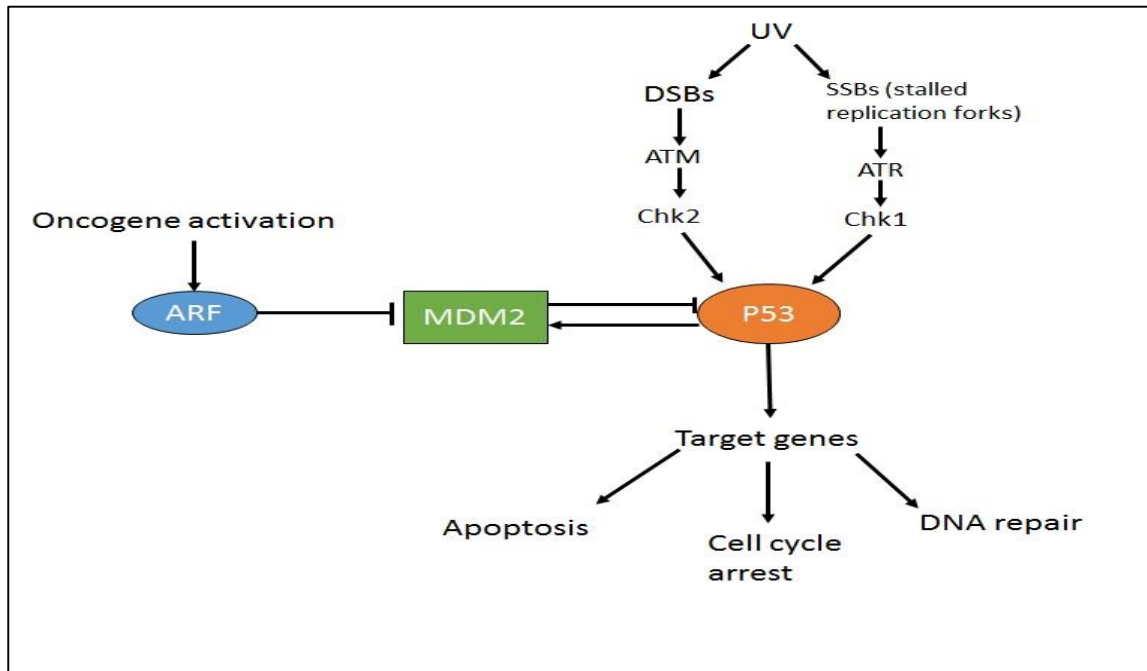


**Figure 1.3 – Simplified pathway of p53 activation**

*Schematic representation of the UV-induced p53 activation via the DNA damage response, as well as the regulation of p53 via ARF/MDM2 pathway. The three main effects of p53 activation are also shown.*

The *CDK4* gene is responsible for encoding the catalytic subunit of cyclin dependant kinase 4 protein. The only inherited mutation currently known in the *CDK4* gene is in codon 24 in exon 2. The mutation is a substitution of Arginine 24 to either Histidine or Cysteine. This substitution results in disruption of the p16 binding site, and results in reduced inhibition of *CDK4* activity (Puntervoll et al, 2012). Reduced inhibition leads to increased activity of *CDK4* activity. The effect of the *CDK4* gene mutation is similar to that seen in the mutation of *CDKN2A* and the changes in p16 activity. Only

three families worldwide have been found to carry the *CDK4* mutations. Despite this, the mutations in these three cases are clustered to the same codon, showing this residue plays a very important role in the function/regulation of *CDK4* (Hayward, 2003).

In recent years, there has been a lot of progress in the characterisation of certain genes that are often mutated in specific cancers. Two of the most notable examples are the tumour suppressor genes *BRCA1/2*, and their role in breast and ovarian cancer development. BRCA1 is a protein that plays a vital role in the resection step of the double strand repair pathway homologous recombination (HR) (detailed mechanism discussed in section VIII). The BRCA2 protein is also involved in HR where it recruits Rad51 to the site of the double strand break. Rad51 is required for the progression of HR via strand invasion (section VIII) (Shahid et al, 2014).

Studies have demonstrated that cells which have defective BRCA1 or BRCA2 proteins are deficient in double strand break repair (Moynahan et al; 1999, Moynahan et al, 2001). Mutations in *BRCA1/2* are most commonly associated with breast and ovarian cancers, but can play roles in the development of other cancers. It is possible to inherit mutations in these genes, which significantly increase a person's risk of developing breast or ovarian cancer by the age of 80. It is estimated that 12% of women will develop breast cancer at some point in their lives, while 72% of women who have inherited a harmful BRCA1 mutation, and 69% who have inherited a harmful BRCA2 mutation will develop breast cancer before the age of 80. 1.3% of women will develop ovarian cancer in their lifetime. 44% of women who have inherited a harmful *BRCA1* gene, and 17% with harmful *BRCA2* mutations develop ovarian cancer before the age of 80 (Howlander et al, 2017; Kuchenbaecker et al, 2017). This increased risk of cancer development through inefficient DNA damage repair reflects the significance of genomic instability in the initiation and advancement of cancer.

## **IV. UVA and Skin cancer**

### **4.1 - NMSC**

The significance of UVB's role in the causation of NMSCs has been widely studied, with UVA being researched less. Keratinocytes absorb UVA/UVB and generate DNA lesions directly, or they can lead to the formation of reactive oxygen species (ROS), which can cause oxidative DNA damage. In the past, UVB was the focus of research into the understanding of the mechanism of UV induced carcinogenesis.

One of the reasons for the focus on UVB was due to the characterisation of mutations in NMSCs. p53 mutations are one of the main carcinogenic alterations found in NMSCs. A study by Berg and colleagues demonstrated high levels of p53 mutants present in the skin tumours of UVB irradiated mice (Berg et al, 1996). A separate study demonstrated that TP53 mutations were present in 66% of aggressive BCCs, and 35% in aggressive SCCs (Bolshakov et al, 2003). The reason for the characteristically high number of mutated TP53 is due to the sequence of the p53 gene, and is discussed further in section V.

While UVA was largely overlooked until recently, studies have shown that UVA plays a role in formation of NMSCs. A study by Agar and colleagues showed that UVA is important in causing DNA damage in deeper basal germinative layer, while UVB induced lesions are found in the upper layers of the epidermis. The UVA induced DNA lesions known as 8-oxoG, result from the generation of ROS linked with UVA exposure. The main UVB induced DNA lesions are called cyclobutane pyrimidine dimers (CPDs). 8-oxoG and CPDs were detected in this study, with the former found in the basal layers of the epidermis, and the later in higher 'superficial' layers. They suggest that the location of the DNA lesions are important, if they occur in stem cells they can lead to permanent genomic mutations (Agar et al, 2004).

## **4.2 - Melanoma**

The mechanism by which melanoma genesis occurs is not fully understood. Given the depth of melanocytes in the skin, UVA is generally accepted as the main factor that can be responsible for the development of melanoma. However, it is not proven that UVA is the definitive factor in melanoma induction and development. Melanoma is the deadliest form of skin cancer, meaning it is important that we develop our understanding of the process in which arises.

There are a number of driver mutations commonly found in melanoma tumours. *BRAF* mutations are found in 50% of melanoma tumours, while *NRAS* mutations have been found in 15-20% of tumours. (Davies et al, 2002). *BRAF* is discussed further in section VI.

## **4.3 - Animal models and other evidence of UVA roles in melanoma formation**

An interesting piece of evidence for UVA playing a role in the development of skin cancer involves aircraft pilots and flight attendants. Airplane windshields are made of a material that blocks almost all of UVB transmission (99%), while UVA was able to pass through by varying levels (0.51-53.3%). The study concluded that pilots flying for 56 minutes are exposed to the same amount of UVA as a 20 minute tanning bed session, and suggest that pilots and cabin crew may be at a higher risk of developing melanoma in their lifetime (Sanlorenzo et al, 2015). A meta-analysis of the rate of melanoma incidence in airline pilots shows that they are twice as likely to develop melanoma in their lifetime compared to the general population (Sanlorenzo et al, 2015.)

The use of animal models in demonstrating that UVA causes melanoma has not proven conclusive. A variety of different animals have been used, although some studies results are questionable depending on the animal chosen. For example, a study used opossums, where they were treated three times a week with UVA. The study showed opossums were more effective at forming melanoma precursors than NMSC tumours. (Ley, 1997). However, opossums are able to utilise an enzyme called photolyase, which is able to repair CPDs using light as a cofactor. Humans do not possess photolyases or an enzyme similar to it, which means the use of opossums as a model for human melanogenesis is questionable.

Xiphophorus hybrid fish are a cross of platyfish (*Xiphophorus maculatus*) and swordfish (*Xiphophorus helleri*), that were developed by Setlow, Woodhead and Grist as models for UV induced melanoma development. It was thought that this hybrid was susceptible to invasive melanoma development when exposed UV (Setlow et al, 1989). However, a more recent study using this model showed that UVA did not induce a significantly different melanoma to untreated fish, indicating the model is poor for UVA induced melanoma development (Mitchell et al, 2010).

Mice are one of the best models for UV induced melanoma, mainly because mouse genetics is well explored. However, one of the main drawbacks of mice is that it can be difficult to initiate melanoma development, and histopathology can be difficult as melanocytes are confined to hair follicles in the dermis, unlike humans, where melanocytes are in the basal layer of the epidermis (Ha et al, 2005). A study by Noonan et al (2012) used hepatocyte growth factor (HGF) transgenic mice as a model for melanoma development. The skin of these mice more closely resemble that of human skin, as they contain ectopic extra-follicular melanocytes in the epidermal/dermal junction, similar to that of a human (Takayama et al, 1996). Noonan et al (2012) also reasons that the pathogenesis of UV induced melanoma has significant similarities to that of a human, as they form 'melanocytic tumours in stages from early lesions to metastases', much like humans. The study showed that CPD formation cannot explain the reason for UVA induced melanomas. Instead, oxidative damage is the main cause of melanoma development, with 8-oxoG being the most abundant type of damage detected in melanocyte nuclei. Noonan also showed that melanin greatly accelerated UVA induced melanoma development, as melanin and UVA cause a photo-oxidative reaction in melanocytes, leading to 8-oxoG formation. (Noonan et al, 2012). UVB was able to induce melanoma in both albino and pigmented mice, suggesting a pathway that is independent of melanin also exists. Collectively, the results suggested that oxidative damage was the most significant UVA induced DNA damage type involved in melanocyte induction.

## **V. DNA damage**

Due to the different energy levels and wavelengths of UVA and UVB, the method by which they can cause skin cancer is different. UVB cannot penetrate the skin as deeply as UVA, and generally only reaches the epidermis layer of the skin, usually only affecting keratinocytes. UVB has enough energy to directly cause DNA damage, and because of this, was the focus of research in understanding the effect of UV on causing skin cancer. The main two types of DNA damage that UVB generates are cyclobutane pyrimidine dimers (CPDs) and (6-4) photoproducts (6-4 PPs).

A trademark sign of mutations caused by UVB radiation is a high number of transition mutations at dipyrimidine sequences containing cytosine (Pfeifer et al, 2005). Most of the time, CPDs and 6-4 PPs are accurately repaired by nucleotide excision repair (NER). If CPDs remain unrepaired, they are detected and processed by polymerase  $\eta$  (Pol $\eta$ ), which is able to insert nucleotides opposite the dimer during translesion synthesis (TLS). If the CPD contains a cytosine base, then a C > T transition mutation can occur. A transition mutation occurs when a pyrimidine base is switched with the other pyrimidine base (C > T or T > C), and the same can occur for purines (A > G or G > C). These C > T or CC > TT transitions have been referred to as signature mutations of UV (Ziegler, 1994).

### **5.1 - Cyclobutane Pyrimidine Dimers (CPDs)**

CPDs are one of the main two UV induced products, and account for around 80% of mutations induced by UVB (Pfeifer et al, 2004). In CPDS, C=C double bonds on two adjacent pyrimidines become bound together (carbons 5 and 6). This binding breaks the base pair with the pyrimidines respective complementary base, resulting in the formation of a lesion. Lesions are usually repaired by nucleotide excision, but it is possible for the lesions to go unrepaired, which can interfere with other processes such as DNA replication, leading to mutation (Choi et al, 2006).

There is evidence that suggests that methylated cytosine's are particularly prone to CPD lesion formation. A study was performed using methylated *lacI* transgene mice. Methylated *lacI* transgene

were used as a target for mutations. The study showed that in 24-32% of CPDs form at 5-methylcytosine containing pyrimidines, which makes up a significant portion of 'solar light-induced' mutations. 5-methylcytosines are a methylated form of the base cytosine (You et al, 1999). Methylated cytosines are prone to deamination, which results in the formation of a thymine base (Sassa et al, 2016). This conversion of C to T is a transition mutation, and is characteristic of UV induced mutations. Many CpGs are methylated on the p53 gene, which can be linked to the high number of p53 mutations observed in skin tumours (Pfeifer et al, 2005).

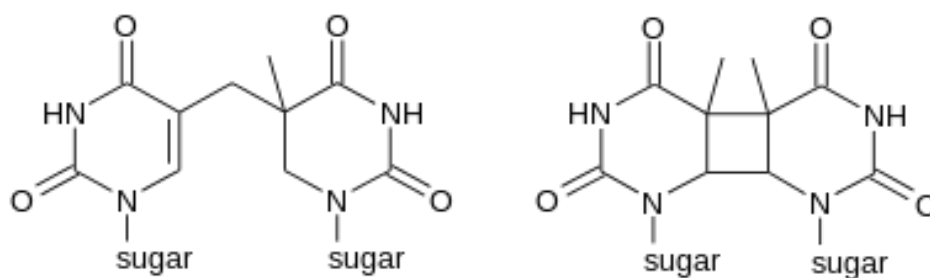


**Figure 1.4 – The structure of 6-4 Photoproduct (left) and Cyclobutane pyrimidine dimers (right)**

CPDs and 6-4 PPs are generated as a result of exposure to UVA and UVB. CPDs form as a result of a carbon double bond forming between 2 adjacent pyrimidine bases (Carbon 5 and 6), forming a cyclobutane ring. 6-4 PPs form when a carbon double bond forms between carbon 6 (5' end) and carbon 4 (3' end) of adjacent pyrimidines. The structures of both these lesions types are represented.

## **5.2 - 6-4 Photoproducts**

6-4 photoproducts are the second most common type of pyrimidine dimer, accounting for ~20% of all lesions, as opposed to the ~80% that CPDs account for (Balajee et al, 1999). Despite being less common, it has been suggested that 6-4 PPs are as significant as CPDs, as they are potentially more mutagenic (Mathews et al, 2000). The experiment that provided evidence of this consisted of UV induced CPD lesions being completely removed from DNA by photoreactivation (via DNA photolyase in the presence of visible light); however, when this DNA is introduced into bacteria, the CPD removal did not affect the frequency of mutations. Much like the study using opossums, the results

are questionable as humans do not possess photolyase, so we cannot accurately use this data to in context to humans.

Much like CPDs, 6, 4 PPs occur at adjacent pyrimidines, and involve the binding of carbons on either base. In 6-4 PPS, a covalent double bond forms between carbon 6 of the 5' base and carbon 4 of the 3' base (figure 1.4) (Yokoyama and Mizutani, 2014). This result is both pyrimidines no longer bind to their respective base, resulting in the formation of a lesion. 6-4 PPs occur most commonly between two adjacent thymidine bases (TT).

### **5.3 - ROS generation and oxidative damage**

As previously stated, UVA has the ability to penetrate the skin to the dermis layer; however, it does not have the energy to break covalent bonds and cause double strand breaks alone, and for a period, was not considered to form DSBs through any mechanism. One of the models suggested is that endogenous photo-sensitizers, such as skin chromophores like flavins and pterins, are required for UVA to cause DSBs (Wondrak, 2005). These cellular photosensitizers are photo-excited by UVA, which result in the formation of reactive oxygen species (ROS) via type one and type two photoreactions (Ikehata and Ono, 2011). The method by which DSBs are generated as a result of ROS is thought to be due to the short diffusion range of the ROS. ROS can lead to the development of DNA lesions, such as 8-oxo-G, which can then cause single strand break (SSBs) formation as a result of faulty repair. The short diffusion range of the ROS results in the clustering of SSBs, which are treated like DSBs by the cell (Greinert et al, 2012). SSBs that occur simultaneously and within 1.5 helix turns are converted to DSBs (O'Neill and Wardman, 2009). ROS have also been found to cause protein oxidation and lipid peroxidation. Both of these products have been considered novel biomarkers for aging, as studies have shown increased protein and lipid oxidation can be linked to increased age, due to their prevalence in age-related diseases, such as cancer (Engelfriet et al, 2013).

8-oxoG is one of the most common forms of oxidative base damage associated with UVA (Rosen et al, 1996). 8-oxoG lesions are responsible for one of the common mutations found in UVA spectra, which is the G > T transversion, where 60% of these mutations result from the photosensitiser riboflavin (Brash, 2015). Various studies have also shown that certain ROS have an effect on gene regulation, often causing increased gene expression, which plays a major role in the development of cancer (Scharffetter-Kochanek et al, 1993).

#### **5.4 DNA lesion Repair and mutation**

It is important that DNA lesions are repaired, as they have the capacity to disrupt DNA replication or RNA transcription machinery. One piece of evidence for the importance of DNA lesion repair is the genetic disorder Xeroderma Pigmentosa (XP). People with XP have a mutation in at least one DNA repair proteins involved in NER. There are various types of XP, with the difference between each form being the specific NER protein that is mutated. Although it varies between each type, XP causes the sufferer to be hypersensitive to UV specific mutations, and consequently skin cancer (Daya-Grosjean, 2008).

#### **5.5 - Nucleotide Excision Repair**

Nucleotide excision repair (NER) is the DNA repair pathway for CPD and 6 – 4 PP lesions. NER can be split into two pathways, the first being transcription-coupled repair (TC-NER) and the other being global genome repair (GG NER). The difference between the two pathways is with their initiation. GG-NER is able to repair both transcribed and untranscribed DNA strands, while TC-NER is initiated when RNA polymerase stalls at DNA lesions. GG-NER initiation relies on the damage-sensing complex DDB/XPC-Rad23, which is able to detect DNA lesions in the entire genome. Both pathways recruit TFIIH, a complex of various XP proteins, to process and repair the lesion (Marteijn et al, 2014).

CPDs that form between adjacent thymidine residues are repaired effectively by nucleotide excision repair pathway. This repair complex is able to bypass the thymidine dimer and correctly pair them with adenine during DNA replication.

However, if the dimer goes undetected by the normal repair complex, Pol  $\eta$  can then target the dimer. Polymerase  $\eta$  is able to synthesise past DNA past the site of UV-induced CPDs, and is even able to synthesise thymine dimers more efficiently than undamaged DNA. Pol  $\eta$  is more error prone with 3' thymine than it is with 5' thymine, which can contribute to the mutagenesis of CPDs (McCulloch et al, 2004).

People who have the XPV (variant) have mutations in the XPV gene responsible for coding Pol  $\eta$ , resulting in an inactive polymerase. Liu and Chen (2006) used Pol  $\eta$  knockout cells to investigate the normal mechanism of Pol  $\eta$  and of XPV cells. They were able to show that Pol  $\eta$  KO resulted in an impaired activation of p53. They also suggest that Pol  $\eta$  is co-localised with phospho-ATM, as Pol  $\eta$  KO results in ATM being unable to phosphorylate CHK2/p53. They went on to show that post UV-induced DNA damage, Pol  $\eta$  KO cells have impaired p53 induced apoptosis due to p53 suppression in early stages. In late stages, Pol  $\eta$  KO caused a suppression of DNA repair but sustained activation of p53, increasing apoptosis events (Liu and Chen, 2006). This data suggests that XPV not only plays a role in TLS, but also in the regulation of the DDR post UV irradiation.

## VI. Mutations seen in skin cancer

Most cancers are induced as a result of a somatic mutation, which are known as driver mutations. These driver mutations result in the hallmarks observed in cancer, leading to uncontrolled cellular proliferation. For skin cancer, there are various known 'signature' mutations. Signature mutations are usually the most common mutation found in a certain cancer type. There a number of different signature mutations that have been identified in skin cancers. The use of next-generation sequencing has allowed to gain a much better understanding of sequence changes present in cancer genomes. A study by Brash (2015), showed that 60% of all mutations are C > T transitions, with 5% being CC > TT transitions at dipyrimidine sites (Brash, 2015).

C > T mutations are the most common mutation seen in cells, while G > T mutations have been observed as the second most common mutation in COLO-829 cells, which are a patient derived malignant melanoma cell line (Pleasant et al, 2010). This study suggests that 8-oxoG may have a significant role in melanoma development. However, a different study which looked at 262 driver mutations amongst 21 genes showed only 9% were G > T tranversions (Hodis et al, 2012). These studies suggest that 8-oxoG and the subsequent G>T transition does play a role in melanoma development, but the significance of this role is still unknown.

As previously mentioned, 5'-CpG residues are often methylated, particularly on p53, and are prone to deamination, resulting in the signature C > T transition mutation. Mutations in p53 can be found in around 50% of all cancer types, but in almost all NMSCs (Basset-Seguin, 1994). The mutations found in NMSCs are usually localised to the highly conserved domains of the gene, which are referred to as the mutation hotspots. Several hotspots have been identified, where at least five are dipyrimidine sequences, with the sequences 5'-CCG or 5'-TCG, which were codons 195, 213, 245, 248 and 282 (Pfiefer et al, 2005). Further evidence for the role of C > T transition mutations was shown when mice were irradiated with UVB. A hotspot at the mouse p53 codon 270 (TCGT) was identified, showing a sequence change of 5'TCGT to 5'TTGT. Mouse p53 codon 270 is the equivalent

of human p53 codon 273 (GCGT). There is no mutational hotspot on the human p53 codon 273, as it does not contain a dipyrimidine sequence, which highlights the significance of dipyrimidine/CPDs in UV induced mutations (You et al, 2000).

If a CPD occurs in certain genes, then it is possible for the cells to become cancerous. These types of mutations are referred to as acquired mutations, as they are separate to inherited mutations as previously discussed. An example of a gene that is commonly found to have an acquired mutation in skin cancers is *BRAF*. *BRAF* is responsible for encoding the B-raf protein. B-raf is a signal transducer protein, more specifically it is a serine/threonine protein kinase, and is responsible for activating the MAPK/ERK pathway (figure 1.5). 50% of melanomas have been found to contain BRAF mutations, with 90% of these having a T > A substitution (V600E) mutation in codon 600. B-raf with a V600E mutation is consistently active, and does not require extracellular factors or signals to become active. As a result, the MAPK/ERK pathway is constantly active, leading to the continual phosphorylation of downstream targets (figure 1.5) such as c-Myc (Asceirto et al, 2012).

C-Myc is able to alter the transcription of various genes, including those that drive cell proliferation – such as cyclins, whilst downregulating genes that aim to prevent cell cycle progression, such as p21 (Dang, 1999). The overexpression of c-Myc has been shown to be a key factor in the development of various hallmarks of cancer, such as increased cellular proliferation, evasion of apoptosis and angiogenesis, and is associated with the progression of various cancer types (Hanahan and Weinberg, 2000; Ascierto et al, 2012). Various studies have shown that C-Myc is often overexpressed in melanoma (Ross and Wilson; 1998, Greulich et al, 2000).

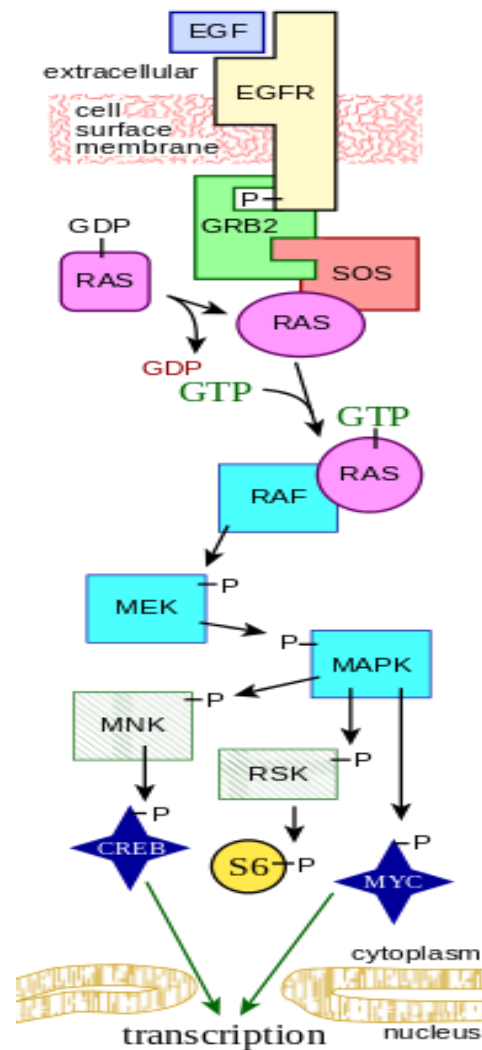


**Figure 1.5 – Simplified diagram of the MAPK/ERK pathway (Wikimedia Commons, 2014).**

*Key components of the MAPK/ERK pathway. 'P' represents a phosphate molecule. The signal cascade is initiated when epidermal growth factor (EGF) bind to the receptor (EGF receptor – EGFR). The intracellular section of the EGFR becomes phosphorylated, allowing for GRB2 to bind. GRB2 binds and consequently activates SOS. SOS catalyses the removal of GDP from ras and allows for GTP to bind. When bound with GTP, ras is active and binds RAF, which phosphorylates MEK and results in its activation. MEK then activates MAPK through phosphorylation. MAPK is then able to activate a transcription factor, such as c-Myc, or CREB via MNK. Through phosphorylation of these transcription factors, the transcription of genes that play a role in the cell cycle is altered. MAPK can also activate RSK which in turn activates S6. S6 is a ribosomal protein that is part of the 40S subunit, and plays a role in translation.*

Studies have shown a link between UV radiation and the stimulation of the MAPK/ERK pathway (figure 1.5), particularly in human keratinocytes. Xu et al (2009) irradiated HaCaT cells with UV radiation (40% UVB/46% UVA), and demonstrated an increase in EGFR activation 1.7 times higher than EGF treated cells (Xu et al, 2009). In a previous experiment, Xu and colleagues demonstrated that UVB-induced signal induction was dependant on EGFR. This was demonstrated using B82 cells and a B82K+ cell line (B82K+ is an EGFR expressing cell line). The B82 cell line are mouse fibroblasts that are devoid of EGFR. When irradiated with UVB, B82K+ showed an induction of the MAPK/ERK pathways and activation of downstream targets, whereas the EGFR devoid B82 cells did not show these changes (Xu et al, 2006). Xu suggests that while UVB is able to cause tumour formation in the skin, the mechanism is dependent on EGFR.

UVA was largely overlooked as a carcinogen until recently, where UVA has been found to play an important role in causing skin cancer, by generating DNA damage indirectly. In a study that involved irradiating embryonic human kidney cells with both UVA and UVB, it was suggested that UVA plays an equal role in carcinogenesis as UVB (Robert et al, 1996).

## **VII. DNA damage response**

It is important that the cell have mechanisms in place to repair any damage that occurs to DNA. If the DNA damage is able to persist, it can lead to various detrimental effects such as the altered gene expression of transcription factors, which can lead to increased proliferation. Another effect that can occur is the evasion of apoptosis. Being able to prevent apoptosis allows mutations to be passed onto daughter cells, causing the development of tumours. Before DNA repair occurs, the cell must stop its progression through the cell cycle, to allow for repair to occur. This involves detection of DNA damage, and consequent signalling to prevent cell cycle progression via cell cycle checkpoints (Huen and Chen, 2010). This signalling cascade is known as the DNA damage response (DDR) (figure 1.6).

Due to UVA only recently coming into focus, our understanding of the mechanism in which it causes DNA damage is limited. There have been contrasting studies regarding UVAs ability to cause DSBs and induce the DDR pathway as a result, particularly in a replication-independent manner. Rizzo et al (2011) irradiated skin fibroblasts with UVA, and saw little  $\gamma$ H2AX foci formation, suggesting that large numbers of DSBs do not form, and that only very low levels of DSBs may be occurring (Rizzo et al, 2011). Other studies contradict Rizzo et al (2011), such as Rapp and Greulich (2004), who showed a clear increase in  $\gamma$ H2AX accumulation with increased UVA exposure time, and demonstrate the activation of DSB repair following irradiation (Rapp and Greulich, 2004). A study was carried out using the Chinese hamster ovary cell line Xrs-6, which are deficient for Ku80, a protein essential for the DSB repair pathway Non-homologous end joining (NHEJ). Fell and colleagues demonstrated Xrs-6 cells were sensitive to UVA induced cytotoxicity, due to their inability to carry out NHEJ, and resulted in chromosome damage. They concluded that this was key evidence for the role of UVA in DSB formation, and the induction of appropriate repair pathway (Fell et al, 2002).

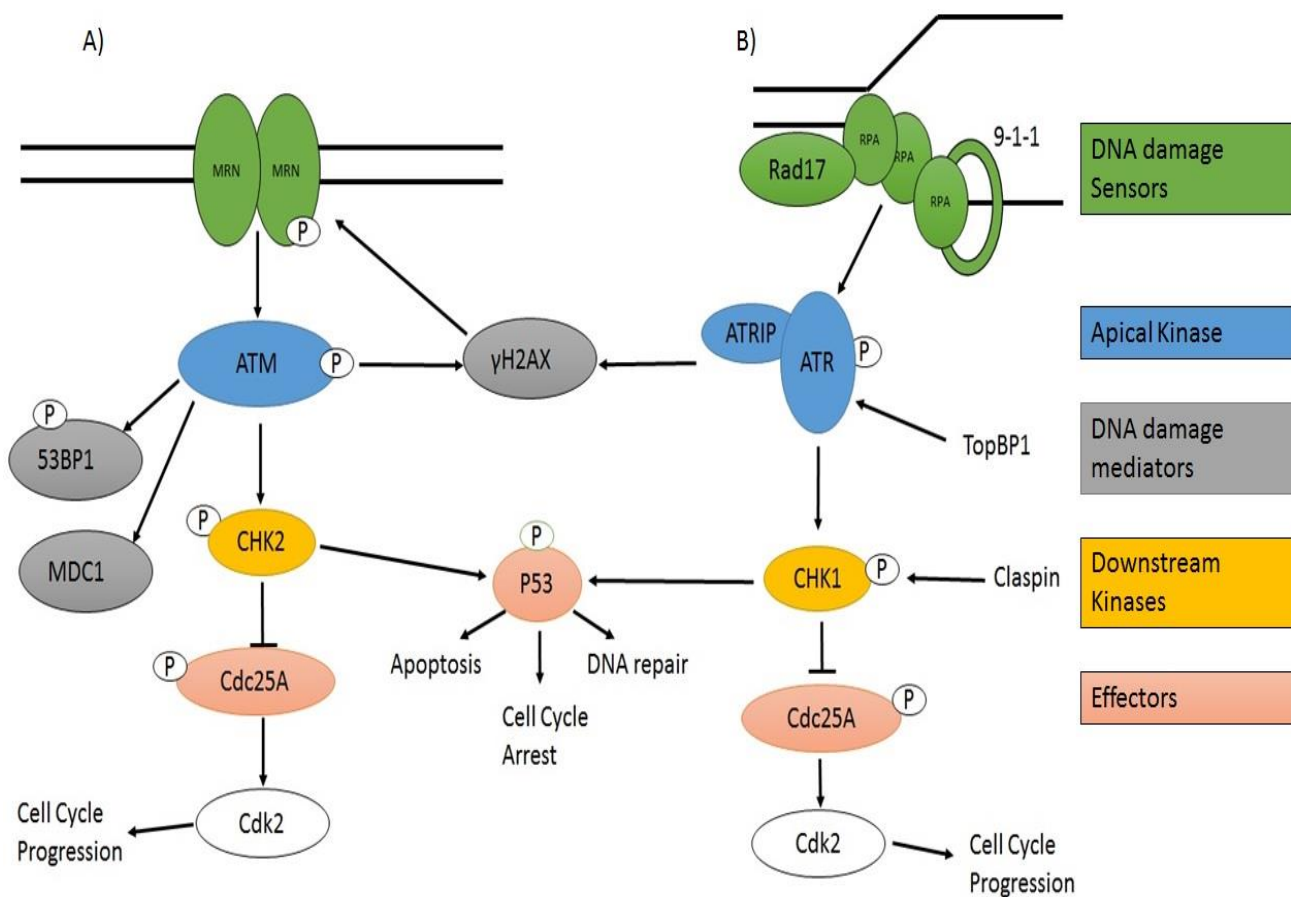


**Figure 1.6 – Simplified Schematic diagram of the DNA damage response**

The DNA damage response (DDR) is a signalling pathway in which cells detect DNA damage and trigger an appropriate response. UV is capable of generating DNA damage which triggers the DDR. A) Double-Strand breaks (DSBs) are detected by the MRN complex. The MRN complex is required for the recruitment of ATM, which is the apical kinase of the DSB DDR pathway. ATM phosphorylates a number of targets, including 53BP1, H2AX (forming  $\gamma$ H2AX) and CHK2. Positive feedback loops can form via  $\gamma$ H2AX and MDC1, where MRN can be recruited by either. CHK2 is the main downstream kinase, and is responsible for the phosphorylation of p53. B) Single-Stranded DNA (ssDNA) damage can occur as a result of UV or through replicative stress. Single-stranded damage is detected by the RPA/9-1-1 complex. RPA is required for the recruitment of the ATRIP/ATR complex, which phosphorylates CHK1 and to an extent H2AX. CHK1 can also phosphorylate p53. P53 phosphorylation leads to cellular response, most notably apoptosis, DNA repair and cell cycle arrest. These responses are important in the prevention of genomic damage persistence in cells, which could otherwise lead to mutations and tumorigenesis.

### **7.1 – Initiation of the DDR**

The detection of DSBs and the consequent activation of the DDR is dependent on the MRN complex. MRN (Mre11, Rad50 and Nbs1) is involved in binding to DNA via the Mre11 and Rad50 proteins (Uziel et al, 2003). The Nbs1 protein contains a FHA/BRCT domain (Fork-head association and BRCA1 C-terminus domain), which is responsible for binding the protein H2AX, and while Nbs1 does not bind DNA itself, it is responsible for localising the Mre11 and Rad50 to the vicinity of the DSB (Kobayashi et al, 2002). The Nbs1 domain also interacts with various downstream proteins via its C terminus, mainly ATM, and is responsible for its recruitment to the site of a DSB via a fork-head association protein (Falck et al, 2005). The function of Rad50 is to bind and hold both ends of the DNA at the break site in proximity to each other. Mre11 is capable of various functions, which include binding DNA and the capability of acting as either an endonuclease or 3'-5' exonuclease (Paull and Gellert, 1998). Cells deficient in MRN were found to be less effective at activating and maintaining ATM (Hartlerode et al, 2015).

### **7.2 - $\gamma$ H2AX generation and accumulation**

One of the most commonly used markers for detecting and measuring the activation of the DDR is  $\gamma$ H2AX. H2AX is a subtype of histone H2A, and varies due to the presence of a C-terminal extension involved in DNA repair. When H2AX becomes phosphorylated at S139, it is then known as  $\gamma$ H2AX. S139 is located in the SQ motif in H2AX, and is significant to the activation and progress of the DDR. Following the SQ motif, there is an acidic residue and a hydrophobic c-terminus which is evolutionary conserved, as it is a common recognition site for DDR kinases (PIKKs) (Kinner et al, 2008). Phosphatidylinositol-3-OH-kinase-like family of protein kinases (PIKKs), make up several components of the DDR, notably ATM, ATR and DNA-PK, which have the potential to generate  $\gamma$ H2AX (Wang et al, 2005). Of the three, ATM is able to be activated by local chromatin modifications, and as a result is likely the cause of  $\gamma$ H2AX generation in response to DSBs (Bakkenist and Kastan, 2003).  $\gamma$ H2AX has been widely accepted as a biomarker for DNA damage, particularly in

studies examining the genomic damage caused by cytotoxic chemicals or environmental factors (Kuo and Yang, 2008). The function of  $\gamma$ H2AX is to recruit other repair proteins to the site of DNA damage, including MRN via its Nbs11 component (Kobayashi et al, 2002). This creates a positive feedback loop in which  $\gamma$ H2AX recruits more MRN, resulting in the amplification of the damage response.

### **7.3 - ATM**

Ataxia-telangiectasia mutated (ATM) is a member of the PIKK family (PI3K related kinases). Members of the PIKK family are serine/threonine protein kinases, meaning that they function by phosphorylating OH groups of serine or threonine groups. ATM is comprised of five domains; the HEAT repeat, kinase, PIKK-regulatory, FAT and FATC domains (figure 1.8) (Lavin et al, 2004). The HEAT repeat domain is responsible for interacting with the C terminus of Nbs1 in MRN, and thus its localisation to DSBs.

Unstimulated ATM exists as a dimer, and requires autophosphorylation for the complex to dissociate, which occurs at the S1981 site (figure 1.7 and 1.8). Autophosphorylation is the process in which a protein is phosphorylated by itself, and can occur in ATM as the kinase domain can bind the phosphorylation domain stably (Bakkenist and Kastan, 2003). Bakkenist and Kastan also demonstrated that mutant ATM, such as the S1981A form, is unphosphorylatable and cannot localise to sites of DNA damage and consequently the DDR is not completed. Other autophosphorylation sites have been identified at S367 and S1893, and have been shown to be functionally significant to ATM activity in response to irradiation-induced DNA damage. ATM with the mutations S367A and S1893A showed a defective DNA damage response, demonstrating a significant delay in p53 phosphorylation, and inability to process genome instabilities and trigger cell cycle arrest (Kozlov et al, 2006).

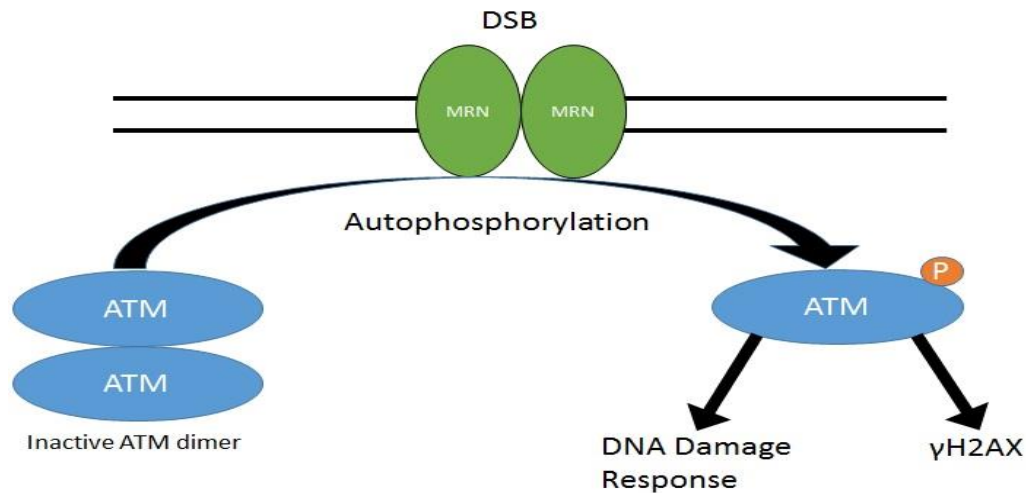


**Figure 1.7 – The simplified diagram of ATM autophosphorylation, showing the dissociation of the inactive dimer forming the active monomer**

When unstimulated, ATM exists as a dimer. ATM can perform autophosphorylation, causing the dimer to break and ATM become active, where it can phosphorylate a number of targets including H2AX and CHK2.

Once the ATM is in its functional monomer form and has localised to the site of DNA damage, it can trigger the DDR. The kinase domain (KD) is the carboxyl-terminal active site, and is responsible for ATM's phosphorylation activity. ATM has been found to have a large range of targets, which result in a range of effects within the cell, including gene expression control and cell cycle control (Shiloh and Ziv, 2013). One of the most well documented targets of ATM is Checkpoint kinase 2 (CHK2). CHK2 is the primary downstream kinase in the DDR, and is responsible for spreading the DDR signal and regulating the cell cycle.

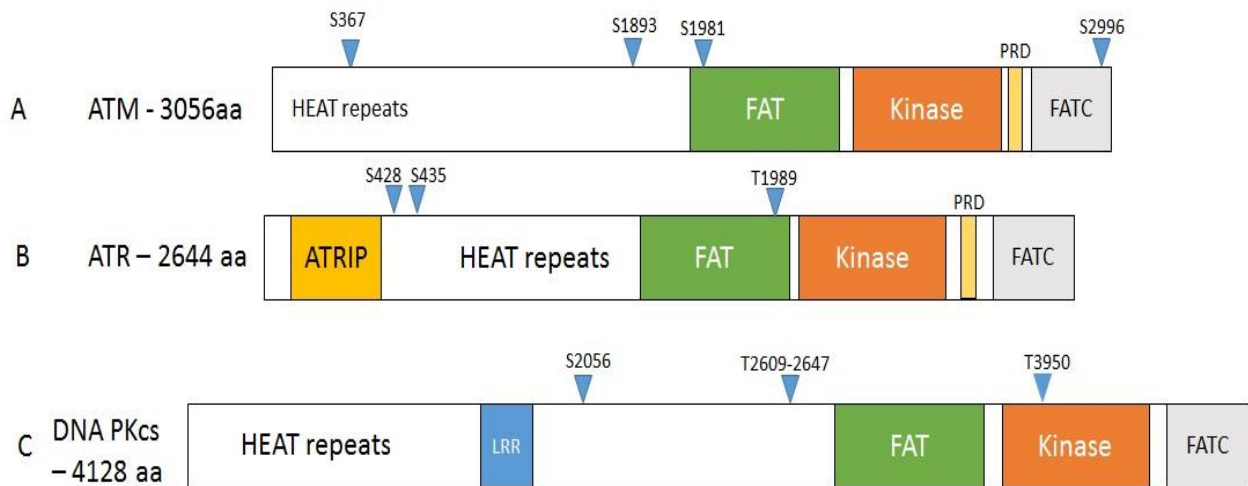


**Figure 1.8 – Simple Schematic diagrams three of the PI3K family members, ATM, ATR and DNA-PKcs**

The blue triangles represent the main sites of phosphorylation of each protein. A) The indicated sites via blue triangles represent the main auto phosphorylation sites required for ATM function. B) Shows the ATRIP site required for ATR localisation to the site of DNA damage. C) DNA-PK structure with blue indication of the main phosphorylation sites. In particular, S2056 and the cluster T2609-2647 being the sites of autophosphorylation.

#### **7.4 – CHK2**

CHK2 is a serine/threonine kinase, comprised of three domains, the N terminal SQ/TQ domain (SCD), central forkhead association (FHA) domain, and the c terminal serine/threonine kinase domain (Ahn et al, 2004). Similar to ATM, the SCD domain is rich in SQ/TQ residues, which are targets of phosphorylation. Thr68 is the primary site of phosphorylation in the SCD, and is important for forming a dimer between two CHK2 monomers. When CHK2 is inactive, it is monomer, however once phosphorylated dimerization occurs where pThr68 interacts with the FHA domain of the other CHK2 (Cai et al, 2009). CHK2 has also been found to be activated by DNA-dependant protein kinase (DNA-PK). Activation via DNA-PKs can occur during mitosis, where CHK2 that is bound to chromatin

and centromeres. This activation is key in preventing mitotic catastrophe, and allowing for spindle stabilisation in the presence of DNA damage that has occurred during mitosis (Shang et al, 2010).

Once activated, CHK2 phosphorylates a range of DDR proteins. 24 proteins have been identified as substrates, making up four groups based on their function. These groups are DNA repair, p53 control, apoptosis and cell cycle regulation (Zannini et al, 2014).

One of the key outcomes of CHK2 activation is coordinating the cell cycle progression at specific checkpoints. By preventing the cell from moving through the cell cycle, the repair of DNA lesions can occur, before they are replicated in S phase, or form a second cell with the lesion during mitosis. The method in which CHK2 triggers this cell cycle arrest can vary. CHK2 can phosphorylate p53 to relieve MDM2 inhibition, leading to p53 driven cell cycle arrest. Alternatively, CHK2 can phosphorylate CDC25A, targeting it for ubiquitination and consequently degradation. A lack of CDC25A activity results in the maintained phosphorylation of CDK2 and consequently remains inactive, preventing the progression from G1 to S phase.

There has been little research carried out on the relationship between UVA and CHK2 activation. Although it is accepted that ATM is one of the main kinases responsible for CHK2 phosphorylation, there has been no evidence presented that CHK2 is activated following UVA irradiation. The effect on CHK2 activation without the presence of functional ATM has also not been investigated.

### **7.5 - p53 structure and function**

The tumour suppressor p53 is arguably one of the most important defences cells have against the development of tumours. Mutations in p53 are a possible cause of many types of cancer, but is more common in certain cancers. Mutations in p53 vary per type of NMSCs. 66% of aggressive BCCs and 35% of aggressive SCC tumours contained p53 mutations. 71% of all p53 mutations detected in all types of SCC and BCC tumours were UV signature mutations (Benjamin and Anathaswamy, 2007).

The main effector protein of the DDR is p53, and once activated, it plays important roles in the

prevention of tumours. The three main pathways p53 is known to trigger is cell cycle arrest, apoptosis and DNA repair.

The structure of p53 is divided into five domains. These domains are; the (N-terminus) transcription activation domain (TAD), the proline rich region (PRR), the DNA binding domain (DBD), the homo-oligomerization domain (OD) and the c terminal domain (CTD).

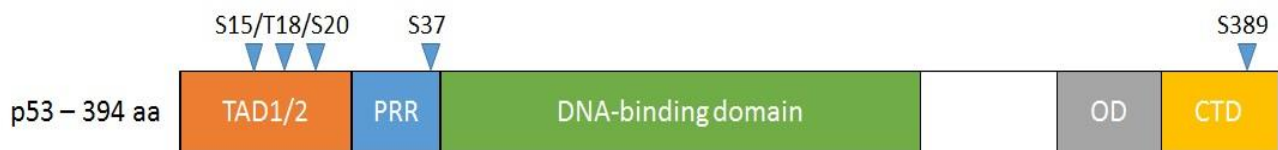


**Figure 1.9 – Simplified schematic diagram of p53 structure**

*Schematic representation of the structure of p53, with the 5 key domains indicated. Blue triangles represent DDR kinase associated phosphorylation sites.*

The proline rich region is required for the induction of apoptosis via p53. Studies where the PRR has been deleted show altered mechanisms of transactivation repression, ROS production and transactivation of the PIG3 gene, which causes inefficiencies of apoptosis (Venot et al, 1998).

The DNA binding domain is key to p53s function as a transcriptional regulator to genes that are transcribed by RNA polymerase II. The transcriptional activity is regulated in a ‘stimulus-specific’ mechanism, meaning that different subsets of target genes can be induced, allowing for a more tailored response to specific stresses (Beckerman and Prives, 2010). The DBD is a hotspot for mutations, accounting for 90% of all known p53 mutations. The majority result in loss of function of p53, as the protein cannot bind to DNA (Vegran et al, 2013).

The oligomerization domain is responsible for the tetramerization of p53. The activity of p53 is dependent on its conformation, where it is active in its tetrameric state and can bind to DNA with

high affinity. The OD is also involved in several protein-protein interactions. While some studies show that p53 is able to bind DNA when the OD has been deleted (monomer conformation), the affinity for DNA is 10-100 times lower than that of a tetrameric full-length protein (Chene, 2001). Several proteins bind directly to the OD, such as casein kinase 2 and  $\text{Ca}^{2+}$  - dependant protein kinase, which both play roles in proliferation and DNA repair (Delphi et al, 1997; Gotz et al, 1999).

The C-terminal domain acts a regulator of p53 function. Its mechanism of action is not fully understood; however it was shown that p53 with a mutant CTD does not activate p21 transcription (Espinosa and Emerson, 2001). McKinney and colleagues demonstrated that wild type p53 is able to diffuse along DNA, but p53 lacking its CTD cannot. The isolated CTD was able to diffuse more efficiently than the whole protein (McKinney et al, 2004). These studies suggests the CTD is required for promoter binding (Hamard et al, 2012).

The TAD domain interacts with MDM2 and CBP/p300 (Lee et al, 2010). CBP/p300 are co-activating transcriptional proteins, and both function to increase the gene expression of their targets (Vo and Goodman, 2001). Nine of the phosphorylation sites of p53 are located in the TAD domain, including S15/T18/S20, which are target sites for CHK2 activity. Phosphorylation of these sites lowers the affinity of MDM2 binding, and increases the affinity for binding CBP/p300 (Krois et al, 2016). In unstressed cells, p53 remains unphosphorylated, which allows MDM2 to remain bound, targeting itself and p53 for ubiquitination and consequently degradation. As a result, p53 cannot arrest the cell cycle or trigger apoptosis, allowing progression to the next phase.

Bruins et al (2004) demonstrated that mice with mutations in p53 at the phosphorylation site Ser389 are deficient in p53 activated mechanisms including apoptosis and cell cycle arrest following UVA irradiation. Ser389 is one of the key phosphorylation sites for DDR kinases, so the mutation of this site resulted in a deficient DDR pathway, leading to development of UVA-induced skin tumours (Bruins et al, 2004). Loughery and colleagues demonstrated the significance of S15, by showing that

mutations at this site cause the failure of p53-mediated transcription or cell cycle arrest in response (Loughery et al, 2014). Loughery also showed that S15 is phosphorylated in response to UVC.

### **7.6 - p53 and apoptosis**

In the event that DNA damage is unable to be fully repaired, apoptosis is induced to prevent the persistence of the lesion, and stop mutations from occurring. Apoptosis has two mechanisms of action, which are the extrinsic and intrinsic pathways. Both pathways involve p53 in some way. The extrinsic pathway (figure 1.9.1) functions by engaging death receptors, which are a part of the tumour necrosis factor receptor (TNF-R) family. The engagement of these receptors results in the formation of death inducing signalling complexes (DISCs). DISCs lead to the activation of caspases-8 and caspase-3, which causes DNA fragmentation and chromatin condensation, key steps in apoptosis (Porter and Jänicke, 1999). p53 can activate the extrinsic pathway by inducing three genes called *Fas*, *DR5* and *PERP*. *Fas* is a member of the TNFR family, and is activated by binding *FasL*, which is a ligand expressed by T cells (Nagata and Golstein, 1995). *Fas* induction via p53 occurs in specific tissue, such as the spleen, thymus and kidney, but not in other tissues including the heart and liver (Bouvard et al, 2000). *DR5* is the death-domain-containing receptor for TNF-related apoptosis-inducing ligand (TRAIL). *DR5* triggers apoptosis via the activation of caspase 8. Increased levels of *PERP* mRNA in cells undergoing apoptosis suggests that they have a role to play in the process, however its mechanism is not fully understood.

The Intrinsic pathway (figure 1.9.1) is associated with the release of cytochrome c from the mitochondria into the cytoplasm. Bcl-2 proteins are heavily involved in the release of cytochrome c, with some of the members being regulated by p53. The bcl-2 family is comprised of both pro and anti-apoptotic signal molecules. *Bax* was one of the first discovered to be induced by p53, and is a member of the pro-apoptotic Bcl-2 proteins (Thornborrow et al, 2002). *Bax* functions by forming a homodimer on the outer-membrane of the mitochondria. This makes the mitochondrial membrane permeable to release cytochrome c. Cytochrome c forms a complex with APAF-1 and procaspase-9

called the apoptosome. The apoptosome activates caspase-9, resulting in the activation of other caspases (Skulachev, 1998). Caspases 3, 6 and 7 are responsible for the proteolytic degradation of intracellular proteins, leading to cell death.

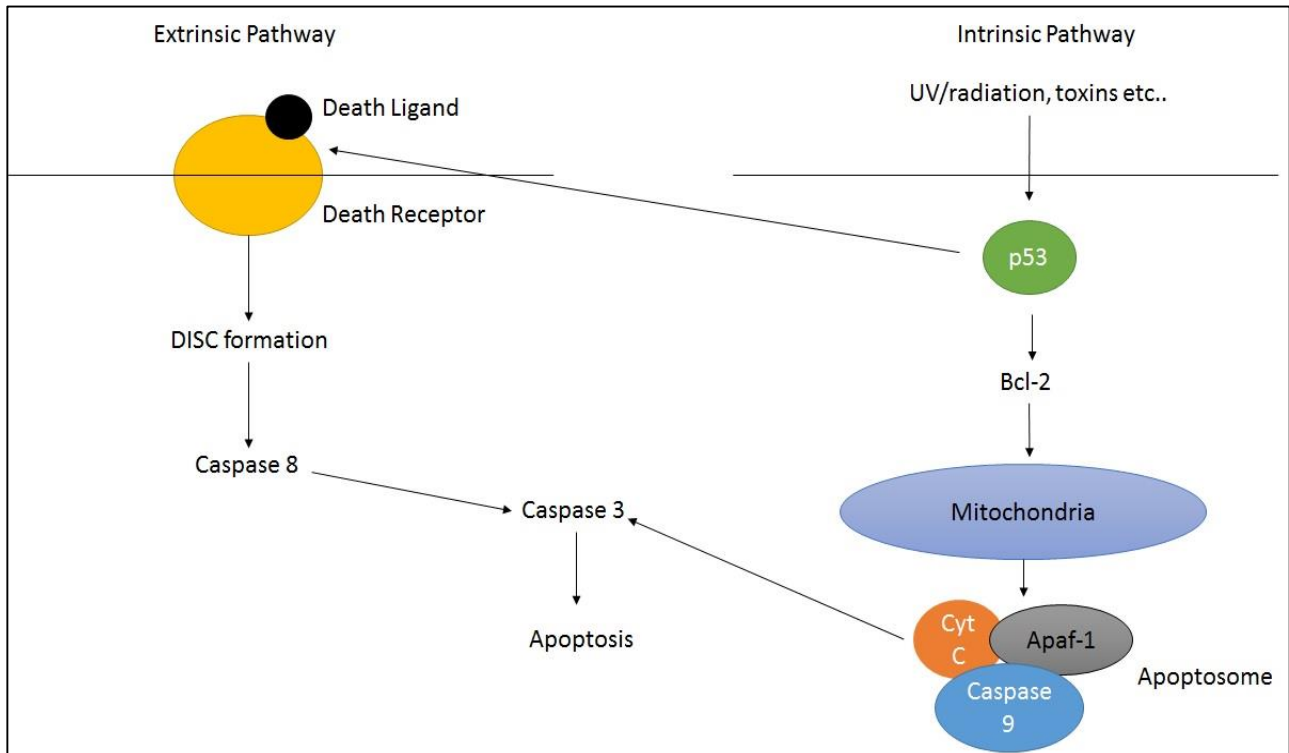


**Figure 1.9.1 – A simplified schematic diagram of the extrinsic and intrinsic pathway of apoptosis activation**

*The induction of apoptosis is required for preventing the persistence of genomic damage, which such damage cannot be repaired. Each pathway has their own initiator caspase (caspase 8 or 9), which results in the initiation of caspase 3, which trigger characteristic apoptosis events such as chromatic condensation and DNA degradation.*

### **7.7 - p53 and growth arrest**

p53 also play a key role in causing cell cycle arrest, particularly in preventing progression from G1 to G2, but also in the G2/M phase transition to some degree. Cell cycle arrest is an important function of p53 as it allows time for DNA repair to occur. One of the main targets of p53 is *WAF1/CIP1*, which

encodes for the protein p21. p21 contains a Cy1 motif in its N-terminal half, which allows it to bind the cyclin subunit and the CDK subunit, preventing CDK activity and complex formation with cyclin. p21 also contains a Cy2 motif in the C terminal half, which binds to the cyclin subunit, however this interaction is weaker and is redundant in comparison to the Cy1 interaction (Chen et al, 1996). If CDK cannot bind with cyclin, then it remains inactive and cell cycle progression cannot occur. P21 is mainly responsible for the inhibition of CDK2, meaning protein Rb remains hypophosphorylated, sequestering the transcription factor E2F1. E2F1 is a transcription factor that targets the genes for DNA replication proteins, and is required for the transition from G1 to S phase (Brugarolas et al, 1999).

p21 can interact with proliferating cell nuclear antigen (PCNA), which is a protein that acts as a DNA clamp, increasing the processivity of leading strand synthesis during DNA replication. Various proteins required for DNA replication and repair tether to PCNA, and are able to slide along DNA (Scovassi and Prosperi, 2006). p21 can compete for PCNA with a number of these protein that rely on PCNA tethering, resulting in the inhibition of s-phase DNA synthesis. p21 was shown to mainly inhibit DNA polymerase  $\delta$  binding to PCNA, by binding to the p50 subunit of the enzyme (Li et al, 2006). DNA polymerase  $\delta$  is heavily involved in leading and lagging strand DNA synthesis.

p53 has also been shown to regulate the G2/M transition, via the control of the cyclin dependant kinase Cdc2. Cdc2 is essential for the progression into M phase. p53 decreases the intracellular level of cyclin B1 by attenuating the promotor for the protein. Cyclin B1 is the regulatory partner of Cdc2, and is required for the initiation of mitosis (Innocente et al, 1999).

### **7.8 - p53 Independent cell cycle arrest**

The mechanism for cell cycle arrest during G1/S transition involves the phosphorylation of Cdc25A phosphatase. CHK2 phosphorylates Cdc25A, which targets the phosphatase for ubiquitination and results in its degradation via the proteasome. This prevents the function of Cdc25A, which is usually to dephosphorylate Cdk2. If Cdk2 remains phosphorylated, it cannot activate and carry out its regular function of phosphorylating a number of substrates required for the transition from G1 to S phase, as well as triggering centrosome duplication (Falck et al, 2001). As a result, the cell cycle is arrested.

### **7.9 - Single Strand DNA damage**

UV has the ability to also cause single strand breaks in DNA, which must be repaired to avoid mutagenesis. UVB can generate CPDs or 6-4 PPs, which can lead to single strand breaks (SSBs) as a result of disruption of DNA repair, or directly through the deposition of energy (Lankinen et al, 1996). UVA has been shown to cause CPDs too (Rochette et al, 2003), but predominately causes SSBs via ROS generation (Osipov et al, 2014). Single strand DNA can also be generated from replicative stress, such as stalled replication forks, as well as enzymatic and helicase activity. The checkpoint responsible for detecting and processing single strand breaks is controlled by ATR. The aim of this ATR driven single strand break response pathway is the same as the DSB driven DDR, which is to arrest the cell cycle and trigger DNA repair or apoptosis. ATR is an essential protein in replicating cells, due to its activation during every S phase cycle, to aid in the control of nucleotide production or origin firing. Mammalian cells with a homozygous loss of ATR function are not viable (Brown and Baltimore, 2000).

Ataxia telangiectasia and Rad3 related (ATR) is a member of the PI3K family and has many similarities to ATM. They are structurally similar (figure 1.8), with the only major difference being the

presence of an ATRIP region in ATR. They are both the apical kinases of their respective pathways. They both phosphorylate SQ/TQ residues on similar target proteins, which continue the DDR cascade. The main difference between the two is that ATR is activated when single strand DNA (ssDNA) breaks are detected, or during replicative stress.

Most ssDNA in a cell is coated by replication protein A (RPA), including that formed during DNA replication. RPA's main function is to prevent ssDNA from forming secondary structures by keeping the DNA unwound. RPA-ssDNA binding is essential for the recruitment of ATR to sites of DNA damage and stalled replication forks, which can be induced by UV (Zou and Elledge, 2003). As a result, the RPA-ssDNA is essential for the progression of the DDR.

ATR alone cannot localise to the site of RPA, it requires binding with ATRIP (ATR-interacting protein) to form the ATR-ATRIP complex. ATRIP is responsible for the localisation of the ATR-ATRIP complex to the RPA-ssDNA. Studies have shown that both ATR and ATRIP are required for the localisation of the other to RPA-ssDNA (Ball et al, 2005). After the localisation of ATR to the site of RPA-ssDNA, there are various criteria that must be met for activation. The ATR-ATRIP complex must bind the RAD9-RAD1-HUS1 complex (simply called 9-1-1). 9-1-1 is similar to PCNA, as it has a ring structure, and is loaded onto primer-template junctions, which in this case is a stretch of RPA-ssDNA. Rad17 is required for loading of 9-1-1 to single stranded DNA (Medhurst et al, 2008). 9-1-1 is required for the recruitment of TopBP1, which is responsible for activating the kinase function of ATR (Delacroix et al, 2007).

The main target of ATR is CHK1. CHK1 is able to phosphorylate cdc25, utilising the same mechanism as CHK2 for p53 independent cell cycle arrest. CHK1 can also phosphorylate p53 as demonstrated in various studies (Ou et al, 2005, Shieh et al, 2000), which results in activation of DNA repair, apoptosis and cell cycle arrest. When activated by ATR, CHK1 must be stabilised by claspin binding (Kumagai and Dunphy, 2000). ATR has also been shown to play a role in the generation of  $\gamma$ H2AX (Ward and Chen, 2001).

## VIII. DNA repair

The purpose of causing cell cycle arrest is to allow time for DNA repair to occur. The repair mechanism that occurs depends on the type of DNA damage that is present. For DSBs, there are two main repair mechanisms: Non-homologous end joining (NHEJ) and homologous recombination. There is a third minor pathway known as microhomology end joining (MMEJ), which serves as a backup pathway should other pathways fail to initiate, particularly HR. Studies have demonstrated that the position of the cell in the cell cycle influences which repair mechanisms predominantly occurs. It is traditionally thought that if the cell is in G1, then NHEJ is dominant, while if the cell is in S or G2, HR is the main repair mechanism (Takata et al, 1998). In contrast, Mao et al (2008) shows that homologous recombination is completely absent in G1 cells, but is also down-regulated in G2/M phase cells, with NHEJ being more dominant (Mao et al, 2008). Takashima demonstrated that NHEJ contributed to 100 fold more repair events than HR. HR frequency increased in S phase cells, while NHEJ never decreased at any stage of the cell cycle, suggesting that the two mechanism do not compete with each other (Takashima et al, 2009). Rapp and Greulich (2004) suggested that both pathways cooperate with each other following UVA irradiation if both are available, particularly in G2 phase cells NHEJ events were visualised using DNA-PKcs foci formation, while HR events were tracked with Rad51 foci formation. They suggest that in G2 cells,  $\gamma$ H2AX marks DSBs, which recruits more MRN complexes and causes the recruitment of proteins involved in both NHEJ and HR (Rapp and Grulich, 2004). The definitive mechanism is not agreed upon, with contrasting data presented in various studies leading to difficulty in deciphering which pathway is dominant in different phases of the cell cycle.

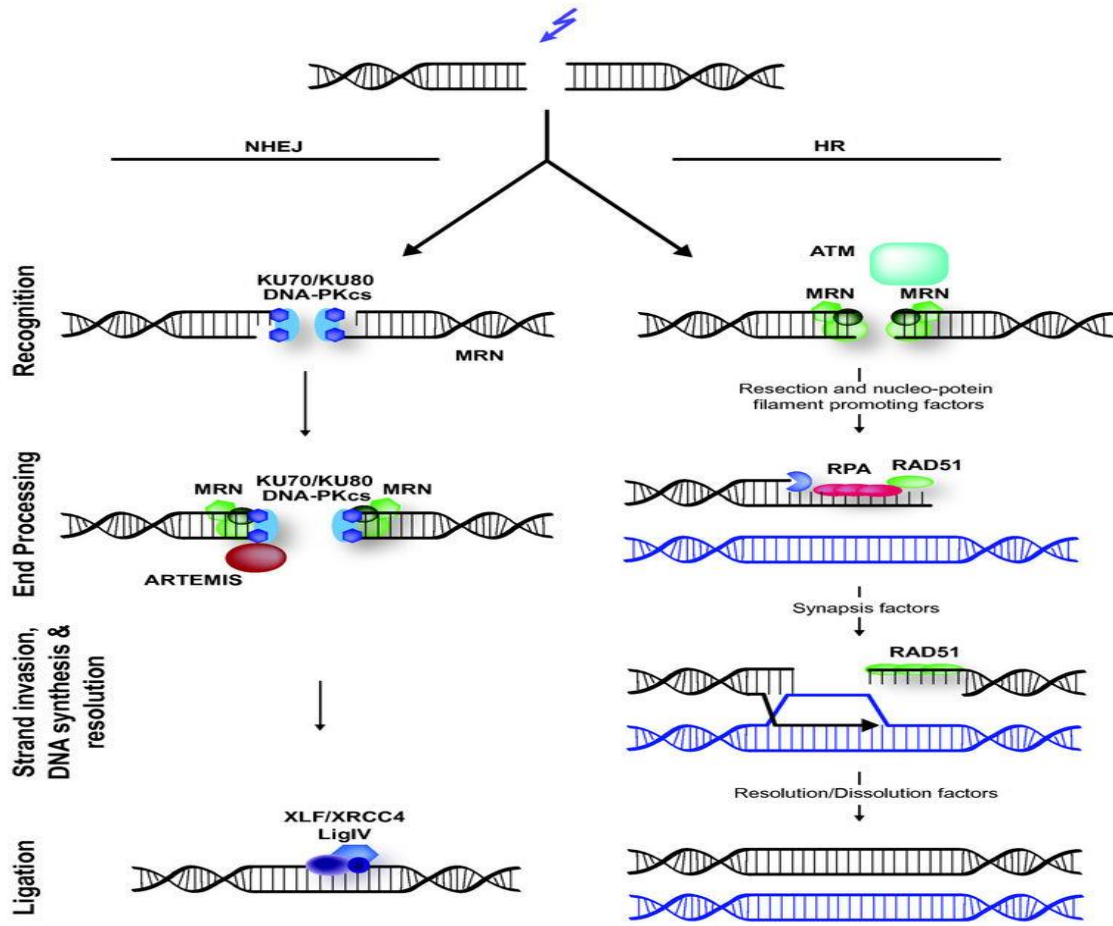


**Figure 1.9.2 – Mammalian DSB repair (Lans et al, 2012)**

DSBs are repaired either through Non-homologous end joining (left) or homologous recombination (right).

NHEJ does not require a homologous template to function, meaning it is the dominant repair pathway in G1

phase cells. NHEJ sometimes requires the trimming of the DNA ends before ligation can occur, which is carried

out by Artemis and DNA-PKcs. The XRCC4/DNA Ligase IV complex carries out ligation. HR is initiated by

resection, and RAD51 is recruited to drive the repair, causing DNA strand invasion to a homologous DS DNA

template, leading to repair.

## 8.1 - Homologous Recombination (HR)

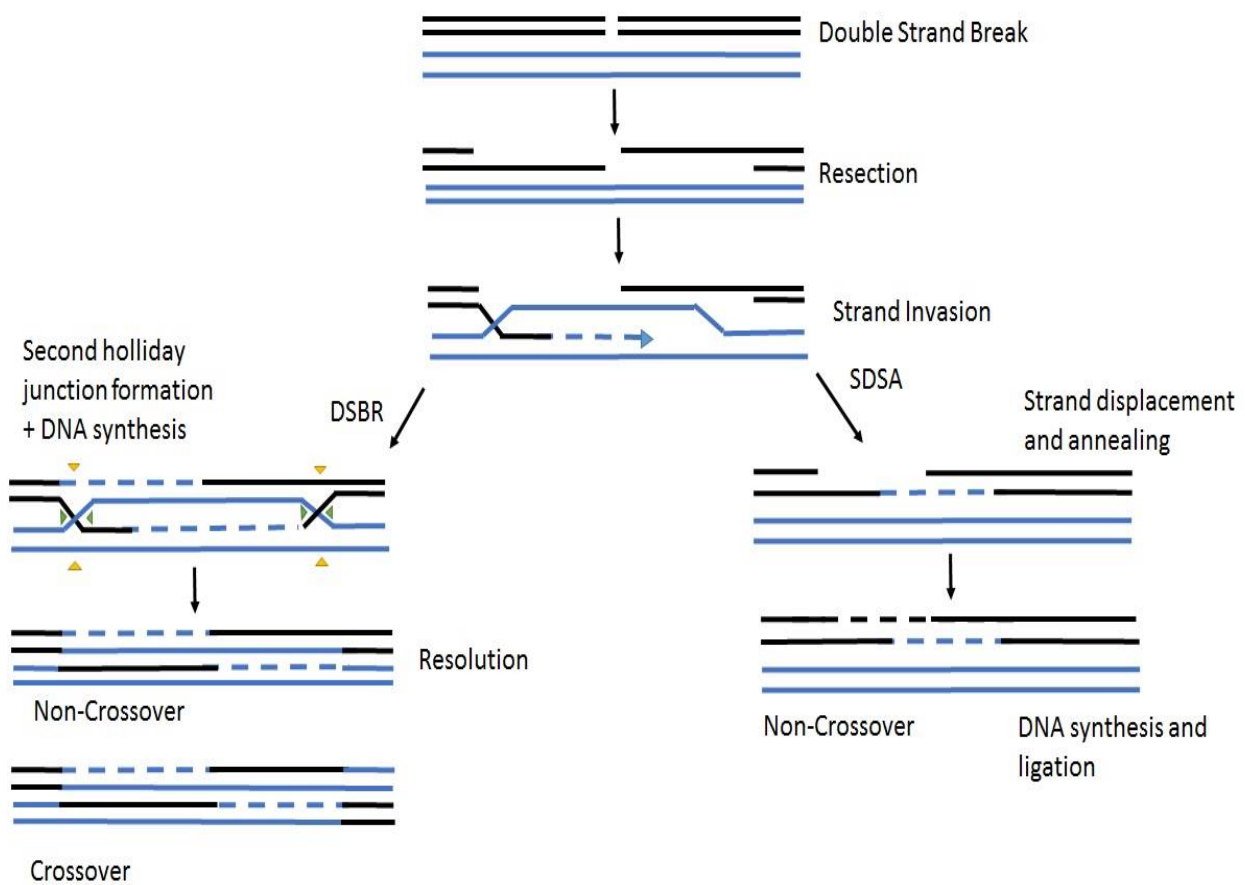


**Figure 1.9.3 - Repair of DNA double-strand breaks by DSBR and SDSA**

Homologous recombination occurs through two possible pathways, double strand break repair (DSBR) and synthesis-dependant strand annealing (SDSA). Both pathways begin the same, with the resection of the breaks to create 3' single strand DNA overhanging breaks. One of the overhanging ssDNA invades a homologous sequence and DNA synthesis occurs. In DSBR, the other DSB end of the strand forms a Holliday junction (HJ). Gap-repair DNA synthesis and ligation occurs. Resolution of the HJ can form either a crossover or a non-crossover result. A crossover will occur when one crossover is cut along the green arrowheads and the other cross over along the black arrowheads. A non-crossover occurs if both crossovers are cut at the black arrowheads. In SDSA, the invading strand is extended and then is then displaced, annealing to the end of the ssDNA at the other side of the break.

Homologous recombination serves multiple roles in the cell, including repair of DSBs, the re-establishment of faulty replication forks and telomere maintenance. HR is dependent on the presence of a homologous sequence in the genome, hence why it occurs post DNA replication (S phase and G2 phase).

The first step of HR is end resection. MRN binds to the end of the DNA at both sides of the double strand break, and the 5' DNA is cut to produce single strand DNA. MRN interacts with CtIP, which is required for the recruitment of RPA. BRCA1 also interacts with MRN, where it promotes HR through the inhibition of 53BP1 (which is required for NHEJ) (Aly and Ganesan, 2011). Further resection requires Exo1, a 5'-3' exonuclease or Sgs1/Dna2 activity. As previously mentioned, RPA binds readily to single stranded DNA, but must be removed via mediators to allow for further steps. The main mediator in humans is BRCA2, and allows for Rad51 binding and filament formation. This filament searches a homologous template for a complementary sequences to that of the 3' overhang, where strand invasion occurs. A displacement loops is formed from the invading strand and the homologous template, and DNA polymerase synthesises new DNA on the 3' overhang (Jasin and Rothstein, 2013). The synthesis of new DNA causes the formation of a Holliday junction, which is a structure of four joined DNA strands. If a second Holliday junction forms it can be resolved via double strand break repair (DSBR) pathway. Alternatively, strand displacement can occur through synthesis-dependant strand annealing (SDSA) pathway.

DSBR (figure 1.9.3) occurs when the non-invading 3' overhang forms a second Holliday junction with the homologous chromosome. Further DNA synthesis fills in gaps, and the strands are separated at the Holliday junctions. Crossovers can occur when one Holliday junction is cut in one plane, and the second junction cut in the other plane (indicated with arrows in figure 1.9.3). Non-crossovers occur when the Holliday junctions are cut in the same plane.

SDSA (figure 1.9.3) does not require the formation of a second Holliday junction. The extended strand is displaced and anneals to the single stranded DNA on the other side of the original double strand break. The remaining gaps are filled in via DNA synthesis and ligation.

## **8.2 - Non-Homologous End Joining (NHEJ)**

NHEJ is the second major method of repairing DSBs. It is referred to as 'non-homologous' as the mechanism does not require the presence of a sister chromatid/homologous template to repair the DNA damage. As a result, it is the dominant DNA repair pathway in G1 phase cells. Evidence has been presented that suggest that NHEJ is not downregulated when HR can be performed (S phase/G2), however the exact role cell cycle status plays is still debated (Takashima et al, 2009).

The NHEJ pathway (figure 1.9.2) can be broken down into three stages. Stage 1) DNA end recognition and bridging. The first step of NHEJ is the binding of the Ku heterodimer (Ku70/80 complex) to both DNA ends at the site of the DSB. The Ku70/80 are circular structures that form a ring round the DNA ends, and allows the binding of DNA-PKcs to DNA as well interacting with the XRCC4-DNA Ligase IV complex, recruiting it to the DNA end. Ku also forms a bridge between the two DNA ends, ensuring the DNA align correctly, as well as preventing degradation and unwanted DNA binding.

DNA-PKcs (DNA dependant protein kinase, catalytic subunit), is a serine/threonine protein kinase and a member of the PI3K family. The actual role of DNA-PKcs is not fully understood, some studies suggest that it is important in the activity of other NHEJ components, in particular Artemis (Ma et al, 2002). DNA-PKcs is capable of autophosphorylation at the Thr2609 site (figure 1.9.2), which is key to its regulation by destabilising the proteins interaction with DNA ends (Uematsu et al, 2007). Ku70/80 also interacts with the XRCC4-DNA Ligase IV complex, recruiting it to the DNA end. DNA-PKcs can

also be responsible for the generation of  $\gamma$ H2AX, contributing to the localisation of DDR components, such as 53BP1 to the site of the DSB (Stiff et al, 2004)

Stage 2) DNA ends can contain moieties that cannot be ligated such as 5' hydroxyls or 3' phosphates, which must be processed in order for NHEJ to continue. PNKP (polynucleotide kinase 3'-phosphatase) is both a kinase and a phosphatase, meaning it is able to appropriately process these molecules that cannot be ligated, and is recruited by DNA-PKcs or XRCC4 (Chappell et al, 2002). The 5' hydroxyl can be phosphorylated and the 3' phosphates can be removed (Bernstein et al, 2005). Artemis is a nuclease that when bound to DNA-PKcs, becomes phosphorylated. When Artemis is phosphorylated, it gains endonucleolytic activity, allowing it to trim the 5' overhangs, and shorten 3' overhangs (Ma et al, 2002). When single stranded overhangs are present, DNA synthesis must be performed in order to generate a blunt end that can be ligated. This type of DNA synthesis is performed by either Polymerase  $\mu$  or  $\lambda$ , which are members of the family X polymerases (Moon et al, 2007).

Stage 3) Ligation of the broken ends at the DSB via the DNA Ligase IV previously bound. XRCC4 stabilises DNA Ligase IV and results in its activation. XRCC4 is also responsible for the localisation of the complex to the site of the DSBs, via its recognition helix (Grawunder et al, 1997). DNA Ligase IV is responsible for filling in the gap caused by a DSB, as it is able to ligate DNA ends that have to potential of base pairing (Gu et al, 2007). The NHEJ complex is removed from the site of the DSB via ATM. Phosphorylated ATM causes a conformational change in DNA-PKcs, resulting in the dissociation of the kinase. It is unknown whether this step occurs before or after the completion of terminal ligation. RNF8, an E3 ubiquitin ligase removes the rest of the NHEJ complex via the polyubiquitination of Ku80 (Feng and Chen, 2012).

### **8.3 - Microhomology-mediated end joining**

Microhomology-mediated end joining (MMEJ), also known as alternative NHEJ, is a method of DSB repair that utilises a 5-25bp resection step. This resection step is somewhat similar to that of HRs, however a much smaller microhomologous region is utilised in MMEJ, as rad51 is not required to progress. MMEJ does not require KU70/80 as NHEJ does. The two microhomologous regions anneal to each other and create 3' flaps on either side of the DSB. The flaps are trimmed via the XPF-ERCC1 endonuclease complex, allowing DNA Ligase III/I to complete the sequence. During the trimming step of MMEJ, a significant portion of the original DNA sequence is removed, meaning that the process is error prone (Wang and Xu, 2017).

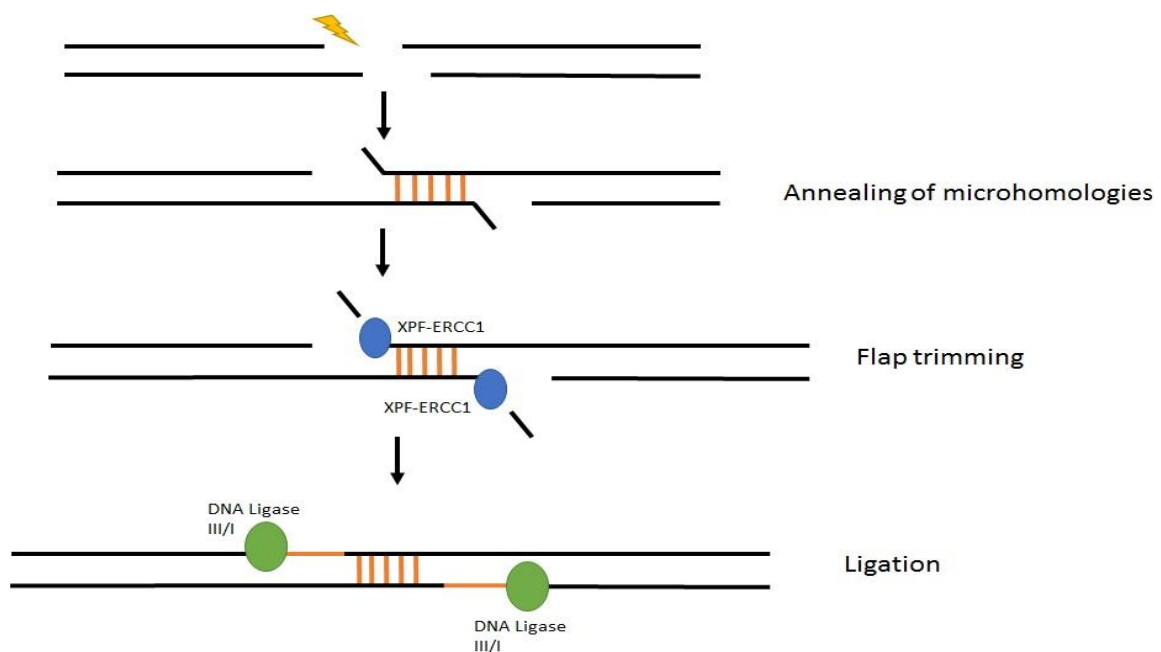


**Figure 1.9.4 – A simplified model of the mechanism for MMEJ**

*A microhomologous region (5-25bp) anneal close to site of the DSB, creating 3' flaps on either side. The flaps are trimmed via XPF/ERCC1 complex and DNA ligase III/I fills in the gaps.*

#### **8.4 – The significance of 53BP1**

53BP1, also known as 53-binding protein 1, is a key factor involved in the DDR, but its exact function and mechanism of action is not fully understood. 53BP1 is localised to sites of DNA damage following the cells exposure to ionising radiation, resulting in the formation of foci. These foci are thought to represents sites of DSBs (Schultz et al, 2000).

The recruitment of oligomerised 53BP1 is not fully understood, but it is thought to be mediated by the E3 ubiquitin ligase RNF8/RNF168 and the generation of  $\gamma$ H2AX via ATM.  $\gamma$ H2AX is recognised by mediator of DNA damage checkpoint protein 1 (MDC1). MDC1 is consistently being phosphorylated by casein kinase 2 (CK2), and causes a positive feedback loop, as more MRN is recruited to the DSB. MDC1 is also phosphorylated by chromatin bound ATM, which causes the recruitment of RNF8. This RNF8 ubiquitylates an unknown substrate, which is recognised by RNF168 (also a E3 ubiquitin ligase, and with the action of both RNF8 molecules and the E2 conjugating enzyme UBC13 form a cascade of ubiquitination that is able to regulate protein action at the site of DNA damage. The RNF8/RNF168/UBC13 complex causes ubiquitinated chromatin to surround the site of DNA damage. RNF168 is able to ubiquitylate H2A, forming the variants known as H2AK13ub and H2AK15ub (depending on the site of ubiquitination – Lys 13 or 15). The RNF8/RNF168/UBC13 complex causes this ubiquitinated chromatin to surround the site of DNA damage. UBC13 is also able to generate lysine-63 linked ubiquitin chains (Doil et al, 2009). A second function of the RNF8/RNF168 mediated chromatin ubiquitylation is the recruitment of oligomerised 53BP1. Di-methylation of Histone 4 lysine 20 (H4K20me<sub>2</sub>) is also important for the recruitment of 53BP1 at DSBs. When DSBs form, there is an increase in local methylation events, which is mediated by MMSET - a histone methyltransferase. A study demonstrated that MMSET downregulation decreases H4K20me<sub>2</sub>, resulting in the decrease of 53BP1 recruitment (Pei et al, 2011). MMSET recruitment is regulated by  $\gamma$ H2AX and MDC1. The recruited 53BP1 is able to bind the H2A variant H2AK15ub (Panier and Boulton, 2013).

The role 53BP1 plays in the DDR involves regulating the type of DNA repair mechanism that is carried out. In G1 cells, NHEJ is the major repair pathway performed due to the lack of sister chromatids, which are required for HR. HR uses a homologous sequence of DNA as a template to repair DNA, so cannot be carried during G1, but is the dominant pathway in G2 and S phase cells (Pandita and Richardson, 2009). 53BP1 promotes NHEJ as the dominant repair mechanism in G1 cells by preventing resection, which is one of the first steps required for HR repair (Bunting et al, 2010). This is achieved by inhibiting the BRCA1/CtIP function in the resection step of HR. As previously mentioned, these are both required for the initiation of resection, and their inhibition prevents HR and causes NHEJ to be upregulated. Inhibition of 53BP1 was shown to rescue cells that were depleted of BRCA1, and resulted in the progression of the resection event, providing evidence of the down regulation of HR via 53BP1 (Escribano-Diaz et al, 2013). RIF1 has also been found to interact with 53BP1, and plays a role in suppressing 5' end resection. It has been demonstrated that NHEJ is impaired in cells which lack RIF1 (Chapman et al, 2013). PTIP have been found to bind to 53BP1, specifically in response to IR and that the association of these two proteins is dependent on ATM. (Jowsey et al, 2004). PTIP is another protein which opposes resection, particularly in the G1 phase of the cell cycle (Feng et al, 2015).

There have been very few studies investigating UVA-induced 53BP1 function. There have been various studies that have used various genotoxic agents, including UV, however these studies often use broad wavelength UV (Rappold et al, 2001) or  $\gamma$ -rays (Anderson et al, 2001).

## **IX. Experimental aims**

UVB was thought to be the major carcinogenic aspect of solar ultraviolet radiation, and resulted in extensive research into the genotoxic effect of UVB. Recently, UVA was shown to play an equal, if not greater role in skin carcinogenesis. Due to this delay in recognition of UVAs genotoxic

capabilities, our understanding of it is lacking, and further research is required to be able to develop better treatments for skin cancer.

Previous studies have investigated DDR activation and DSB repair pathways, but have not used UVA as the source of DSBs. Reynolds et al (2012) utilised near-infrared microbeams as a way of generating DSBs, whilst other studies have used ionizing radiation or restriction enzymes (Mao et al, 2008; Stiff et al, 2004,). Although these studies are useful in investigating DSB-induced repair pathways, it cannot be assumed that the mechanism are the same with UVA-induced DSBs.

Previous experiments carried out in our laboratory (Steel, 2016) explored the effects of UVA on the DDR, and how inhibition of certain components of this pathway effect the activation of other components and repair mechanisms. One finding from Steel (2016) was that the ATM inhibitor KU-55933 caused a significant decrease in the accumulation of UVA-induced  $\gamma$ H2AX. Other inhibitors of ATM have been developed, including the more potent KU-60019, but had not been investigated in our laboratory. The effect of ATM inhibition on DDR components or DNA repair pathways had not been fully investigated in. Western blotting had been attempted to investigate UVA-induced PNKP phosphorylation, but have not been successful.

The data provided in previous experiments both within and outside our laboratory provided justification to developed aims to investigate the effect of UVA-induced DSBs, and how the DDR is activated as a result.

The first aim of these experiments was to investigate the effect of UVA on HaCaT cells, specifically its ability to cause DSBs. The second aim was to optimise the use of the ATMi inhibitor KU-60019, by testing various concentrations for their ability to disrupt various aspects of the DDR, as well as checking the presence of phosphorylated ATM. Once optimised, the effect of both UVA and the combination of KU-60019 and UVA on the activation of various components of the DDR was investigated. The main components of the DDR tested for the phosphorylated forms of CHK2, p53,

and PNKP, which indicate activation. We also looked at  $\gamma$ H2AX accumulation post UVA irradiation, as well as 53BP1 localisation.

## 2. Materials and Methods

### I. Media and Buffers

**Table 2.1**

<u>Buffer or media name</u>	<u>Components and supplier</u>
10x TBE	0.89 M Tris, 0.89 M Boric Acid, 0.02 M EDTA
10x TBST	10x TBS solution (Melford) – 0.5 M Tris, 1.5 M NaCl, 0.5% Tween20
10x TGS	0.25 M, 1.9 M Glycine, 1% SDS
RIPA Buffer	0.05 M Tris, 150 mM NaCl, 0.1% SDS, 0.12 M Sodium deoxycholate, 1% Triton X100 Supplemented with Roche Complete™ Mini, EDTA-free protease inhibitor cocktail tablets and Roche PhosSTOP phosphatase inhibitor cocktail tablets
PBS	0.14 M NaCl, 0.01 M NaPO <sub>4</sub> , buffer, 3 mM KCl

### II. Cell Culturing – HaCaT

HaCaT cells were grown in DMEM containing Phenol Red with 10% FCS, 100 $\mu$ g/ml of penicillin and 100 $\mu$ g/ml streptomycin. Cells were cultured in T75 flasks (NUNC) in a 37°C humidified incubator with

5% CO<sub>2</sub>. The HaCaT culture was split by removing the media and adding 10ml of PBS-EDTA (0.05%) (Gibco) to the flask and incubating at 37°C for 12 minutes. The PBS-EDTA was then removed and 2ml of Trypsin-EDTA (0.5M) was added to the flask for 15 – 25 s and then removed. The cells were then incubated at 37°C for approximately 5 minutes, or until the cells had visibly detached. The cells were then physically removed from the flask surface by pipetting 8ml of fresh media over the cells until all were in suspension. For cell maintenance, 1ml from the 8ml of media is added to a new T75 flask, and then 15 ml of fresh media added.

### **III. Treatment - UVA Irradiation**

Cells that were to be exposed to UVA had their media changed to phenol red free DMEN + L-glutamine and 10% FCS. Phenol red free media had to be used for UVA irradiation, as phenol red is known to absorb UV. The ability of Phenol red to absorb UV could influence the effect of UVA on the cells, generating unreliable results.

UVA irradiation was carried out using Pro-lite Plus 240 V 25 W UVA bulbs with a 70 W m<sup>-2</sup> output. A 25 minute incubation results in a dose of 100 KJ m<sup>-2</sup>. Any possible UVB output generated by the bulbs was mitigated by placing a Mylar sheet over the dishes during UV exposure. Cells were exposed for 25 minutes. The temperature of the cells was kept constant by a Grant RC 400 cooling system set to 25°C which was sufficient for maintaining 37°C during irradiation. This ensured temperature wasn't a factor contributing to changes in cells. Control cells were kept in the 37°C/5% CO<sub>2</sub> incubator.

Cell samples were processed immediately after irradiation (0 hour), or left to rest for either 1, 2 or 4 hours (specified) in the 37°C incubator.

### **ATM inhibition**

In previous experiments in the laboratory, the ATM inhibitor KU-55933 at 1  $\mu$ M had been used. In the experiments presented in this study, the ATM inhibitor KU-60019 has been used at a concentration of either 200 nM or 2  $\mu$ M.

#### **IV. Comet Assay**

$4 \times 10^5$  HaCaT cells in 4 ml of Phenol Red DMEM + 10% FCS + 1 mM L-glutamine were seeded into culture dishes containing two coverslips, and were incubated for one day at 37 °C and 5% CO<sub>2</sub>.

The Enzo Comet SCGE assay kit was used to generate comet assay data. 40 ml of Lysis solution and PBS was chilled at 4°C prior at least 20 minutes before use. The low melting point agarose was heated up in a beaker of hot water until molten, and then left to cool to 37°C in an incubator. Cells were treated, and then harvested at their appropriate time point by scraping the dish with the phenol red free media still present. The suspension was added to a 15 ml falcon tube and centrifuged at 500rpm for 5 minutes. Supernatant was carefully extracted, and the pellet then resuspended in 1 ml of PBS. The suspension was centrifuged again, and the supernatant removed. The pellet was then resuspended in 200  $\mu$ l of PBS and kept on ice.

200  $\mu$ l of 37°C low melting point agarose, and 20  $\mu$ l of the cell suspension was added to an Eppendorf tube and quickly mixed. 75  $\mu$ l of this mixture was pipetted onto a pre-treated comet assay slide. If the mixture did not cover the whole of the sample area, the pipette tip was used to spread the suspension evenly, before it was able to solidify. The slides were left to set for 10 minutes at 4°C. The slides were then immersed in the pre-chilled lysis solution for 1 hour at 4°C. The next steps depended on whether a neutral or alkaline comet assay was being performed.

### **Neutral Comet assay**

Slides were removed from the Lysis solution and immersed in 50 ml of 1x TBE buffer. The slide was then placed in a gel tank, equal distance from either electrode, and filled with 1x TBE buffer. The gel was run at a voltage equal to the distance between the electrodes in centimetres – 18 V for 10 minutes. The slide was removed; excess TBE was tapped off, rinsed with water and then submerged in 70% ethanol for 5 minutes. All slides were left to air-dry until the samples were completely flat.

### **Alkaline Comet Assay**

Slides were removed from the Lysis solution and immersed in 50 ml of freshly prepared alkaline solution (pH >13) for 1 hour, at room temperature in the dark. After this, the slides were then placed in a gel tank, equal distance from either electrode, and filled with 1x TBE buffer. The gel was run at a voltage equal to the distance between the electrodes in centimetres – 18 V for 10 minutes. The slide was removed; excess TBE was tapped off, rinsed with water and then submerged in 70% ethanol for 5 minutes. All slides were left to air-dry until the samples were completely flat.

### **Staining and visualisation**

CYGREEN® Nucleic Acid Dye (Enzo) stock was made up (999 µl water + 1 µl CYEGREEN DYE solution) and 100 µl was added to each sample area. The slides were left for 30 minutes in the dark at room temperature. The dye solution was the tapped off and the samples rinsed with water. The slides were left to dry at 37°C, until all moisture had evaporated. Samples were visualised using epifluorescence microscopy.

## V. Western Blotting Analysis

### Protein Isolation

2.5x10<sup>6</sup> HaCaT cells were seeded into 40 mm culture dishes, and incubated for one day at 37 °C and 5% CO<sub>2</sub>. Once dishes containing HaCaTs had been treated, the phenol red free media was removed, and then cells washed with 2 ml PBS. The PBS was removed and 50 µl of RIPA added. The dish was scraped and the cells and RIPA extracted into Eppendorf tubes. The extracts were centrifuged at 13000 rpm at 4°C for 10 minutes. The supernatant was transferred into a different Eppendorf tubes and the pellet discarded.

### Protein Concentration determination

A Bradford assay was performed to find the concentration of protein in each sample. Protein standards were made up using a stock 10 mg/ml BSA (Sigma Aldrich). A 1 mg/ml (1.0) standard was made using 90 µl of TE and 10 µl of stock BSA. A serial dilution was performed, removing 50 µl of 1.0, and adding it to 50 µl of TE for a 0.5 mg/ml (0.5). 50 µl of 0.5 was added to 50 µl of TE to create a 0.25 mg/ml standard. 10 µl of each standard was added to 1 ml cuvettes. 2.5 µl of sample and 7.5 µl of TE (pH – 7.4) was added to cuvettes. A blank was made using 10 µl of TE. 0.5 ml of Bradford reagent was added to all cuvettes and mixed. The absorbance was read using a spectrophotometer at 595 nm. The spectrophotometer was calibrated using the blank and then the absorbance of the standards and samples recorded. A standard curve was produced using the standards absorbance. The equation of the curve was used to calculate the protein concentration in each sample. The calculated protein concentration was used to work out the volume of each sample needed to make up 20 µg for western blotting analysis. The samples were made up to 10 µl and 5 µl of 3x SDS PAGE loading buffer added.

### **SDS PAGE Gel electrophoresis**

10 µl of sample were run on either a 10% gel or a 4-15% gradient gel (BioRad). The protein marker Precision Plus Protein Standard All Blue (BioRad), was loaded at a volume of 5 µl in lane 1. The gel was run for 35 minutes at 200 V, in 1x TGS buffer in the Mini-PROTEAN®Tetra Vertical Electrophoresis Cellsetup.

### **Gel transfer to membrane**

Proteins were transferred to Immobilon® PVDF Membrane. The membrane had to be hydrated in 100% methanol for 30 seconds, washed briefly in water, and then soaked in Pierce™ 1-Step Transfer Buffer for 2 minutes. 4 sheets of blotting filter paper were soaked in only transfer buffer for 5 minutes prior to transfer. The Thermo Scientific™ Pierce™ Power Blotter was used, with the setting varying depending on the size of the protein of interest.

### **Membrane Probing**

After the transfer was complete, membranes were briefly washed in 1x TBST for 2 minutes, and blocked in 5% Milk for 1 hour. Membranes were then probed with a primary antibody, with concentrations and incubation times specified in table 2.2. Actin was used as a load control.

After the secondary antibody incubation, the membrane was washed with TBST. To develop the membrane for imaging, a ThermoFisher Pierce™ ECL Plus Western Blotting Substrate was used. Substrate A and substrate B were mixed together at a ratio of 40:1 (2000µl:50µl), and then washed over the membrane for 5 minutes. Excess imaging solution was allowed to drip off the membrane and it was then placed in a BioRad Chemidoc XRS+ Imaging System. The exposure time was adjusted to generate images with optimum band intensity and background signal.

Table 2.2 - Antibodies and the conditions used for Western Blotting

Primary Antibody	Concentration and incubation conditions	Supplier	Secondary Antibody	Concentration and incubation conditions	Supplier
Anti-gamma H2AX Mouse monoclonal (Ser139)	1/2000 – 1 hour RTP	Abcam (ab111174)	Anti-mouse IgG, HRP-linked Antibody	1/4000 for 1 hour at RT	Cell Signal Technology® #7076
Anti-ATM (phospho S1981) antibody	1/1000 - Overnight at 4°C	Abcam (ab36810)	Anti-mouse IgG, HRP-linked Antibody	1/4000 for 1 hour at RT	Cell Signal Technology® #7076
Phospho-p53 (Ser15)	1/1000 - Overnight at 4°C	Cell Signal Technology® #9286	Anti-mouse IgG, HRP-linked Antibody	1/4000 for 1 hour at RT	Cell Signal Technology® #7076
Phospho-PNKP1 (Ser114/Thr118)	1/1000 - Overnight at 4°C	Cell Signal Technology® #3522	Anti-rabbit IgG, HRP-linked	1/4000 for 1 hour at RT	Cell Signal Technology® #7074
Phospho-CHK2 (Thr68)	1/1000 - Overnight at 4°C	Cell Signal Technology® #2661	Anti-rabbit IgG, HRP-linked	1/4000 for 1 hour at RT	Cell Signal Technology® #7074
Purified mouse anti-actin Ab-5 monoclonal antibody	1/2000 -1 hour at RT	BD Bioscience (612656)	Anti-rabbit IgG, HRP-linked	1/4000 for 1 hour at RT	Cell Signal Technology® #7074

## VI. Immunofluorescence

### Coverslip retrieval and processing

4x10<sup>5</sup> HaCaT cells in 4 ml of Phenol Red DMEM + 10% FCS + 1 mM L-glutamine were seeded into culture dishes containing two coverslips, and were incubated for one day at 37 °C and 5% CO<sub>2</sub>.

Post irradiation and rest time, coverslips were removed, washed briefly with PBS, and added to a 24 well dish. Each coverslip was fixed using 4% PFA at room temperature for 20 minutes. PFA was removed and 200  $\mu$ l of PBS was added to each coverslip, and stored at 4°C until further processing.

Coverslips were then permeabilised by adding 0.5 ml of 0.5% Triton X-100 for 20 minutes, and then washed for 5 minutes 3 times with 1 ml of PBS. Coverslips were then transferred to a Parafilm lined humidified chamber. 100  $\mu$ l of 3% BSA was added to each coverslip for 1 hour at room temperature to block the cells. The BSA was removed and coverslips washed 3x with PBS. Coverslips were then treated with primary and secondary antibodies, specified in table 2.3. Coverslips were washed 3x with PBS after each antibody treatment, and then mounted on slides using Vectashield containing DAPI (Vector Labs). Excess vectashield was wiped away and the slides sealed with nail varnish. Slides were stored at 4 °C in the dark until visualisation via confocal microscopy. Slides were visualised using Zeiss LSM 880 confocal microscope and Zen (Zeiss) software was used to generate images. When visualising, at least 100 nuclei was imaged per sample, and images were processed using imageJ.

**Table 2.3 – Antibodies and the conditions used for Immunofluorescence**

<b>Primary Antibody</b>	<b>Concentration and Incubation Conditions</b>	<b>Supplier</b>	<b>Secondary Antibody</b>	<b>Concentration and Incubation conditions</b>	<b>Supplier</b>
Anti-gamma H2AX Mouse monoclonal (Ser139)	1/4000 for 1 hour at RT	Abcam (ab111174)	Goat anti – mouse IgG (H+L), Alexa Fluor 488 conjugate	1/1000 for 1 hour at RT	Life Technologies (R37120)
53BP1 antibody	1/500 – Overnight at 4°C	GeneTex (GTX70310)	Goat anti Rabbit IgG (H+L), Alexa Flour 488 conjugate	1/1000 for 1 hour at RT	Life Technologies (R37116)

## **VII. EdU Assay**

Cells were pulse labelled with EdU 20 minutes prior to UV irradiation, by adding 4 µl of 10 µM EdU to dishes. EdU treated dishes were incubated at 37 °C and 5% CO<sub>2</sub>. After UVA irradiation, coverslips were removed from dishes, washed briefly in PBS, and placed in a 24 well dish. Each coverslip was washed twice in 3% BSA in PBS, and then permeabilised in 1 ml of 0.5% Triton X-100 for 20 minutes. The Triton was removed and the coverslips washed with 3% BSA in PBS twice, and transferred to a humidified chamber. The Click-iT® reaction cocktail was made up to a volume of 1ml, using Alexa Flour® Azide 555. 100 µl of the cocktail was added to each coverslip, and incubated in the dark for 20 minutes. The cocktail was removed, and the coverslips was 3x with 3% BSA in PBS and then 3x with PBS.

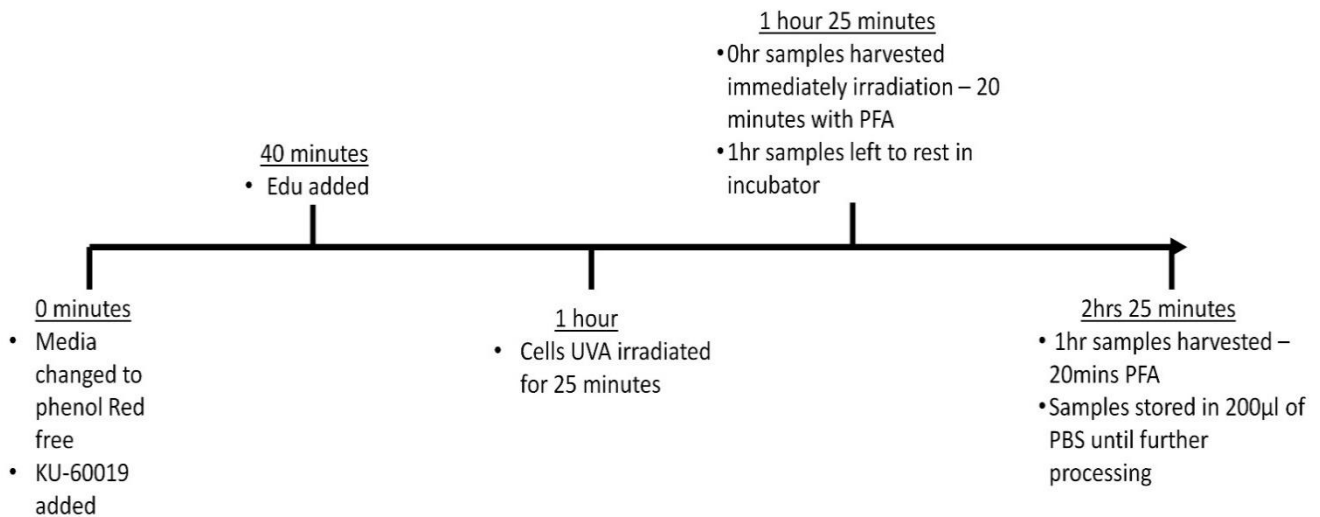


**Figure 2.1 – The timeline of key stages of Edu staining and immunofluorescence process**

*0 minutes - The experiment began when the growth media was removed and phenol red free DMEM added.*

*Appropriate samples were also treated with 2 µM of KU-60019 at this point. 40 minutes – The EdU component was added 20 minutes before UVA irradiation. 1 hour – appropriate samples were treated with 100 KJ/m<sup>2</sup> UVA for 25 minutes. 1 hour 25 minutes – samples that did not require rest (0 hour) were harvested at this point. 1 hour samples were left to rest in a 37°C/5% CO<sub>2</sub> incubator. 2 hours 25 minutes – 1 hour rest samples were harvested at this point.*

The coverslips were then incubated with 3% BSA in PBS for 1 hour at RT, then washed 3x in PBS, and incubated with the either γH2AX or 53BP1 primary antibodies. The concentrations and conditions for the primary antibodies were the same as those used in the immunofluorescence (table 1.2), and the secondary for γH2AX samples was the same. The 53BP1 treated coverslips required a rabbit secondary with Alexa Flour 468, as to avoid the EdU fluorescence overlapping with the 53BP1 signal. Coverslips were incubated for the secondary antibodies for 1 hour, and then washed with PBS, then mounted onto slides with DAPI Vectashield. Excess Vectashield was wiped away and the coverslips were sealed with nail varnish.

### 3. Results

The sun is the main source of ultraviolet radiation that humans are exposed to. Ultraviolet radiation is comprised of three different wavelengths, UVA, UVB and UVC. UVC has little clinical relevance as it is completely absorbed by the atmosphere. 95% of ultraviolet radiation that reaches Earth's surface is UVA, with the remaining 5% being UVB. UVA and UVB have both been shown to cause genotoxic stress in skin cells, and play a major role in the development of skin cancer. The mechanism in which UVA and UVB cause DNA damage varies, due to their different energy levels and ability to penetrate the skin. UVB can be absorbed directly by DNA leading to dipyrimidine dimers. The mechanism in which UVA causes DNA damage is not fully understood. One model for UVA induced DNA damage requires endogenous cellular photosensitiser excitation, leading to the generation of ROS and oxidative damage. Both UVA and UVB induced damage results in the activation of the DNA damage response, which is responsible for detecting the damage, triggering a signal cascade that leads to cellular responses such as cell cycle arrest, apoptosis and DNA repair.

UVB was thought to be the major factor in skin carcinogenesis, resulting in extensive research. Until recently, UVA was not thought to be carcinogenic, which meant there was little research carried out investigating UVAs genotoxic ability. This research project aims to investigate the effect of UVA on DNA, and how the DNA damage response is activated and sustained post UVA irradiation.

#### **Inhibition of ATM**

The accumulation of  $\gamma$ H2AX is one of the most commonly used biomarker of DNA damage currently used. It is widely accepted that ATM is one of the main kinases responsible for the phosphorylation of H2AX, while it is unknown how much DNA-PKcs and ATR contribute to  $\gamma$ H2AX generation in response to UVA irradiation.

Previous experiments in our laboratory has shown that the use of the ATM inhibitor KU-55933 (Selleckchem) completely prevents the generation of  $\gamma$ H2AX (figure 3.1). The ATM inhibitor KU-

55933 has an IC<sub>50</sub> of 12.9 nM for ATM. In these previous experiments, the working concentration of KU-55933 used was 1 μM, which is below the stated IC<sub>50</sub> of other pathways, such as DNA-PK (2.5 μM), but much higher than that of the intended target. The results of these experiments suggested to us that ATM is solely responsible for the generation of γH2AX in UVA irradiated cells. IC<sub>50</sub> values were determined in cell free assays.

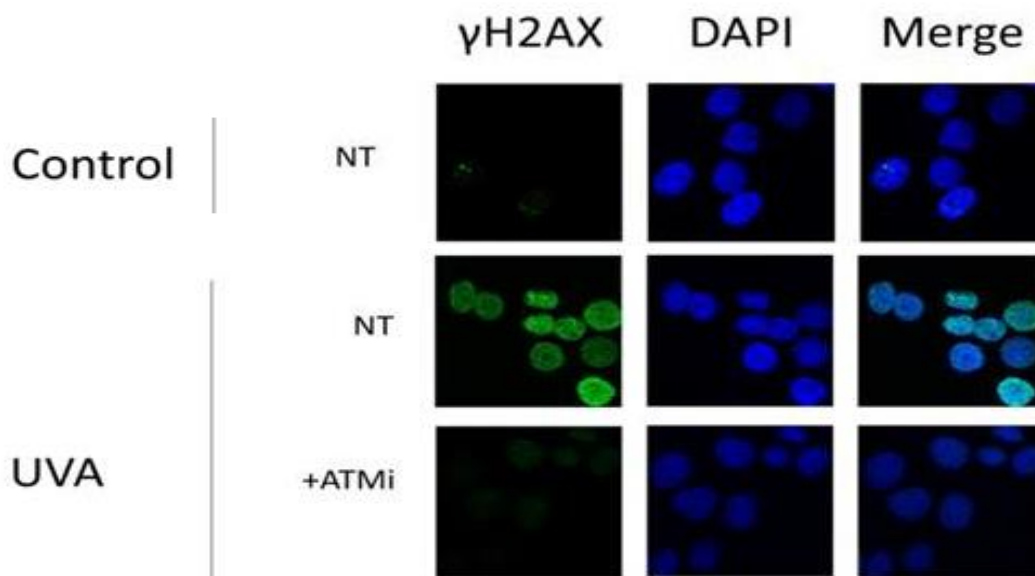


**Figure 3.1 – The ATM inhibitor KU-55933 abrogates the γH2AX response of UVA (Steel, 2016)**

*Samples were harvested 1 hour post UVA irradiation. HaCaT cells that were treated with only UVA show a high amount of γH2AX fluorescence compared to untreated cells. Cells that were treated with UVA and KU55933 show almost no γH2AX.*

Given the results of these previous experiments, the aim of the experiments presented in this report was to further investigate the effect of UVA on HaCaT cells, as well as test the ATM inhibitor KU-60019. According to the information provided by selleckchem, KU-60019 is a much more potent ATM inhibitor than KU-55933, with an IC<sub>50</sub> of 6.3 nM for ATM. Golding and colleagues reported that KU-60019 was three to ten times more effective than KU-55933 at preventing the phosphorylation of targets of ATM post ionising irradiation (Golding et al, 2009). The IC<sub>50</sub> for DNA-PKcs and ATR is 1.7 μM and >10 μM respectively (Golding et al, 2009).

It is important to remember that while autophosphorylation is an important step in the activation of ATM, historical evidence shows that mutant ATM with no kinase activity is still able to autophosphorylate (Barone et al, 2009). This means that it cannot be concluded with complete certainty that the phosphorylation of ATM is representative of its activation.

### **I. UVA induces double strand breaks in HaCaT cells, but is repaired quickly**

When DNA damage is detected, the DDR is activated, leading to key processes such as cell cycle arrest and DNA repair. Cell cycle arrest is important as it prevents DNA damage being replicated and persisting in the genome. Arrest also allows time for DNA repair before the cell transitions to the next phase of the cell cycle. By detecting the presence of DSBs in cells immediately after UVA exposure allows us to confirm the genotoxic ability of UVA. By allowing a period of time (1hr) after irradiation, we can investigate the speed in which potential damage can be repaired.

Comet Assays, also known as Single Cell Gel Electrophoresis Assay (SCGE), are a sensitive technique used to detect the presence of DNA damage in individual cells. The purpose of performing the comet assay was to confirm that UVA radiation causes DNA damage, and investigate the time parameters in which this damage is repaired. There are a variety of different comet assay types that can be used to show different forms of DNA damage. An alkaline comet assay can be used to detect a wide range of DNA damage types, such as ssDNA breaks, DSBs and apurinic/apyrimidinic sites, as the use of a high pH solution causes the DNA helix to denature and unravel to become single stranded. A neutral comet assay can be used to visualise mainly DSBs, making it ideal for the investigation in the ability of UVA to cause DSBs.

The presence of comet tails indicates the accumulation of DNA damage, only damaged DNA is small enough to be pulled out the nucleoid cavity towards the anode during electrophoresis. A comet

assays was chosen as the technique to visualise DNA damage, due to the methods high sensitivity, and its simple visualisation of DNA damage.

Although the main aim of this experiment is to investigate the ability of UVA to form DSBs, an alkaline comet assay was performed first, to optimise the technique and ensure UVA lamp output was not compromised, and was suitable for further use.

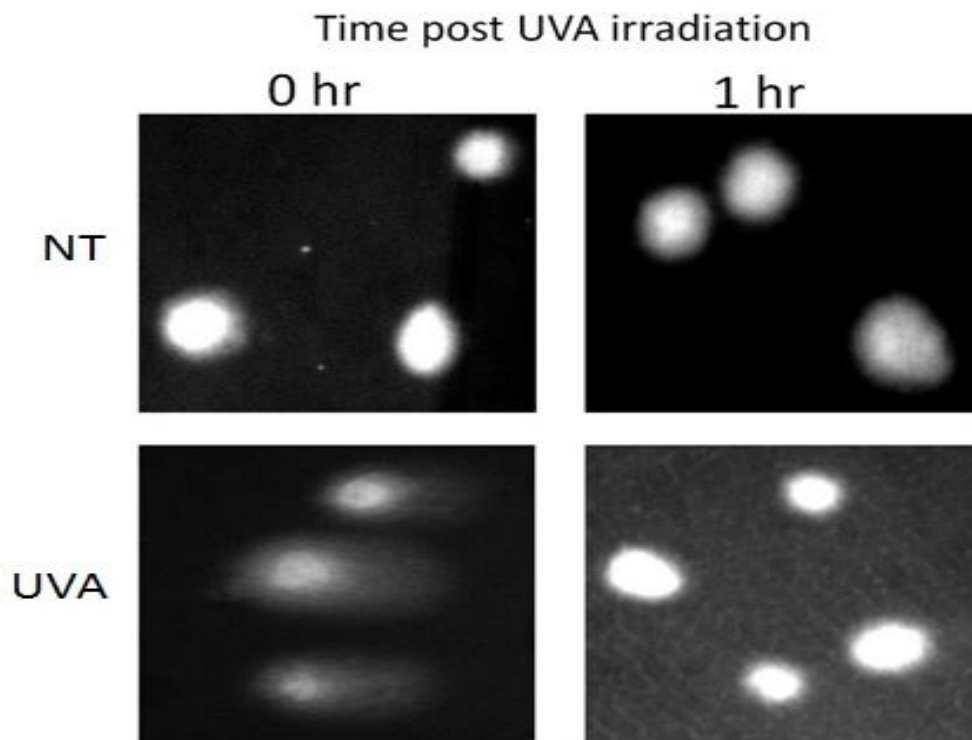


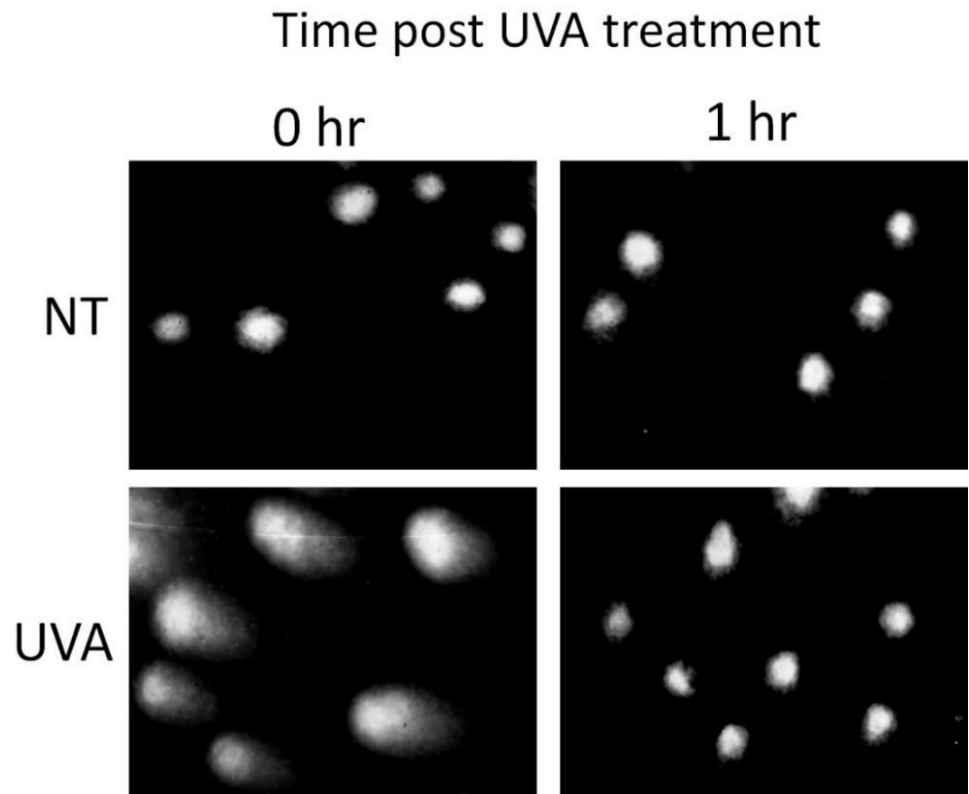
**Figure 3.2.1 – Alkaline comet assay of UVA treated HaCaT cells**

*HaCaT cells were seeded into dishes and allowed to adhere. UVA treated HaCaT cells were irradiated with  $100 \text{ KJ m}^{-2}$  UVA for 25 minutes, and either harvested immediately (0 hour) or allowed to rest for 1 hour in a  $37^\circ\text{C}/5\% \text{ CO}_2$  incubator. During processing, after cells had been lysed they were incubated in a  $\text{pH} > 13$  alkaline solution for 1 hour. The data shown are representative of three individual experiments.*

The presence of DNA damage is indicated with the generation of comet tails, which appear as smudge like residues from cell nuclei. It was expected that untreated cells would not result in the formation of DNA damage, and that UVA treated cells would display DNA damage. However, we

were unsure what amount of DNA damage would be present after 1 hour of rest. Figure 3.2.1 shows that our predictions were largely correct, with untreated cells showing no DNA damage. UVA treated cells immediately harvested post irradiation (0 hour) showed large comet tails, indicating the presence of DNA damage. However, only 1 hour post UVA irradiation, many of the comet tails were not present and no DNA damage was present, suggesting that DNA damage was repaired quickly. As this was an alkaline comet assay, we cannot assume that the damage caused by UVA is DSBs. To check for only DSBs, a neutral comet assay was performed.

A



B

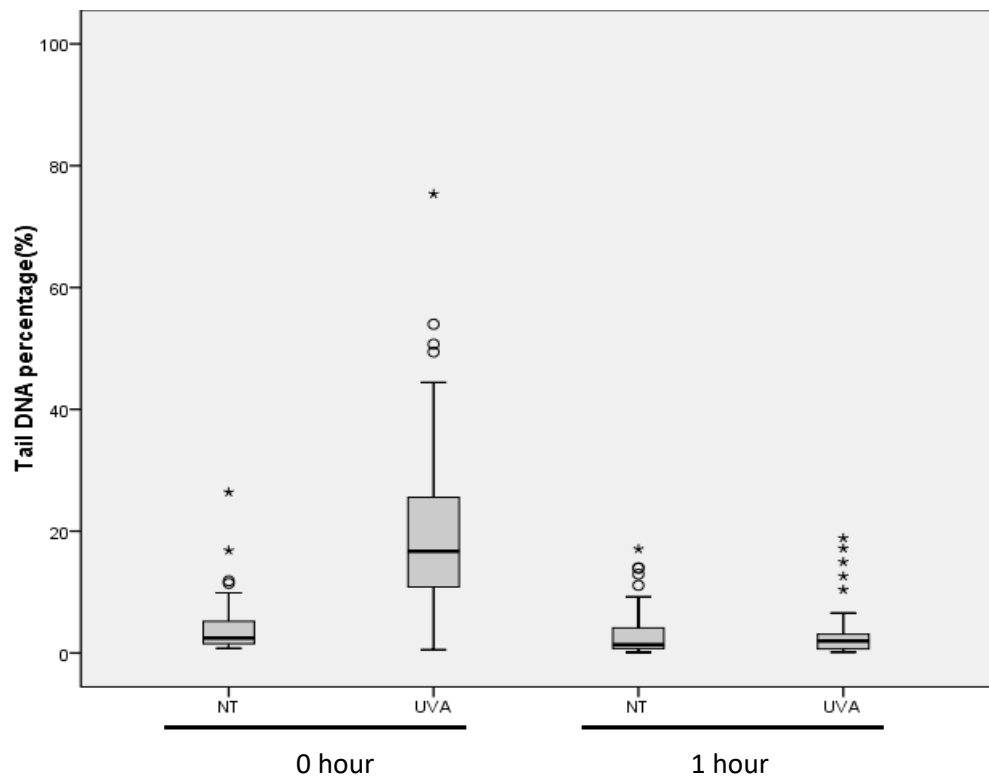


### Figure 3.2.2 – Neutral comet assay of UVA treated HaCaT cells

*UVA treated HaCaT cells were irradiated with 100 KJ m<sup>-2</sup> UVA for 25 minutes. 0 hr cells were harvested immediately after UVA treatment. 1 hr cell samples were left to rest for 1 hr after UVA treatment in a 37°C/5% CO<sub>2</sub> incubator, and then harvested. Unlike the alkaline comet assay, the samples are not incubated in an alkaline solution during processing. Instead, electrophoresis is carried out immediately after the lysis solution incubation stage.*

- A) Representative epifluorescence images of comet assays*
- B) Comet assay images were analysed using imageJ and the plugin OpenComet. The tail DNA percentage was determined and plotted in a box plot, indicating the median and the range of data. The median and the interquartile ranges are represented by the boxplot, while the whiskers show the 95% percentiles. NT = No treatment/ UV = UVA treated. The number indicates how long the samples were rested for – 0 = 0 hours, 1 = 1 hour. Circles above the plots represent outliers while the stars represent extreme outliers. The data shown is of the only repeat of this experiment.*

The neutral comet assay showed similar results to that of the alkaline comet assay, indicating that UVA is effective at generating DSBs. Untreated cells had an average of 4.25% ( $\pm 4.25$ ) and 3.20% ( $\pm 4.31$ ) (NT0 and NT 1 respectively). 0 hour UVA treated cells saw a significant increase in tail DNA percentage ( $p < 0.001$ ), showing an average tail DNA percentage of 21.5% ( $\pm 14.90$ ). When cells were rested for 1 hour post UVA irradiation, there was no significant difference between them and untreated cells ( $p = 0.751$ ), showing an average of 3% ( $\pm 4.0$ ).

Figures 3.2.1 and 3.2.2 suggest that DNA damage that is present immediately post UVA irradiation (0 hours), is rapidly repaired after 1 hour. From this experiment, it was decided that other techniques should be performed to visualise the presence of DNA damage, but also investigate the activation of the DNA damage response. It is worth noting that more repeats are required for these comet assays, to be able to make accurate and confident conclusions.

## **II. Inhibition of ATM via 200 nM KU-60019 alters the phosphorylation of H2AX and other components of the DDR post UVA irradiation**

After investigating the ability for UVA to generate DSBs, we went to look at how the DDR is activated after UVA irradiation, and how inhibition of the apical kinase ATM may alter the pathway. Western blotting was chosen as one of the techniques to demonstrate this. HaCaT cells were pre-treated with 200 nM of KU-60019 for 1 hour prior to UVA irradiation.

CHK2 is a one of the main targets of ATM kinase activity, and is a key downstream kinase in the DDR, responsible for the phosphorylation of various other effector proteins of the DDR including p53. p53 is arguably one of the most important proteins in the prevention of tumourgenesis of almost any cancer type, and is one of the main effector proteins of the DDR, making its phosphorylated form an ideal candidate for this investigation. PNKP is both a kinase and a phosphatase, and plays a key role during NHEJ, where it trims molecules that cannot be ligated from the end of DNA, allowing for Artmeis to bind and DNA repair continue. Mutations in PNKP can result in defective DNA repair, and cause cells to be sensitive to radiation (Shen et al, 2010). We believed PNKP to be a suitable protein to investigate during these experiments, as it plays an important role in DNA repair, and the overall success of the DDR.

Western blotting is a very useful method of showing the presence of a protein in cell extracts.

Phosphorylation of CHK2, p53 and PNKP is a key event in their respective pathway and is required for their engagement and interactions with other components, and are suitable biomarkers of their activation.  $\gamma$ H2AX is a well-established indicator of DNA damage as it is generated by various components of the DDR, including ATM and DNA-PK.  $\gamma$ H2AX (Ser139) was ideal as the indicator of DNA damage in western blotting.

KU-60019 is a potent inhibitor of ATM, with an  $IC_{50}$  of 6.3 nM. It is much more specific than the previous ATM inhibitor used in our laboratory - KU-55933, which has an  $IC_{50}$  of 12.9 nM for ATM.

200 nM was chosen as the initial working concentration for KU-60019, as it is much higher than the reported IC<sub>50</sub> for ATM, but is much lower than the IC<sub>50</sub> of other potential targets, such as DNA-PKcs and ATR, with IC<sub>50</sub> values of 1.7 μM and >10 μM respectively.

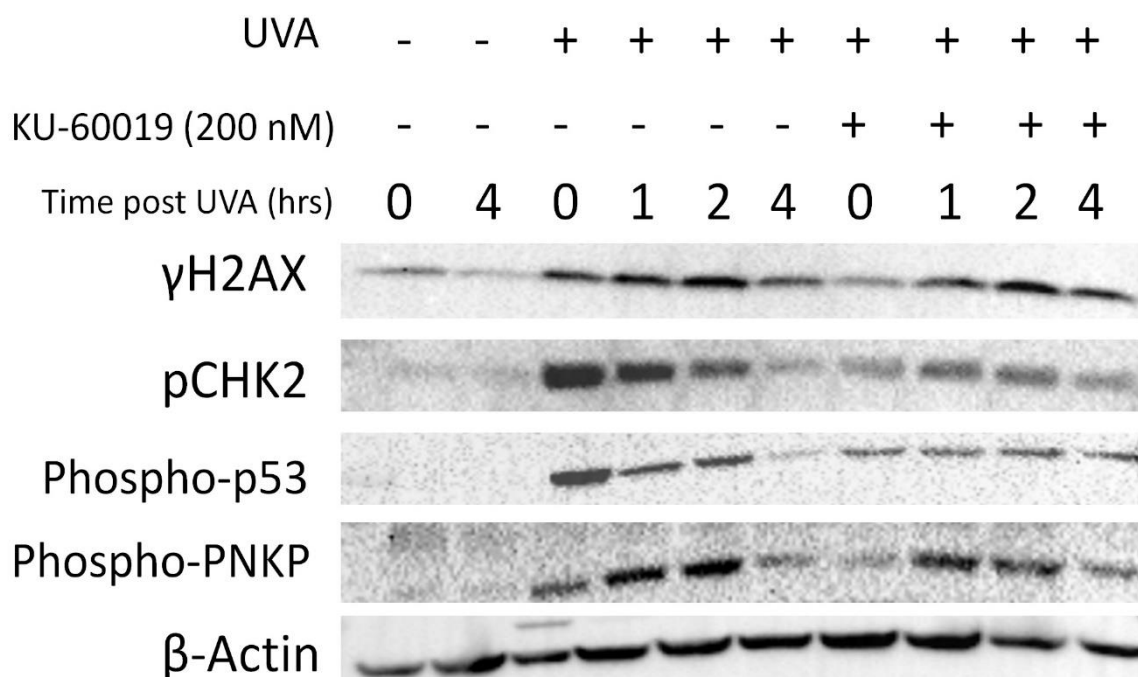


**Figure 3.3.1 – Western blotting detection of various components of the DDR when treated with the ATM inhibitor KU-60019 at 200 nM**

HaCaT cells were pre-treated with 200 nM of KU-60019 for 1hr before irradiation with 100 KJ m<sup>-2</sup> UVA for 25 minutes. Samples were then used to make cell extracts either immediately post irradiation (0 hr) or after rest (in a 37°C/5% CO<sub>2</sub> incubator) for the indicated amount of time. When harvested, the cells were washed with PBS, and then extracted using RIPA buffer containing protease and phosphatase inhibitors. Protein concentrations were determined using a Bradford assay. Samples were loaded in a 4-15% gradient TGX gel. Each component was probed for via western blotting. β-Actin was used as a load control. The data shown is representative of three individual experiments.

It was expected that KU-60019 would have a sizable effect on the accumulation of γH2AX, as previous studies in our laboratory showed that a less specific inhibitor (KU-55933) could almost completely prevent the formation of γH2AX (figure 3.1). However, figure 3.2.1 shows that the use of 200 nM KU-60019 only caused a delay in the accumulation of γH2AX post UVA irradiation. Cells only

treated with UVA showed a large amount of  $\gamma$ H2AX immediately post irradiation (0 hr), with the intensity peaking at 2 hrs post UVA exposure. When treated with both KU-60019 and UVA, the  $\gamma$ H2AX accumulation was lower immediately post irradiation compared to non ATMi pre-treated cells. However, the intensity of  $\gamma$ H2AX increased to a similar level after only 1hr post irradiation, and peaking again at 2 hrs.

The activation of CHK2 (pCHK2) in UVA treated cells peaks immediately post irradiation (0 hr), and decreases in intensity over the course of the next 4 hours. The intensity of CHK2 activation at 4 hours is almost at the same level as the untreated control cells. When treated with both KU-60019 and UVA, CHK2 activation does not reach the same level as uninhibited cells. There is a peak at 1-2 hours, but the intensity of said peak is much less than that of only UVA treated cells, and does not vary much across the 4 hours.

Phospho-p53 activation shows a similar pattern to that of pCHK2, in cells that are treated with UVA only and those that are treated with both UVA and KU-60019. A peak at 0 hours in UVA treated cells, with a gradual decrease over the next 4 hours can be seen, while ATMi and UVA treated cells have a small amount of activation which remains consistent over the 4 hours.

The accumulation of phospho-PNKP is similar to the pattern seen with  $\gamma$ H2AX than pCHK2/phospho-p53. In UVA treated cells, the response gradually increases, peaking at 2 hours post irradiation and decreasing to almost control levels at 4 hours. When treated with KU-60019, there is a large decrease in the initial phosphorylation of PNKP, but between 1 – 2 hours post UVA irradiation, the intensity increased to a similar level as uninhibited cells.

To go alongside the western blotting data, we also utilised immunofluorescence to show the effect of UVA and KU-60019 on HaCaT cells and the accumulation of  $\gamma$ H2AX. Using a secondary antibody with Alexa Fluor 488, we measured the intensity UVA-induced  $\gamma$ H2AX fluorescence in a minimum of 100 cells immediately after irradiation (0 hr) and 1 hour post exposure. We also included KU-60019 treated samples, to gain a more visual representation of the effect of ATM inhibition on  $\gamma$ H2AX

accumulation, and to be able to compare the effect with previous work in the laboratory using the KU-55933 ATM inhibitor.

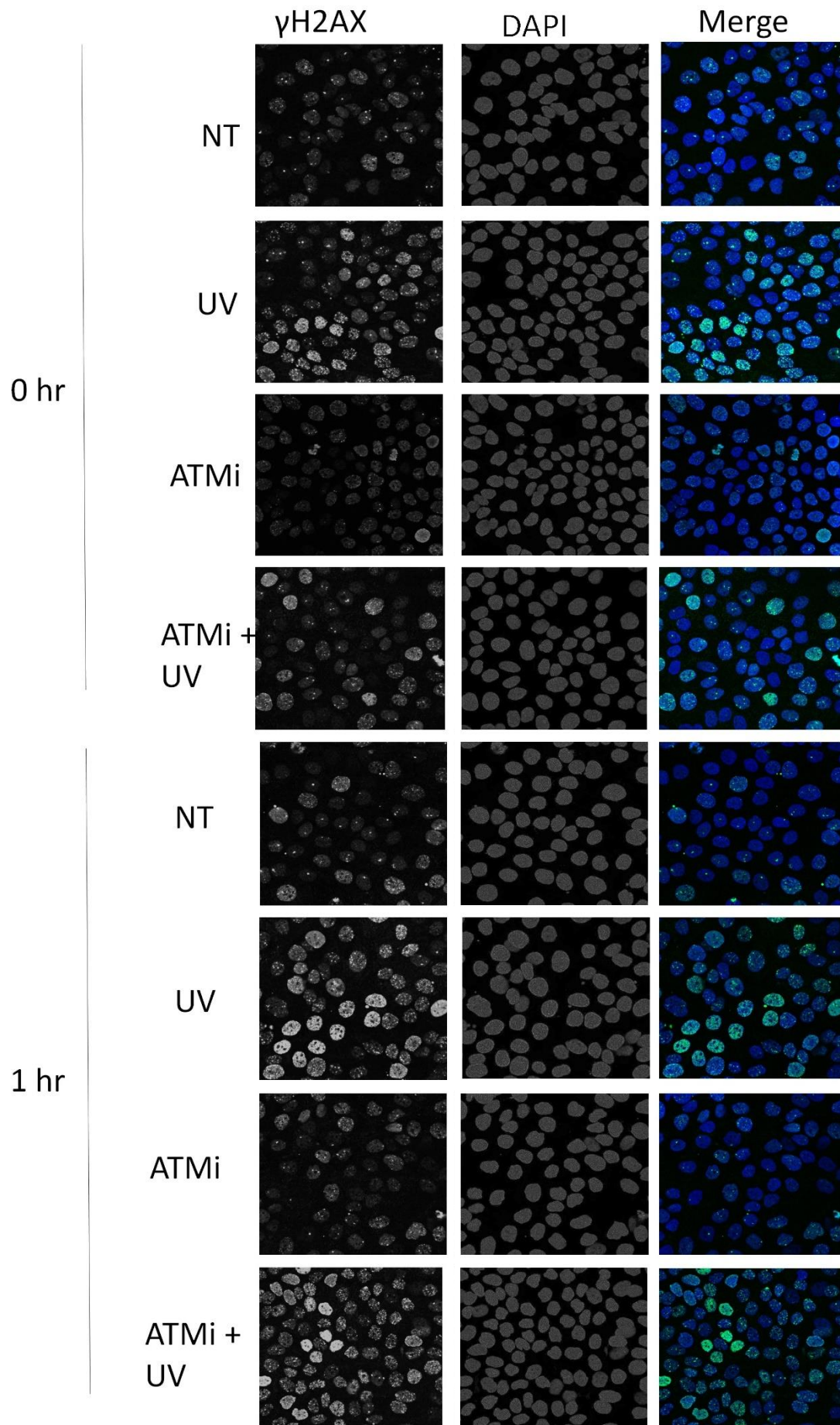


**Figure 3.3.2 – Immunofluorescence detection of  $\gamma$ H2AX after UVA irradiation and the addition of the ATM inhibitor KU-60019**

HaCaT cells were seeded onto coverslips and allowed to adhere overnight. Cells were pre-incubated with 200 nM KU-60019 for 1 hour, then irradiated with 100 KJ m<sup>-2</sup> UVA for 25 minutes. Cells were fixed either immediately after irradiation (0 hr) or after 1 hr rest in a 37°C/5% CO<sub>2</sub> incubator. Cells were stained with a  $\gamma$ H2AX primary antibody, and then stained with an AlexaFluor 488-labelled secondary antibody. Coverslips were mounted onto a slide using DAPI containing mounting medium. Cells were visualised using confocal microscopy and ZEN software. Representative confocal images of immunofluorescence showing  $\gamma$ H2AX, DAPI and a merge of the two. The data shown is representative of three individual experiments.

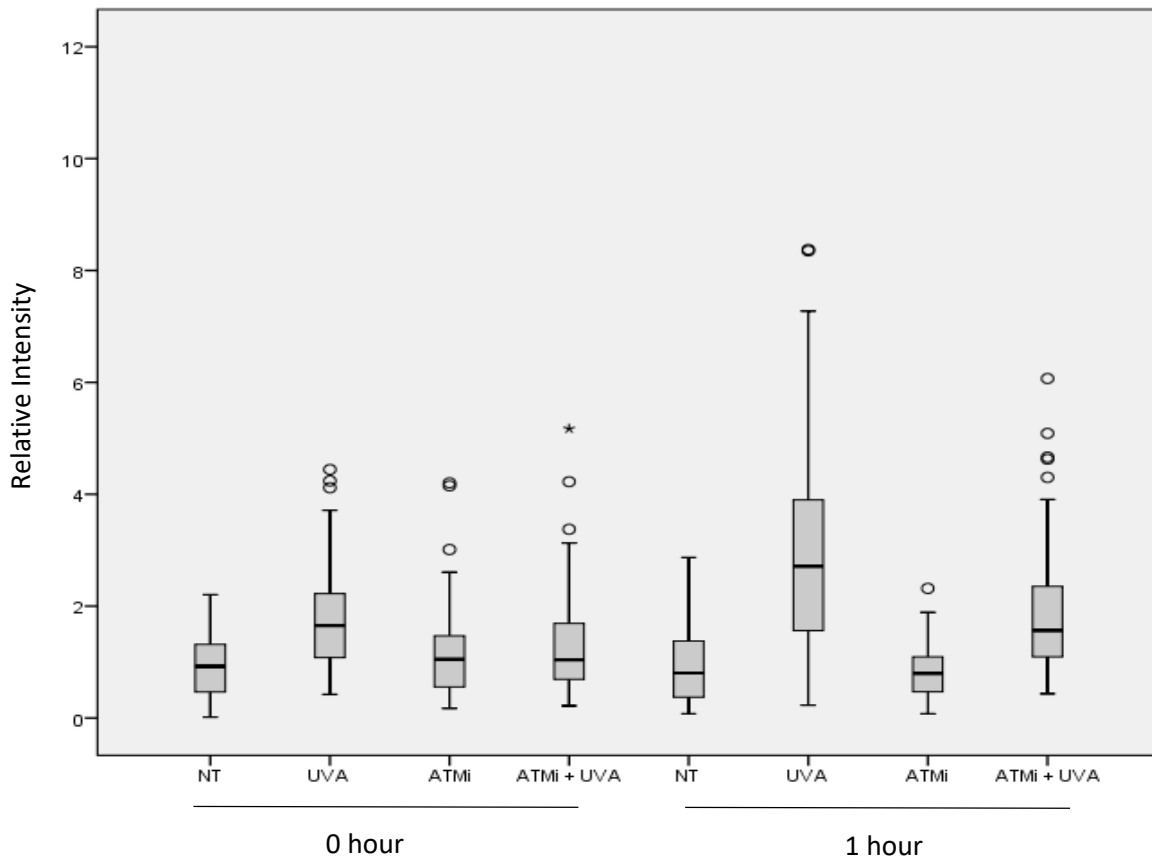


**Figure 3.3.3 – Quantification of immunofluorescence images**

The relative intensity of the immunofluorescence was quantified using ImageJ software. The intensity quantities were normalised to the respective control group (NT). A box plot was created, indicating the median and the range of data. The median and the interquartile ranges are represented by the boxplot, while the whiskers show the 95% percentiles. NT = No treatment / UV = Ultraviolet light / ATMi = KU-60019. Circles above the plots represent outliers while the stars represent extreme outliers. The data shown represents the mean relative intensity from three individual experiments.

$\gamma$ H2AX accumulation seen in immunofluorescence (figures 3.3.2 and 3.3.3) follows a trend similar to that seen in the western blotting analysis (figure 3.3.1). Irradiated only Cells showed a significantly increased level of UVA-induced  $\gamma$ H2AX fluorescence at 0 hour compared to the control ( $p < 0.001$ ). There was a further increase in fluorescence 1 hour post irradiation compared to the 0 hour value

( $p = <0.001$ ) which increased when left to rest for 1 hour post irradiation, as seen with the increase in brightness as seen in figure 3.3.2. When cells were treated with both 200 nM of KU-60019 and UVA, there is a significant increase in  $\gamma$ H2AX fluorescence, compared to ATMi only treated cells at both 0 and 1 hour time points ( $p=0.01$  and  $p= <0.001$  respectively). There was no significant difference between control cells and KU-60019 treated cells ( $p=0.760$ ).

When a combination of both UVA and KU-60019 is used, there is a slight yet significant increase in the  $\gamma$ H2AX fluorescence compared to the untreated samples ( $p=<0.001$ ) and KU-60019 only treated cells ( $p=0.01$ ). When UVA and KU-60019 treated cells are rested for 1 hour post irradiation, there is a much larger increase in fluorescence compared to untreated cells ( $p=<0.001$ ).

### **III. 200 nM KU-60019 is not enough to fully inhibit ATM phosphorylation**

After investigating the effect of 200 nM of KU-60019 on other components of DDR, we looked if ATM itself is being fully inhibited. A concentration of 200 nM is around 30 fold higher than the  $IC_{50}$  for ATM (6.3 nM), but it was believed to be worth investigating as the results were somewhat different that when the ATM inhibitor KU-55933 was used in previous experiments. Western blotting was chosen to as the appropriate technique to check for ATM inhibition, and phospho-ATM (pATM) was probed for. Due to the size of the pATM (350 kDa), the transfer step of western blotting procedure was increased, to ensure the protein was efficiently transferred to the membrane.

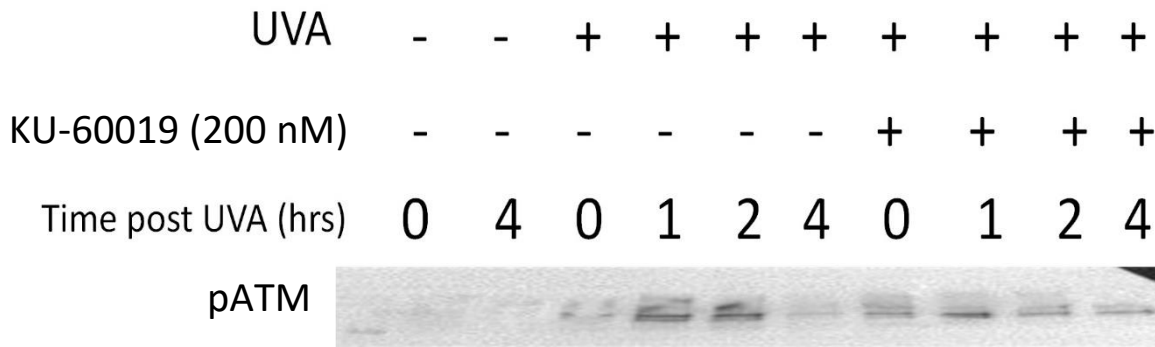


**Figure 3.4 – Western Blotting of phospho-ATM when HaCaTs treated with either UVA or UVA and 200 nM KU-60019**

HaCaT cells were pre-treated with 200 nM of KU-60019 for 1hr before irradiation with 100 KJ m<sup>-2</sup> UVA for 25 minutes. Samples were then used to make cell extracts either immediately post irradiation (0 hr) or after rest (in a 37°C/5% CO<sub>2</sub> incubator) for the indicated amount of time. When harvested, the cells were washed with PBS, and then extracted using RIPA buffer containing protease and phosphatase inhibitors. Protein concentrations were determined using a Bradford assay. Samples were loaded in a 4-15% gradient TGX gel. Transfer was ran for slightly longer than previous western blotting, to account for the size of pATM. No actin control was run for these samples. The data shown is representative of a single experiment.

Figure 3.4 shows that when treated with only UVA, the accumulation of pATM follows a similar pattern as  $\gamma$ H2AX and phospho-PNKP (figure 3.3.1). The intensity of pATM increase immediately following UVA irradiation, peaking at 2 hours, then decreases rapidly between 2 and 4 hours. When treated with both UVA and 200 nM of KU-60019, we expected to see little ATM phosphorylation, particularly immediately after irradiation. However, figure 3.4 shows the pattern to be somewhat similar to that of uninhibited cells, with a clear accumulation of pATM at 0 hours and increasing at 1 hour.

Due to ATM still being phosphorylated with the addition of 200 nM KU-60019, we decided to increase the concentration of the inhibitor to 1.83  $\mu$ M, to attempt to fully inhibit ATM phosphorylation.

**IV. 2  $\mu$ M KU-60019 is enough to inhibit the immediate phosphorylation of ATM following UVA irradiation**

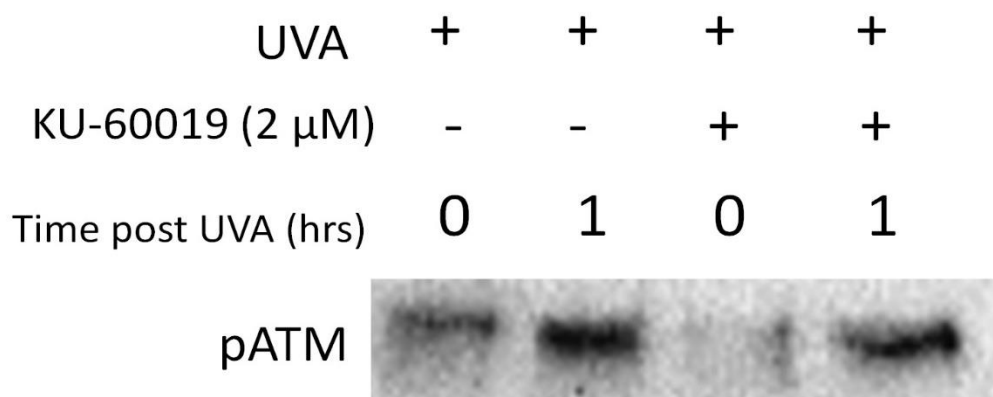


**Figure 3.5 – Western blotting of pATM in HaCaTs treated with UVA or UVA and 2  $\mu$ M of KU-60019**

*HaCaT cells were pre-treated with 2  $\mu$ M of KU-60019 for 1hr before irradiated with 100 KJ m<sup>-2</sup> UVA for 25 minutes. Samples were then used to make cell extracts either immediately post irradiation (0 hr) or after rest (in a 37°C/5% CO<sub>2</sub> incubator) for the indicated amount of time. When harvested, the cells were washed with PBS, and then extracted using RIPA buffer containing protease and phosphatase inhibitors. Protein concentrations were determined using a Bradford assay. Samples were loaded in a 4-15% gradient TGX gel. Transfer was ran for slightly longer than previous western blotting, to account for the size of pATM. No actin control was run for these samples. The data shown is representative of a single experiment*

Increasing the concentration of KU-60019 to 2  $\mu$ M resulted in the abrogation of pATM accumulation immediately post UVA treatment, but the effect did not persist for longer than 1 hour (figure 3.5).

We were satisfied with using 2  $\mu$ M KU-60019 to inhibit the early phase of the ATM phosphorylation post UVA irradiation. We decided to then investigate the effect of 2  $\mu$ M KU-60019 on the same components of the DDR as seen in figure 3.3.1.

## V. ATM inhibition with 2 $\mu$ M KU-60019 reduces the intensity of $\gamma$ H2AX formation and DDR activation

By increasing the concentration of KU-60019, we were expecting to see a more adverse effect on various components of the DDR, particularly in the 0 to 1 hour time points, due to a lack of ATM activity in the early stages post UVA exposure, as demonstrated in figure 3.5

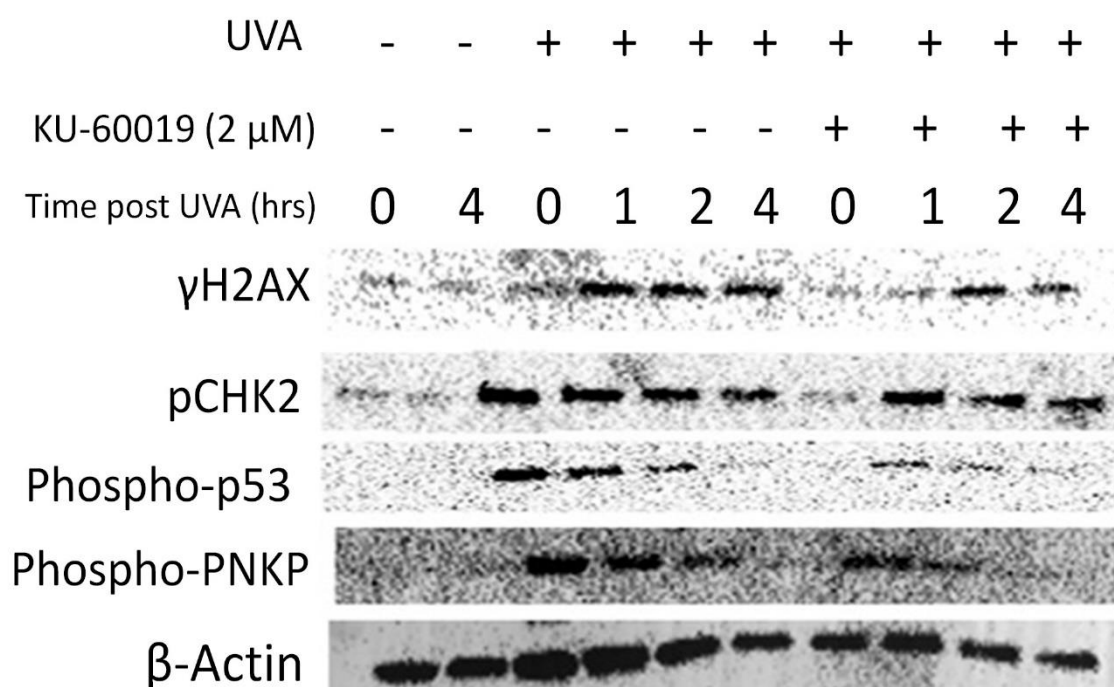


**Figure 3.6.1 – Western blotting detection of various components of the DDR when treated with UVA or UVA and 2  $\mu$ M KU-60019**

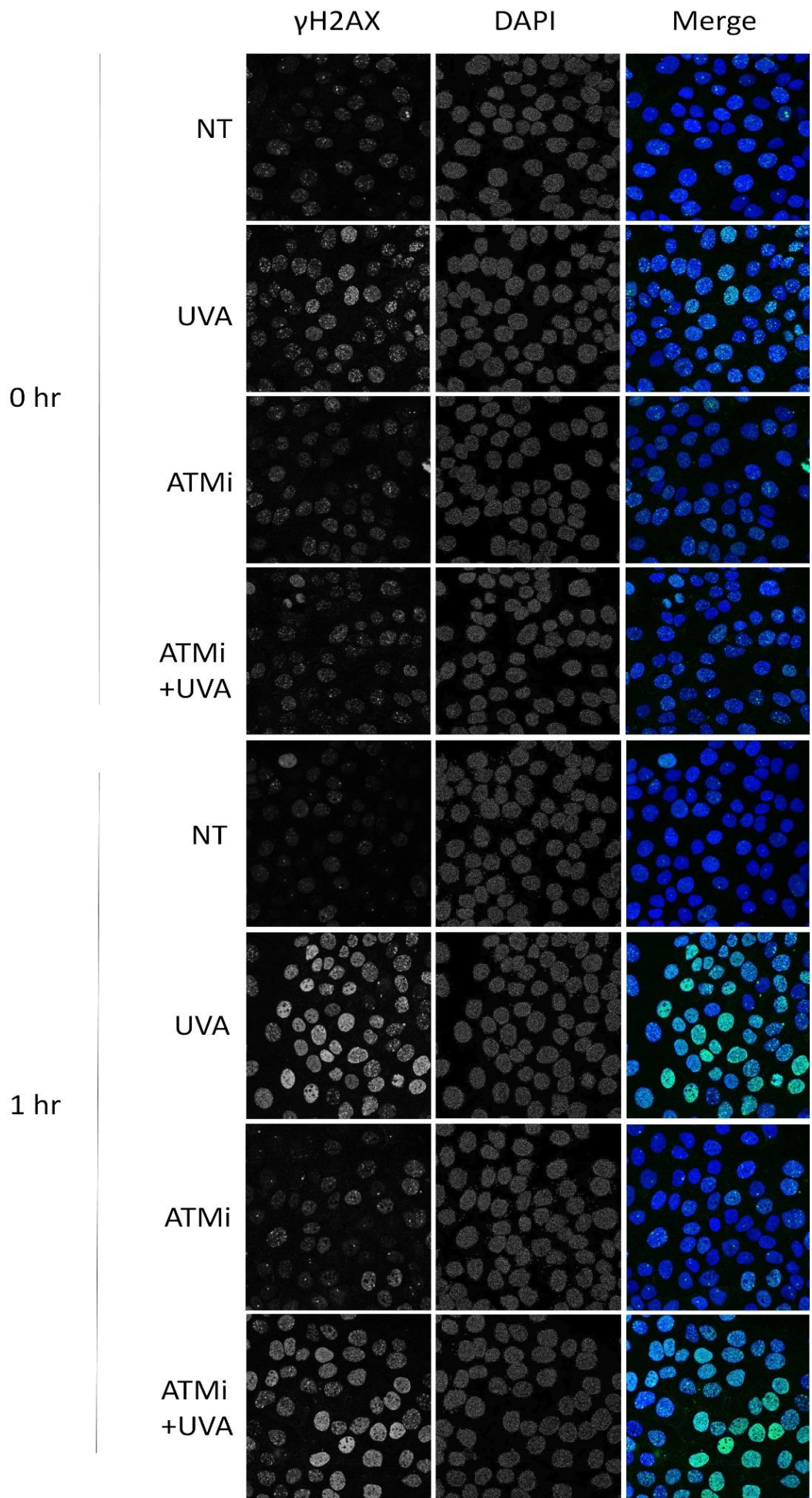
*HaCaT cells were pre-treated with 2  $\mu$ M KU-60019 for 1 hour prior to UVA irradiation (100 KJ m<sup>-2</sup> for 25 minutes). Cell extracts were made immediately after UVA irradiation, or after the indicated amount of rest time in a 37°C/5% CO<sub>2</sub> incubator. Extracts were probed for various components of the DDR and  $\beta$ -Actin was used a load control. The data shown is representative of two individual experiments.*

Figure 3.3.1 shows that 200 nM KU-60019 resulted in a delay in the immediate accumulation (0 hour) of  $\gamma$ H2AX post UVA irradiation, and after 1 hour the level of  $\gamma$ H2AX was similar to that of uninhibited cells. When 2  $\mu$ M KU-60019 is used instead,  $\gamma$ H2AX accumulation is delayed for longer, with decreased accumulation persisting for over 1 hour post irradiation (figure 3.6.1).  $\gamma$ H2AX rapidly increases between 1 to 2 hours post irradiation, and then decrease slowly past 4 hours.

pCHK2 displays a greatly reduced initial response to UVA irradiation, showing very little accumulation at 0 hours. pCHK2 then increases at 1 hour post irradiation and remaining at a relatively consistent intensity up to 4 hours post irradiation (figure 3.6.1) The pattern is very similar to that in cells treated with 200 nM KU-60019 (figure 3.3.1).

Phospho-p53 showed a very consistent level of accumulation when treated with 200 nM KU-60019 (figure 3.3.1). When treated with 2  $\mu$ M KU-60019, there is very little initial accumulation of phosphorylated p53, which only increased slightly 1 hour post UVA irradiation, which decreased gradually between 1 to 4 hours. Phospho-p53 and pCHK2 still have a similar pattern of accumulation, as seen previously in figure 3.3.1. Phospho-PNKP showed almost no difference between 200 nM (figure 3.3.1) and 2  $\mu$ M (figure 3.6.1) of KU-60019.

As with 200 nM KU-60019, immunofluorescence was carried out using 2  $\mu$ M KU-60019 to support the findings of the western blotting analysis.



**Figure 3.6.2 - Immunofluorescence detection of  $\gamma$ H2AX after UVA irradiation and the addition of the ATM inhibitor KU-60019**

*HaCaT cells were seeded on coverslips and allowed to adhere. Cells were pre-treated with 2  $\mu$ M of KU-60019 for 1 hour, and then irradiated for 25 minutes with 100 KJ m<sup>-2</sup> UVA. Cells were fixed immediately post irradiation (0 hour) or after 1-hour rest in a 37°C/5% CO<sub>2</sub> incubator. Cells were stained with a  $\gamma$ H2AX primary antibody, and then with an AlexaFluor 488-labelled secondary antibody. Coverslips were mounted onto a slide using DAPI containing mounting medium. Cells were visualised using confocal microscopy and ZEN software. Representative confocal images of immunofluorescence showing  $\gamma$ H2AX, DAPI and a merge of the two. The data shown is representative of three individual experiments.*

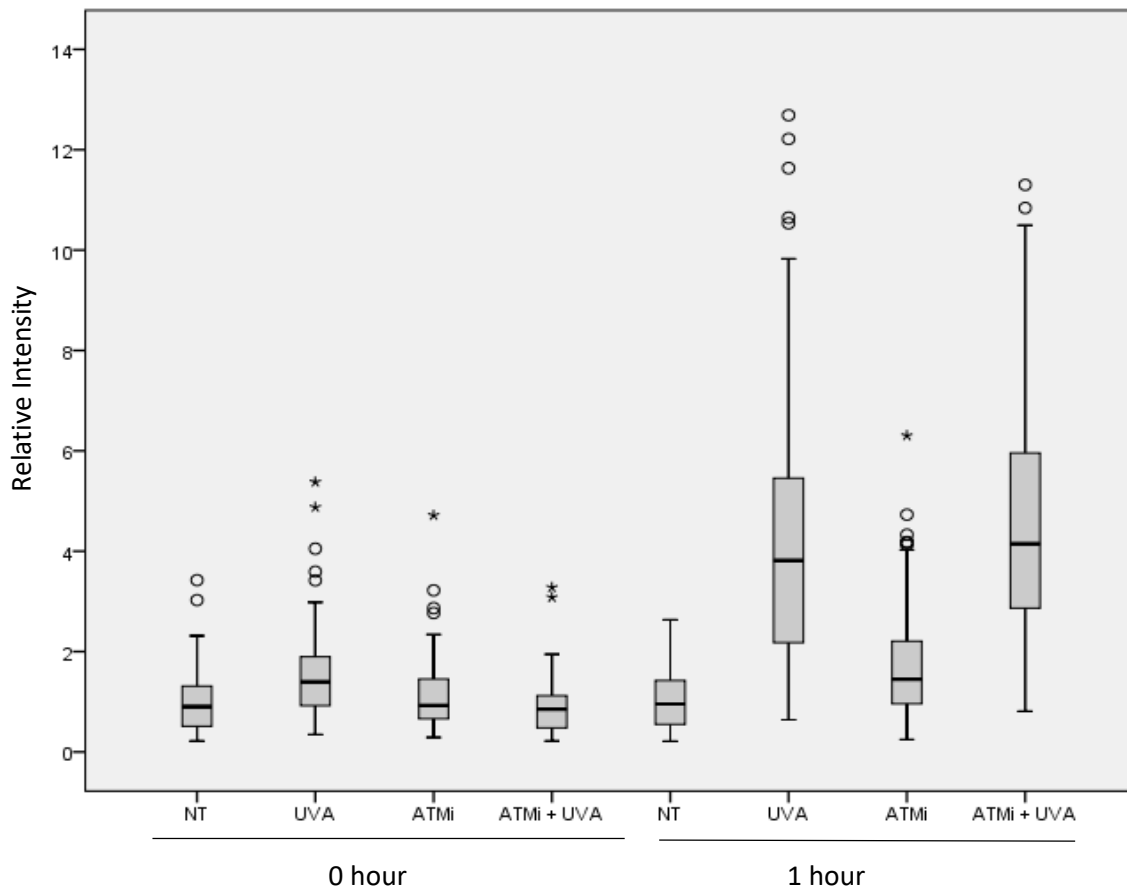


**Figure 3.6.3 – Quantification of immunofluorescence images from 2  $\mu$ M KU-60019 experiments**

The relative intensity of the immunofluorescence was quantified using ImageJ software. The intensity quantities were normalised to the respective control group (NT). A box plot was created, indicating the median and the range of data. The median and the interquartile ranges are represented by the boxplot, while the whiskers show the 95% percentiles. NT = No treatment / UV = Ultraviolet light / ATMi = KU-60019. The data shown is representative of a single repeat of three separate experiments. Circles above the plots represent outliers while the stars represent extreme outliers.

$\gamma$ H2AX accumulation seen in the immunofluorescence images (figure 3.6.2/3.6.3) shows a similar pattern to that seen in the western blotting analysis for UVA only treated cells (figure 3.6.1). There is some difference between the inclusion of 2  $\mu$ M KU-60019 in the western blotting analysis and the immunofluorescence.

Cells treated with UVA and 2  $\mu$ M of KU-60019 saw no significant change in the level of  $\gamma$ H2AX fluorescence compared to untreated cells at 0 hours ( $p=0.529$ ), which can be seen in the western blotting data too. However, 1 hour post irradiation, there was a significant increase in  $\gamma$ H2AX fluorescence in UVA and KU-60019 treated cells compared to untreated cells ( $p<0.001$ ), while the western blotting data shows that  $\gamma$ H2AX doesn't increase until 2 hours post irradiation. KU-60019 only treated cells saw no significant change in fluorescence intensity compared to untreated cells ( $p=0.098$ ). There is not a significant increase in fluorescence between UVA and KU-60019 treated cells those treated with only KU-60019 at 0 hours ( $p=0.798$ ). However, there is a significant difference increase between the same two groups at 1 hour post irradiation ( $p<0.001$ ).

## **VI. The influence of UVA and cell cycle status on 53BP1 foci formation in HaCaT cells**

53BP1 is an essential protein in promoting NHEJ in G1 cells. 53BP1 prevents resection occurring, which is the first major step of homologous recombination. As a result, NHEJ becomes the dominant repair type. As HR requires the presence of a homologous template, it cannot function during G1 where DNA has not been replicated and there is no homologous DNA. Therefore, it is thought that 53BP1 is mainly active during G1, and during the S/G2 phases it is less active. Some studies suggest that HR is only dominant during S phase, and the NHEJ is carried out during G2-phase cells (Mao et al, 2008).

EdU staining is technique that is able to distinguish between cells that are in S or G2 to those that are in G1. EdU is a thymidine analogue, and when it is introduced into active replicating cells, it is taken up and incorporated in newly synthesised DNA. When cells are processed, a reaction occurs between the EdU and a fluorescent azide (with copper catalysis), known as a cycloaddition. This is generally referred to as a 'Click' reaction. The result is that cells that are in S phase or have transitioned to G2 when EdU was introduced fluoresce, while cells that are in G1 do not, allowing for a distinction between actively replicating cells and G1 cells.

The initial aim was to investigate the effect of UVA on 53BP1 foci formation, to explore the activation of NHEJ following irradiation. However, upon finding contrasting reports of cell cycle status on foci formation, we decided to investigate this too (Takata et al, 1998, Mao et al, 2008, Takashima et al, 2009).

To investigate the activity of 53BP1 and its relationship with cell cycle status, EdU staining was combined with standard immunofluorescence, and visualised using confocal microscopy. The same experimental design was used as with previous experiments, however EdU was added 20 minutes before the UVA irradiation. EdU staining is processed before the immunofluorescence stages.

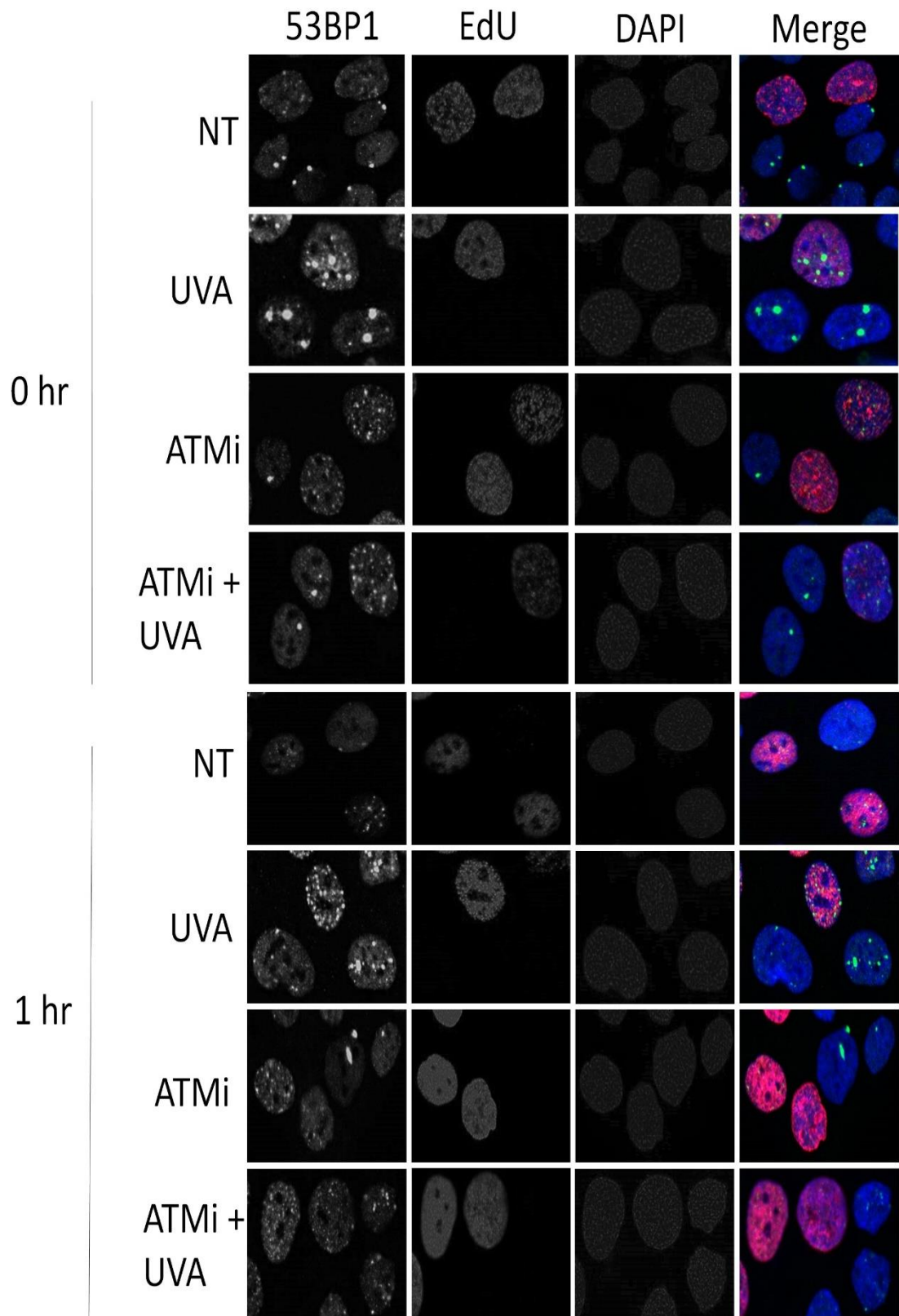


**Figure 3.7.1 – Combination of immunofluorescence and EdU staining of HaCaT cells when treated with either UVA or UVA and 2  $\mu$ M of KU-60019**

HaCaT cells were seeded onto coverslips and allowed to adhere. Cells were treated with 2  $\mu$ M KU-60019 for 1 hour prior to UVA irradiation. 20 minutes before UVA irradiation, EdU was added. Cells were then treated with 100 KJ m<sup>-2</sup> of UVA for 25 minutes. 0 hour cells were fixed immediately post UVA treatment, and 1 hour samples were incubated at 37°C/5% CO<sub>2</sub>. Samples were processed for EdU first, then the standard immunofluorescence procedure was carried out. Samples were incubated with a 53BP1 rabbit primary antibody, and then with a 488 anti-rabbit secondary antibody. Coverslips were mounted onto slides using DAPI containing mounting medium. Cells were visualised using confocal microscopy and ZEN software. Representative images of the confocal microscopy, showing 53BP1, EdU, DAPI and a merge of the three are presented. The data shown is representative of a single experiment.

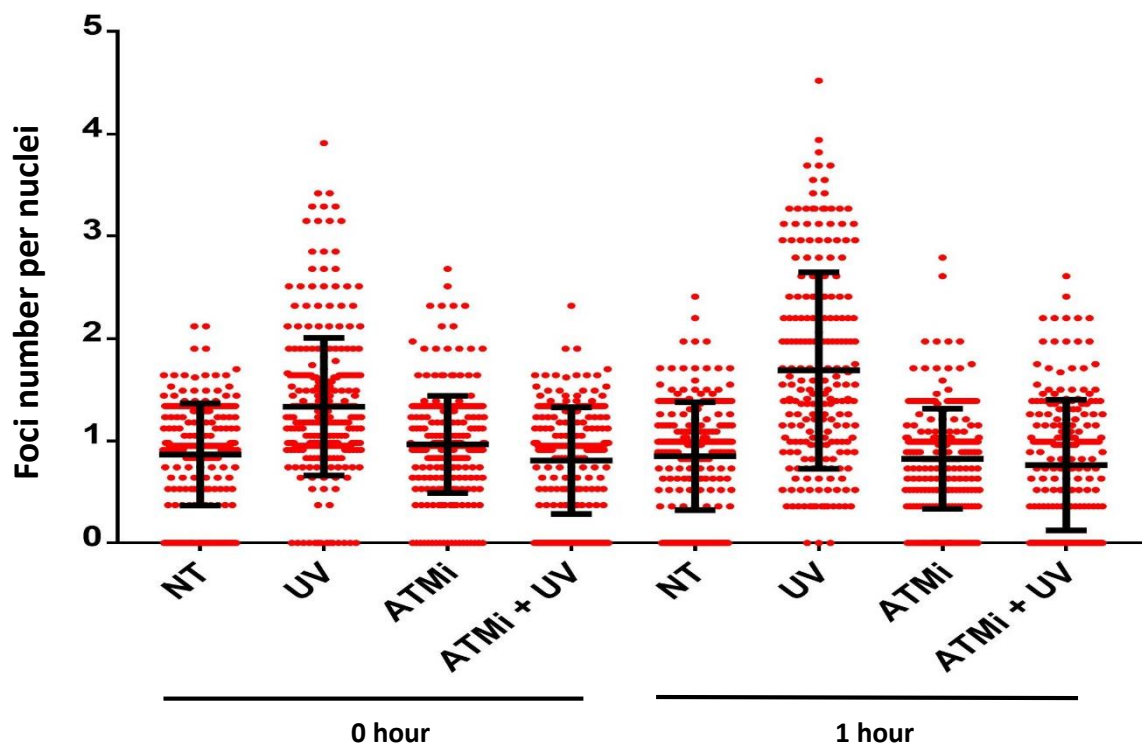


**Figure 3.7.2 – Quantification of the number of foci per nuclei presented in a swarm plot**

53BP1 foci were quantified from the confocal images using imageJ software. The number of foci were plotted on a Swarm plot using GraphPad Prism. The mean and the SD are plotted for each treatment type. NT = No treatment / UV = Ultraviolet light / ATMi = KU-60019. The data shown is representative of a single experiment

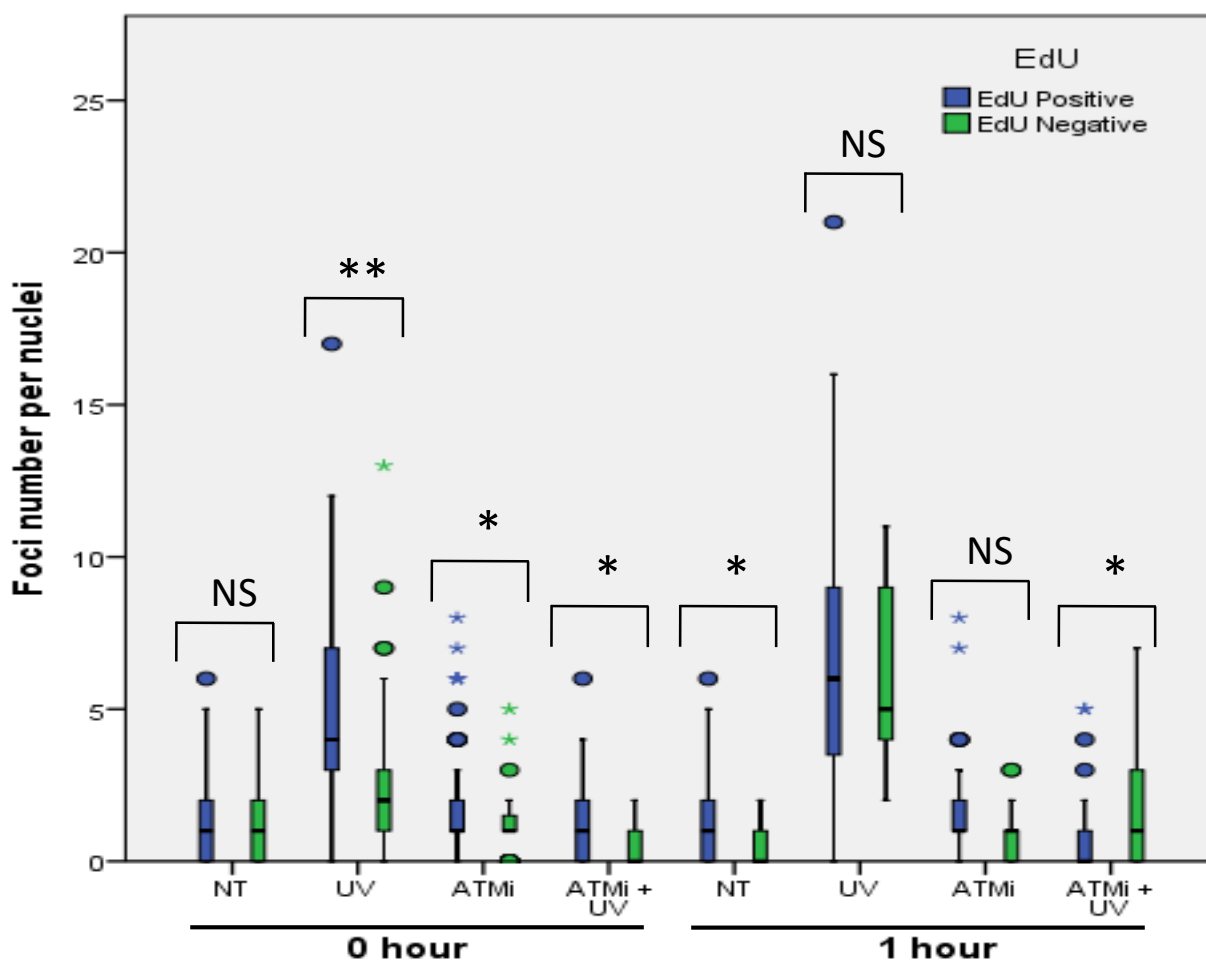


**Figure 3.7.3 – The difference in the number of foci between EdU positive and negative cells in each treatment**

A Clustered bar chart displaying the average number of foci in each treatment and EdU status. EdU positive cells were determined using imageJ, where cells that fluoresced with EdU were deemed positive, while those that showed no fluorescence were deemed negative. Error bars indicate the standard deviation. NS indicates that the difference in the number of foci between Edu positive and EdU negative cells of the same treatment is not significant, while \* indicates a significant difference, with a threshold between  $p = 0.05 - 0.001$ . \*\* indicates a highly significant difference, with a threshold  $p = <0.001$ . Circles above the plots represent outliers while the stars represent extreme outliers. The data shown is representative of a single experiment. . Circles above the plots represent outliers while the stars represent extreme outliers.

Treating cells with UVA caused a significant increase in 53BP1 foci formation compared to untreated samples immediately following irradiation ( $p < 0.001$ ). There was also a significant increase in foci in UVA treated cells 1 hour following radiation, compared to untreated cells ( $P < 0.001$ ), with the increase being significantly larger following 1 hour rest than 0 hours ( $p < 0.001$ ). The addition of KU-60019 alone does not cause a significant increase in the number of foci in either 0 or 1 hour samples ( $p = 0.276$  and  $0.156$  respectively). Treatment with both UVA and KU-60019 showed no significant

increase at both 0 hour and 1 hour time points ( $p=0.249$  and  $p=0.065$  respectively). There is also no significant difference in foci number between both the UVA and KU-60019 treated time point samples ( $p=0.712$ ) There is no significant difference between the two control (NT) groups ( $P=0.644$ ).

By including EdU staining in this experiment, we can investigate which stage of the cell cycle 53BP1 is most active, by seeing how foci numbers change depending on replication status. There were some significant differences in foci number and replication, however other treatments did not see a significant difference. In 0 hour control cells (NT), there was no significant difference in foci number between EdU positive and negative cell ( $p=0.479$ ). However, 1 hour control cells did show a significant difference in foci number ( $p=0.006$ ). In UVA treated samples with 0 hours rest, there was a highly significant difference in foci number, with more foci forming in EdU positive cells ( $p<0.001$ ), while samples that were rested for 1 hour did not have a significant difference ( $p=0.974$ ). In KU-60019 treated cells, 0 hour samples showed a significant increase of foci in EdU positive cells ( $p=0.033$ ) while 1 hour rested cells showed no significant difference ( $p=0.070$ ). KU-60019 and UVA treated cells at 0 hours showed that EdU positive cells had significantly more foci than EdU negative cells ( $p=0.003$ ), while 1 hour rested cells had showed a significantly more foci in EdU negative cells ( $p=0.001$ ).

## 4. Discussion

The repair of DNA damage is essential to the prevention of the development of tumours and cancer. Detecting and triggering the appropriate cellular response is the main function of the DNA damage response, and defects in this pathway can cause increased sensitivity to UV radiation. Solar radiation accounts for most of the Ultraviolet light people are exposed to. 95% of the UV that reaches Earth's surface from the sun is UVA, with the remaining 5% being UVB. Oxygen (atmosphere and ozone layer) absorbs all the UVC wavelengths, and most UVB wavelengths. UV radiation has been proven to be one of the main factors associated with the development of skin cancer, including non-melanoma skin cancers and cutaneous malignant melanoma. People with the genetic disorder Xeroderma Pigmentosa (XP) are particularly prone to UV induced skin cancer, as they have at least one of a variety of mutations in proteins that are important to the repair of DNA damage.

Although both UVA and UVB have been shown to induce DNA damage, UVB was the focus of initial research, as UVAs carcinogenic effect had not been demonstrated. Only recently has UVAs mutagenic capabilities come into focus, making a lot of current research aimed mainly at developing our understanding of the mechanism behind UVA induced genotoxicity. Our understanding of UVA to induce the DDR is one of the key areas of current research, and is the main aim of the experiments presented in this report. The ability of UVA to induce DNA damage, and more specifically double strand breaks is investigated, as well as UVA induced activation of the DDR. The inhibition of ATM, and the resulting effect on both DNA damage generation and DDR activation was also investigated. The role of cell cycle status on certain aspects of DNA repair was a point of focus too in this investigation.

## **I. UVA causes double strand breaks in HaCaT cells, but is rapidly repaired**

There are various studies that suggest different conclusions on the ability of UVA to cause DSBs.

Rizzo et al (2011) concluded that UVA did not produce any significant DSBs, even with high doses of UVA. Rizzo also demonstrated that UVA, both 100 and 200 KJ m<sup>-2</sup> did not produce any significant comet tails (neutral comet assay), either immediately following irradiation or after 1 hour rest (Rizzo et al, 2011). Other studies have demonstrated UVA-induced DNA damage using neutral comet assays (Wischermann et al, 2008; Greinert et al, 2012). To investigate UVAs genotoxic capacity for ourselves, we irradiated HaCaT cells with 100 KJ m<sup>-2</sup> UVA and performed both alkaline and neutral comet assays.

Comet assays are a useful technique when investigating DNA damage generation. There are various values that can be used for further analysis. The three that are most commonly used are DNA tail percentage, tail moment and olive tail moment. DNA tail percentage is the proportion of the DNA content in the tail compared to the entire comet DNA content. Tail moment is the length of the tail DNA multiplied by the tail DNA percentage. Olive tail moment is the product of the tail length and the fraction of the total DNA in the tail. All three parameters are useful when describing comet assay data, with each having their benefits and drawbacks. Kumaravel and Jha (2006) claim that olive tail moment and tail DNA percentage are effective at correlating with doses of genotoxic agents. Their study also states that due to tail moment and olive tail moment measurements having arbitrary units, it can be difficult to compare to other studies (Kumaravel and Jha, 2006). Tail DNA percentage can be compared across different studies, and can be easily visualised, and as a result was chosen as the parameter for this study.

Figure 3.2.1 shows UVA has the capacity to generate DNA damage in general. The alkaline comet assay is able to detect ssDNA breaks, DSBs as well as apurinic/apyrimidinic sites. Irradiating cells with UVA causes large amounts of DNA damage shown by the presence of comet tails at 0 hours and

UVA. However after just 1 hour of rest, the comet tails are no longer present, indicating that most if not all UVA-induced DNA damage has been repaired. Although this does provide evidence for the general genotoxic capabilities of UVA, we are more interested in UVA induced DSBs.

To investigate DSB generation, a neutral comet assay was performed. Neutral comet assays have been used to visualise DSB accumulation in previous studies, and has been shown to effectively differentiate between ssDNA breaks and DSBs (Cortes-Gutierrez et al, 2012). A previous study by Wischerman et al (2008) investigated the effect of UVA induced DNA damage on HaCaTs using comet assays, and saw a similar pattern as presented in this study. However, a neutral comet assay was only used to investigate the immediate effect of UVA (60 J/cm<sup>2</sup>) on HaCaTs, so the repair kinetics was not seen (Wischermann et al, 2008).

Figure 3.2.2 provides evidence for ability of UVA to generate DSBs, as seen with the presence of comet tails immediately following UVA. Interestingly, there is no significant difference in tail DNA percentage in controls and cells treated with UVA and allowed to rest for 1 hour. This finding suggest that the bulk of DSBs have been repaired within 1 hour of UVA irradiation. Wischermann demonstrated that general DNA damage (alkaline comet assay) is repaired rapidly within 4 hours of UVA irradiation, with the 2 hour time point showing a large decrease in DNA tail percentage compared to 0 hour samples (Wischermann et al, 2008). We provide further evidence that DNA damage is rapidly repaired following UVA exposure, particularly DSBs.

After demonstrating the rapid repair of DNA damage using comet assays, we moved onto investigating the activation of the DDR following UVA, and how it may reflect comet assay results.

## **II. UVA causes an increase in $\gamma$ H2AX accumulation, which peaks between 1 and 2 hours post irradiation**

$\gamma$ H2AX has been widely accepted as a biomarker for DNA damage, and has been used in the past as a biomarker for UVA generated damage (Valdiglesias et al, 2013). Although some studies have questioned the ability of UVA to cause  $\gamma$ H2AX formation, numerous other studies have presented contradicting data. Rizzo et al (2011) demonstrated that UVA did not form  $\gamma$ H2AX foci, and that UVB is only capable of inducing a significant number of  $\gamma$ H2AX. Rizzo claims that a possible reason for differences in their data to other studies which show significant  $\gamma$ H2AX foci formation may be because their study counted  $\gamma$ H2AX positive cells when over ten foci were present, to avoid ambiguity (Rizzo et al, 2011). There are more studies that demonstrate the accepted mechanism of  $\gamma$ H2AX accumulation post UVA irradiation (Grienert et al, 2012; Wischermann et al, 2008; Lu et al, 2006). Along with these studies and many more, the data presented here supports the use of  $\gamma$ H2AX as a biomarker for UVA induced DNA damage.

Western blotting analysis (figure 3.3.1 and 3.6.1) and immunofluorescence data (figure 3.3.2/3.3.3 and 3.6.2/3.6.3) shows that  $\gamma$ H2AX accumulation increases immediately after exposure to UVA radiation, and continues to increase to peak between 1 to 2 hours post exposure. This increase in  $\gamma$ H2AX accumulation in this time span can be attributed to the positive feedback loop mechanism that  $\gamma$ H2AX causes. MRN detects DSBs, which in turn recruits ATM. ATM is one of the main kinases responsible for the phosphorylation of the histone variant H2AX, becoming  $\gamma$ H2AX.  $\gamma$ H2AX can act as a coordinator of the DDR, and causes the recruitment of more MRN molecules via an interaction with the Nbs1 domain (Kobayashi et al, 2002,) or via the recruitment of MDC1. MDC1 is recruited by  $\gamma$ H2AX which is initially generated via ATM. MDC1 is then continuously phosphorylated by CK2, causing phosphorylation dependant interactions with the Nbs1 domain of MRN. MRN increases ATM recruitment, leading to more  $\gamma$ H2AX formation and so on (Kinner et al, 2008).

Further evidence of the link between ATM and  $\gamma$ H2AX can be seen in figure 3.3.1, which shows the pattern of ATM phosphorylation after UVA irradiation. Similar to  $\gamma$ H2AX accumulation, ATM phosphorylation increases between 0 and 1 hour post UVA exposure, peaking between 1 and 2 hours, before decreasing up to and beyond 4 hours. When DSBs have been repaired,  $\gamma$ H2AX accumulation gradually decreases (figure 3.3.1 and 3.6.1). The decrease is not instant as the feedback mechanism will still be occurring, however there will be natural recruitment of MRN to the site of the DSB.

### **III. The ATM inhibitor KU-60019 prevents the accumulation of $\gamma$ H2AX in the early response to UVA irradiation**

KU-60019 is an inhibitor of ATM, and is more specific than previously used inhibitors such as KU-55933. KU-60019 has an  $IC_{50}$  of 6.3 nM for ATM, compared to KU-55933s 12.9 nM. KU-60019 has  $IC_{50}$  values of 1.7  $\mu$ M and  $>10$   $\mu$ M for DNA-PK and ATR respectively, compared to KU-55933s 2.5  $\mu$ M for DNA-PK and 16.6  $\mu$ M for PI3K, and  $\sim 100$   $\mu$ M for ATR (Hickson et al, 2004). KU-55933 has previously been used in the laboratory, with similar experimental designs as stated in this report, however a consistent concentration of 1  $\mu$ M was used. The use of KU-55933 resulted in the complete abrogation of  $\gamma$ H2AX accumulation in cells that were treated with UVA (figure 3.1). The study suggested that  $\gamma$ H2AX formation is dependent on ATM activity, and that UVA initiates DSBs (Steel, 2016). Steel also used an ATR inhibitor and investigated  $\gamma$ H2AX accumulation, but saw no effect, suggesting  $\gamma$ H2AX does not form as a result of ssDNA breaks or replication fork stalling.

The data presented in this study both support and contradict the findings of Steel (2016). The use of the ATM inhibitor KU-60019 did cause a decrease in the accumulation of  $\gamma$ H2AX, as seen in western blot analysis (figures 3.3.1 and 3.6.1) and immunofluorescence data (3.3.2/3.3.3 and 3.6.2/3.6.3). However this decrease is only apparent in the immediate response to UVA irradiation, with large decreases in  $\gamma$ H2AX levels only present at 0 hour time points, when cells are treated with both KU-60019 and UVA. In cells treated the same but rested for 1 hour post UVA irradiation,  $\gamma$ H2AX had

accumulated significantly higher levels than cells treated with only KU-60019, regardless of the concentration of the inhibitor.

The difference between the results seen in figure 3.3.1 and 3.3.2 using KU-60019, and those presented in Steel (2016) using KU-55933 presented issues. The expected result when using KU-60019 was that it cause a very similar effect on cells, causing a complete abrogation of the accumulation of  $\gamma$ H2AX. When this result was not seen, it was decided that increasing the working concentration of KU-60019, from (200 nM to 2  $\mu$ M) may result in the same effect as KU-55933.

We also decided to investigate to what degree 200 nM KU-60019 was inhibiting ATM. Figure 3.4 shows that 200 nM was not fully inhibiting ATM phosphorylation, particularly in the early phase of the UVA induced DDR. This data was further evidence that increasing inhibitor concentration was required.

2  $\mu$ M KU-60019 was chosen as the new working concentration, and western blotting was carried out to ensure it was inhibiting ATM to a satisfactory degree. Golding et al (2009) used KU-60019 at various concentrations (1, 3 and 10  $\mu$ M), and demonstrated reduced  $\gamma$ H2AX accumulation at all three concentration (Golding et al, 2009). The results of this study provided suitable reason to test 2  $\mu$ M as a potential working concentration. Golding's study also shows that 2  $\mu$ M KU-60019 should not pose inhibitory effect on DNA-PK, despite being over the supplied  $IC_{50}$  of 1.7  $\mu$ M.

Figure 3.5 shows that 2  $\mu$ M of KU-60019 almost completely inhibits UVA-induced ATM phosphorylation immediately following irradiation (0 hours). At 1 hour post UVA irradiation, ATM phosphorylation had increased back to a similar level as uninhibited cells. It was decided 2  $\mu$ M would be the working concentration, and we would investigate how a delay in the initial phosphorylation of ATM after UVA irradiation would effect other aspects of the DDR with 2  $\mu$ M KU-60019 and  $\gamma$ H2AX accumulation.

The western blotting analysis (figure 3.6.1) shows that using 2  $\mu$ M KU-60019 resulted in an increased delay time of  $\gamma$ H2AX accumulation, where there is little increase at 0 and 1 hours post UVA irradiation in inhibited cells. However, the immunofluorescence data (figure 3.6.3) shows that  $\gamma$ H2AX levels had increased significantly at 1 hour post irradiation. There was no significant increase in UVA and KU-60019 treated cells at 0 hours post irradiation.

Even with the increase of KU-60019 concentration to 2  $\mu$ M, UVA-induced  $\gamma$ H2AX accumulation was increasing at 1 hour post irradiation, to levels similar to uninhibited UVA treated cells (figure 3.6.2/3.6.3). When 1  $\mu$ M of KU-55933 was used, there was a huge reduction in the accumulation of  $\gamma$ H2AX at 1 hour post UVA irradiation (Steel, 2016). When considering the results presented by Steel, and the results presented in this study, we suggest that the ATM inhibitor KU-55933 at 1  $\mu$ M may also be inhibiting the action of DNA-PK, while KU-60019 at 2  $\mu$ M is only inhibiting the action of ATM.

The  $IC_{50}$  values of KU-55933, and the study by Golding et al (2009) using KU-60019, suggest that neither should be inhibiting DNA-PK at the working concentrations. A study by Stiff et al (2004) concluded that both ATM and DNA-PK play a significant role in the formation of  $\gamma$ H2AX. Stiff and colleagues demonstrated that cells that were lacking ATM and treated with a specific DNA-PK inhibitor (LY294002) would not elicit an IR-induced  $\gamma$ H2AX response. Cells that contained a functional form of either ATM or DNA-PK, but not both, could still elicit an IR-induced  $\gamma$ H2AX response.

Importantly, Stiff also showed that the  $\gamma$ H2AX accumulation was slowed in cells that were lacking ATM, but not DNA-PK, suggesting that the early response to irradiation is dominated by ATM (Stiff et al, 2004).

The conclusions put forward by Stiff et al (2004) suggest that the less specific ATM inhibitor KU-55933 may also be inhibiting DNA-PK at 1  $\mu$ M, while KU-60019 at 2  $\mu$ M is not. KU-60019 was only able to prevent the accumulation of  $\gamma$ H2AX in the early response to UVA irradiation. At 1 hour post UVA irradiation, DNA-PK was able to compensate for the lack of ATM activity, and present a  $\gamma$ H2AX response similar to that in uninhibited cells. 1  $\mu$ M KU-55933 can inhibit both ATM and DNA-PK,

explaining why there was large abrogation of a UVA-induced  $\gamma$ H2AX response. Our findings support the idea that ATM is important in the formation of  $\gamma$ H2AX in the early response to UVA, and that DNA-PK plays a significant role in the later response. The reported  $IC_{50}$  of  $\sim 100 \mu\text{M}$  for ATR by KU-55933 allows us to conclude that ATR does not play a major role in  $\gamma$ H2AX formation.

To be able to draw accurate conclusions from the immunofluorescence data, a control should be performed using an agent that is known to cause DSBs, such as Zeocin. This would confirm whether the results seen in UVA treated samples were a result of DSB formation.

It also important to point out the difference between  $\gamma$ H2AX foci formation and  $\gamma$ H2AX pan staining as a tool for investigating DSBs. Many studies use  $\gamma$ H2AX foci formation as a method of investigating DSB formation.  $\gamma$ H2AX foci indicate the presence of a DSB, and can be easily quantified, either through counting by eye or through automated systems. Pan stained  $\gamma$ H2AX has also been investigated as an indicator of DSB formation, however less is known as the reason why pan staining may occur instead of foci formation. A study by Meyer and colleagues suggests that  $\gamma$ H2AX pan staining varies depending on the amount of DNA damage, particularly clustered DNA lesions, and is mediated by ATM and DNA-PK (Meyer et al, 2013). Another study suggests that UV-induced  $\gamma$ H2AX pan staining does not occur due to DSB formation, but rather is a result of NER factors exposing the S139 site to kinases, and that intensity can vary depending on the cell cycle status of the cell (Marti et al, 2006).

Given the broad use of  $\gamma$ H2AX foci in other studies, and the mechanism for  $\gamma$ H2AX pan staining not being fully understood, a possible improvement to this study may be the quantification of  $\gamma$ H2AX foci instead of fluorescence intensity.

Future work could investigate the link between  $\gamma$ H2AX foci formation and pan staining. 53BP1 foci formation is a widely accepted biomarker of DSB formation, even following UV exposure.

Immunofluorescence could be carried out that probes for  $\gamma$ H2AX and 53BP1 in the same nuclei. If  $\gamma$ H2AX foci are associated with DSB formation, then we would expect to see overlapping  $\gamma$ H2AX and

53BP1 foci. EdU could also be incorporated into  $\gamma$ H2AX immunofluorescence studies, to investigate the claim that  $\gamma$ H2AX fluorescence varies with cell cycle status.

#### **IV. ATM inhibition causes significant decreases in the activation of UVA-induced DDR**

Western blotting analysis was chosen as a suitable method of investigating the activation of different DDR components in response to UVA exposure. pCHK2 was chosen as a component to investigate as it is one of the main targets of ATM activity, and plays a key role in the DDR by acting as a downstream kinase, activating other components such as p53. p53 is considered one of the most important proteins involved in the prevention of tumours and cancer, as it is key for activating apoptosis, cell cycle arrest and DNA repair in response genotoxic stress. PNKP has both kinase and phosphatase activity, where it is able to trim molecules that cannot be ligated from DNA ends during NHEJ, allowing the repair pathway to continue. The activation of all three of these proteins require phosphorylation for their activation and consequent interaction with other DDR components. As a result, the phosphorylated forms of these proteins were used as biomarkers of their activation in this study.

##### **CHK2**

Figures 3.3.1 and 3.6.1 shows that CHK2 is rapidly phosphorylated immediately after UVA irradiation, and then decreases slowly over the course of the next few hours, where the level at 4 hours is only slightly higher than that of untreated cells. When the ATM inhibitor KU-60019 is introduced, the initial peak at 0 hours does not occur. There is evidence of some pCHK2 accumulation at 0 hours, but it is only slightly higher than untreated levels. At 1 hour and onwards, the level of pCHK2 has increased but does not reach levels equal to that of uninhibited cells. As ATM is one of the main phosphorylators of CHK2, its inhibition severely decreases pCHK2 accumulation. There is a small

degree of pCHK2 present at the 0 hour time point, suggesting that there may be other kinases responsible in CHK2s phosphorylation.

ATR is another candidate that may be responsible for the phosphorylation of CHK2, as seen in the study by Wang and colleagues, which saw ATM inhibited GM 5399 (human diploid fibroblasts) cells display enhanced ATR activity, as well as CHK2 phosphorylation in response to UV radiation (Wang et al, 2006). DNA-PK has also been shown to phosphorylate CHK2, and could explain the delayed increase in phosphorylation when ATM is inhibited (Li and Stern 2005). This suggests an ATM independent pathway of CHK2 activation, which is consistent with a similar pathway of  $\gamma$ H2AX accumulation as previously discussed. It would be worth investigating the effect of combining ATM and DNA-PK inhibitors to investigate the potential effect on CHK2 phosphorylation, and how the previously mentioned ATM inhibitor KU-55933 may change this pattern.

### **p53**

The pattern of p53 phosphorylation in response to UVA exposure is similar to that of CHK2 (figure 3.3.1 and 3.6.1). There is an immediate peak in phospho-p53 following UVA irradiation, which decrease gradually over the course of the next 4 hours, where the level at 4 hours is close to that of untreated cells. The pattern seen here is the same as CHK2 activation, suggesting a close link between the two proteins.

When ATM is inhibited, there is a sizeable reduction in the phosphorylation of p53. The immediate response to UVA irradiation is lost, with an intermediate amount of p53 phosphorylation occurring between 1 and 4 hours post UVA exposure. These results suggest that UVA-induced p53 phosphorylation is heavily mediated by ATM, particularly in the early response. Zhang and colleagues demonstrated a similar pattern, with Ser15 and Ser20 being heavily phosphorylated, which are both two key target sites of CHK2 activity (Zhang et al, 2002). It could be expected that p53 phosphorylation would mirror CHK2 activation when ATM is inhibited. A larger decrease in phospho-p53 suggested that there is a mechanism in which Ser15 is phosphorylated independent of

CHK2 activity (figure 3.6.1). There are other pathways which have p53 as a target effector protein, including the ATR mediated DNA damage response, which could explain the mild increase in phospho-p53. It would be interesting to investigate the effect of DNA-PK inhibition on p53 phosphorylation, particularly on Ser15 following UVA exposure, to check if it is a kinase responsible for p53 activation.

### **PNKP**

The phosphorylation of PNKP indicates the activation of the NHEJ repair mechanism. Figures 3.3.1 and 3.6.1 show that the pattern of PNKP phosphorylation is very similar to that of  $\gamma$ H2AX accumulation. There is an increase between the untreated cells and 0 hour UVA treated cells, which increases further, peaking between 1 to 2 hours. After this peak, the level of UVA-induced PNKP phosphorylation drops, with the amount at 4 hours being only slightly higher than that in untreated cells.

Cells treated with KU-60019 do not show a large difference in PNKP phosphorylation. The general response appears to be slightly dampened, but the pattern is the same. The peak does occur at 1 hour though, and appears to have decreased at 2 hours post irradiation. Increasing the inhibitor concentration also seems to decrease the overall intensity of the response. This suggests that the activation of PNKP is only partially attributed to an ATM dependant pathway, and that other pathways play an equal if not more important role. Ku70/80 is one of the complexes responsible for the initiation of NHEJ. Ku70/80 binds the DNA ends at DSB sites, and recruits DNA-PK and XRCC4, which is required for the recruitment and activation of PNK. Reynolds and colleagues suggest that Ku70/80 is responsible for the faster mechanism of NHEJ mediated repair of simpler DSBs, whereas ATM is required for the slower repair of more complex DSBs (Reynolds et al, 2012). If ATM is required for the more delayed mechanism of DSB repair, then the results seen here support this, as PNKP phosphorylation after 2 hours is reduced, particularly with an increase in KU-60019 concentration (figure 3.6.1) compared to uninhibited cells.

A study showed that PNKP phosphorylation occurs mainly at serine 114 and 126. The study also demonstrated Ser114 phosphorylation following ionizing radiation is ATM dependant, while Ser126 phosphorylation required DNA-PK (Zolner et al, 2011). Zolner also states that Thr118 is phosphorylated following DNA damage, which may be a reason why ATM inhibition has not caused an abolition of phospho-PNKP signal in this study, as the primary antibody detects both pSer114 and pThr118. There has been little investigation into Thr118, and we have little understanding of how it is phosphorylated in response to DNA damage. It would be interesting to investigate the effect of KU-55933 on the phosphorylation of Ser126, as we might expect to see little signal if the inhibitor is preventing both ATM and DNA-PK action, while the use of KU-60019 should allow for some phosphorylation if DNA-PK is still functional. Using a primary antibody which detects only Ser114 phosphorylation could also be carried out in the future, to investigate if KU-60019 completely prevents phosphorylation at Ser114.

To be able to draw accurate conclusions from the western blotting data in figure 3.6.1, more controls should be performed alongside the experimental blots. For example, unphosphorylated forms of CHK2, p53 and PNKP should be probed for, to ensure that differences seen in phosphorylated versions are not as a result from abnormal amounts of protein in the cells.

## **V. 53BP1 foci formation increase following UVA irradiation**

The formation of 53BP1 foci is used as a biomarker for the sites of DSB repair for some time. Schultz et al (2000) demonstrated that 53BP1 foci form with the use of DSB-inducing agents such as ionising radiation. However, Schultz also showed that 53BP1 foci did not form following exposure to UVC light (Schultz et al, 2000). There may be several reasons for this finding.  $50 \text{ J m}^{-2}$  of UVC (254nm) was applied dosage in this experiment. This is a very large amount of UVA to irradiate cells with, and likely caused extensive DNA damage that was beyond repair, preventing repair mechanisms from occurring and 53BP1 foci formation not occurring. UVC has been shown to generate DSBs, but in doses

much lower than the ones used here. Bogdanov used  $0.1 - 2 \text{ J m}^{-2}$  of 257 nm UVC and saw the immediate formation of DSBs (Bogdanov et al, 1997).

Stiff demonstrated that cells lacking both ATM and DNA-PKcs activity do not generate 53BP1 foci, and suggest that the formation of 53BP1 is dependent on  $\gamma$ H2AX formation, and not of ATM or DNA-PKcs themselves. Reynolds suggested that ATM was required for the slower repair of complex DSBs, but not the more rapid repair of simpler breaks (Reynolds et al 2012).

For some time, it was accepted that NHEJ was the dominant repair mechanism in G1 phase cells, and HR was dominant in S and G2 phase cells (Takata et al, 1998). In 2008, Mao suggested that HR was mainly dominant in S phase, and was down regulated in G2, with NHEJ being the main mechanism in G1 and G2 (Mao et al, 2008). Takashima and colleagues saw that NHEJ remains active at all stages of the cell cycle, with HR increasing three fold in late S/G2 phase cells in response to endonuclease-induced DSBs. The frequency of NHEJ events didn't decrease at any stage of the cell cycle, and suggest that it does not compete with HR (Takashima et al, 2009).

To investigate how NHEJ is activated in response to UVA, and how it may change over the course of the cell cycle, we combined 53BP1 foci immunofluorescence and EdU assays. KU-60019 was used to investigate how ATM inhibition may alter the activation of NHEJ.

Figures 3.7.1/3.7.2 shows that UVA-induced 53BP1 foci formation increases immediately, with the response increasing in intensity after 1 hour rest. This demonstrates that UVA does have the ability to generate 53BP1 foci, meaning NHEJ is activated as a result, with the number of NHEJ events increasing at 1 hour.

ATM inhibition had a significant effect on the formation of 53BP1 foci. There was no significant increase in foci number in either 0 hour or 1 hour rested cells that were treated with both UVA and KU-60019. Furthermore, there was no significant difference in foci number between either time

point in cells treated with both UVA and KU-60019. These results suggest that ATM plays an important role in both the early and later activation of the NHEJ, in response to UVA exposure.

By including EdU staining, we can investigate how cell cycle status may affect the formation of 53BP1 foci, and consequently the activation of NHEJ. If the early model of NHEJ activation is true, then we should expect to see a significantly higher number of 53BP1 foci in G1 cells i.e. EdU negative cells. If the findings in the studies by Mao et al (2008) and Takahsima et al (2009) are accurate, then there should be no significant difference between EdU fluorescence and the number of foci.

The results for the EdU aspect of this experiment vary substantial, and do not follow a general pattern. There were some significant differences in the number of foci between EdU positive and negative cells, as seen in 0 hour UVA, KU-60019 and dual treated cells, which also showed an increase in EdU positive cells. However, the 0 hour control, as well as 1 hour UVA treated cells and KU-60019 treated cells showed no significant difference. 1 hour rested cells that were treated with both UVA and KU-60019 showed the opposite effect, with a significantly higher number of foci in EdU negative cells. There are some conclusions that can be drawn from this data.

The comet assay data (figure 3.2.2) indicate a large presence of DSBs in UVA treated cells immediately following irradiation. Figure 3.7.3 shows that there is a large increase in the number of 53BP1 foci immediately following UVA irradiation, and that there is significantly more foci in actively replicating cells (EdU positive). Cells that are allowed to rest for 1 hour following irradiation show that the difference in the number of 53BP1 foci between EdU positive and negative cells is not significant. This suggests that there may be alternate mechanisms for NHEJ activation depending on which phase of the cell cycle the cell is in. The increase in foci number 1 hour of rest in G1 cells (EdU negative) may suggest that this response is much slower than NHEJ activation in actively replicating cells.

The inclusion of an ATM inhibitor causes a significant reduction in 53BP1 foci formation in both EdU positive and negative cells immediately following UVA irradiation, which indicates a major

dependence on ATM activity for the activation of NHEJ. However, in dual treated cells that are rested for 1 hour, there is a significantly higher number of 53BP1 foci in EdU negative cells. This suggests that the delayed G1 activation of NHEJ is less dependent on ATM activity, while actively replicating cells are more dependent on ATM. This finding contradicts Reynolds (2012), which suggested that ATM was required for the slower repair of DSBs (Reynolds et al, 2012). Stiff demonstrated that cells with neither ATM nor DNA-PK activity did not form 53BP1 foci (Stiff et al, 2004). Our data suggests that NHEJ that occurs immediately following UVA irradiation, and the NHEJ that occurs in actively replicating cells is dependent on ATM. Later and G1 associated NHEJ events may be more dependent on DNA-PK activity. It would be interesting to incorporate DNA-PK inhibitors into these experiments, to investigate if G1/late based 53BP1 foci formation is DNA-PK dependant.

Figure 3.7.1 shows that some nuclei have a small number of large foci, particularly those that are EdU negative. These large foci are known as OPT domains, and form as a result of incomplete DNA synthesis during the S phase of the previous cell cycle. The incomplete DNA synthesis leads to a DNA damage response, which recruits 53BP1 and other DNA repair proteins to the site. OPT domains present themselves as large 53BP1 foci in G1 phase cells (figure 3.7.1). Harrigan and colleagues demonstrated that ATM plays a key role in the formation of OPT domain. By using the ATM inhibitor KU-55933, they were able to largely abrogate OPT domain formation. Interestingly, Harrigan also demonstrated that AT (Ataxia Telangiectasia) cells and ATM<sup>-/-</sup> MEFs were still able to form smaller OPT domains, and suggest that DNA-PK plays a role in their formation (Harrigan et al, 2011). This finding suggests that KU-55933 may be inhibiting other proteins such as DNA-PK, and could explain why OPT domain formation was abrogated in treated cells.

Only one repeat was carried out which combined EdU and 53BP1 foci immunofluorescence, so accurate conclusions cannot be drawn from this aspect of the experiment. In the future, it may be worth synchronising the cell cycle of the cell population, to gain a better understanding of cell cycle

position and 53BP1 foci formation, as it allows us to more easily determine the precise phase the cell is in.

53BP1 is not a bona fide biomarker of NHEJ activation, but rather a biomarker of DSB sites. 53BP1 is closely associated with NHEJ, as it plays a crucial role in promoting the DNA repair pathway over HR, however it cannot be accepted as a biomarker of NHEJ. To investigate NHEJ activation more accurately, a true biomarker of the repair pathway should be used, such as DNA-PK (T2609).

## **VI. Future work**

There are various avenues that have been investigated in this project, which can be looked into further, to advance our understanding of the carcinogenic effect of UVA and its effect on the DDR. One of the most important experiments that should be carried out should aim at validating the claim that KU-55933 at 1  $\mu\text{M}$  is able to inhibit DNA-PK, despite being below the supplied  $\text{IC}_{50}$ . Given the results presented in this study, and that of Steel (2016), KU-55933 may have the capacity to inhibit DNA-PK, while KU-60019 is much more specific. Studies have already demonstrated that KU-60019 is up to ten times more potent at inhibiting ATM (Golding et al, 2009). Hickson et al (2004) concluded that KU-55933 was a potent ATM inhibitor, and demonstrated an  $\text{IC}_{50}$  of 2.5  $\mu\text{M}$  (Hickson et al, 2004). Studies have gone on to use 10  $\mu\text{M}$  of KU-55933 as a potent inhibitor of ATM (Li and Yang, 2010, Orthwein et al, 2015). If KU-55933 is able to inhibit DNA-PK significantly at these concentrations, it could cause question amongst studies that have assumed KU-55933 is only inhibiting ATM.

To investigate this claim, an experiment could be carried out that combines KU-60019 and a DNA-PK inhibitor, such as NU7441, and perform western blotting analysis and immunofluorescence looking for  $\gamma\text{H2AX}$  accumulation. A combination of these two inhibitors could result in the abrogation of  $\gamma\text{H2AX}$  generation, similar to that seen in Steel (2016) with KU-55933.

The main focus of this study has been on ATM, and how it plays a role in the cellular response to UVA. UVA has the ability to generate single strand breaks (Osipov et al, 2014), suggesting ATR

activation is likely to occur to repair such damage. Some studies suggest ATR is able to generate  $\gamma$ H2AX, particularly in the absence of ATM and DNA-PK (Wang et al, 2005). Other studies have concluded that ATR does not play a role in ionizing radiation induced  $\gamma$ H2AX formation in early stages (Stiff et al, 2004). To develop our understanding of ATR in response to UVA, the use of an ATR inhibitor should be considered, to see how the DDR is activated following UVA exposure, and how  $\gamma$ H2AX accumulation is affected. It is worth noting that  $\gamma$ H2AX formation via ATR can occur when ssDNA arises at stalled replication forks during the repair of bulky DNA lesions, which does not reflect DSB induced  $\gamma$ H2AX.

Another area of interest for future work is based on the studies that have demonstrated a difference between cells with inhibited ATM and cells which lack ATM altogether. ATM-KO mice have characteristics similar to the genetic disease ataxia-telangiectasia (AT) - except neurodegeneration, and are commonly used as a model for AT (Barlow et al, 1996; Elson et al, 1996). Other mice lines have been produced that have mutated ATM that are kinase-dead. These particular mice lines die early in embryonic life, and demonstrate genomic instability, more so than cells that have no ATM protein (Yamamoto et al, 2012). A different study suggested that certain ATM mutations result in defective homologous recombination during embryonic development, which results in lethality (Daniel et al, 2012). A review by Shiloh and Ziv (2013) suggests that when a kinase-dead ATM protein is recruited to the site of DNA damage, the DDR is detrimentally effected, significantly more so than ATM absence (Shiloh and Ziv, 2013).

CRISPR/Cas9 has been developed in the past few years and has opened up many possibilities in genetic manipulation, as it allows for the relatively simple removal of DNA sequences from the genome. HaCaT cells have been developed that would allow us to use the CRISPR/Cas9 system to manipulate genes that code for proteins of interest. We can use these cells to remove ATM, and investigate the difference in the UV-induced DDR between inhibited cells and KO cells easily. If

mutations can also be introduced in the ATM gene, then we can investigate the difference between ATM-KO and kinase dead ATM, and the effect these have on the DDR and genome stability.

Previous studies in our laboratory, as well as this one present the effect of UVA on HaCaT cells. HaCaT cells provide a good model for keratinocyte reaction to UVA, but skin is made up of a variety of cells, including melanocytes and fibroblasts. The microenvironment of the skin may also play a role in UVA-induced responses, so it is important that future work is carried out that examines skin tissue completely, so we can gain a more clinical understanding of UVA-induced tumourgenesis. To further develop the point of clinical relevance, solar radiation is comprised of both UVA (95%) and UVB (5%), meaning cells are exposed to both. Experiments should be carried out which examines the effect of simultaneous UVA and UVB irradiation, for a more clinical understanding of the effect on solar radiation on skin cancer.

## **VII. Conclusion**

The aim of this project was to build upon findings made in previous experiments in our laboratory, such as those seen in by Steel (Steel, 2016). The experiments described and discussed in this report have provided insight in the kinetics of the DNA damage response following cellular exposure to UVA. New data has been presented on how PNKP and CHK2 is phosphorylated following UVA exposure, but also how dependant these components are on ATM activity. Data on DNA damage accumulation has also been presented, which explores how fast DSBs build up following UVA exposure, and also how fast this damage is repaired. The effect of ATM inhibition via KU-60019 has also been investigated, which has caused us to question the specificity of the previously used inhibitor KU-55933. 53BP1 foci formation following UVA exposure has been studied very little prior to this project. This report presents and discusses how UVA effects 53BP1 foci formation, and also explores how the cell may affect the localisation of 53BP1, which is a topic that is still not fully understood. Overall, this project has helped develop our limited understanding of the effect of UVA

on human skin cells, and has highlighted key areas of interest that should be investigated in the future.

## References

- AGAR, N. S., HALLIDAY, G. M., BARNETSON, R., S, ANANTHASWAMY, H. N., WHEELER, M. & JONES, A. M. 2004. The basal layer in human squamous tumors harbors more UVA than UVB fingerprint mutations: A role for UVA in human skin carcinogenesis. *Proceedings of the National Academy of Sciences of the United States of America*, 101, 4954-4959.
- AHN, J., URIST M FAU - PRIVES, C. & PRIVES, C. 2004. The Chk2 protein kinase. *DNA Repair*. 3, 1039-47.
- AI, L., STEPHENSON KK FAU - LING, W., LING W FAU - ZUO, C., ZUO C FAU - MUKUNYADZI, P., MUKUNYADZI P FAU - SUEN, J. Y., SUEN JY FAU - HANNA, E., HANNA E FAU - FAN, C.-Y. & FAN, C. Y. 2003. The p16 (CDKN2a/INK4a) tumor-suppressor gene in head and neck squamous cell carcinoma: a promoter methylation and protein expression study in 100 cases. *Modern Pathology*. 16, 944-950.
- ALY, A. & GANESAN, S. 2011. BRCA1, PARP, and 53BP1: conditional synthetic lethality and synthetic viability. *Journal of Molecular Cell Biology*, 3, 66-74.
- AMERICAN CANCER SOCIETY. 2016. *Key statistics for Basal and Squamous Cell Skin Cancers*. American Cancer Society [Online]. Available: [https://www.cancer.org/cancer/basal-and-squamous-cell-skin-cancer/about/key-statistics.html#written\\_by](https://www.cancer.org/cancer/basal-and-squamous-cell-skin-cancer/about/key-statistics.html#written_by) [Accessed 13 Sep 2017].
- ANAND, P., KUNNUMAKARA, A. B., SUNDARAM, C., HARIKUMAR, K. B., THARAKAN, S. T., LAI, O. S., SUNG, B., AGGARWAL, B. B. Cancer is a Preventable Disease that Requires Major Lifestyle Changes. *Pharmaceutical Research*. 25, 2097-2116.
- ANDERSON, L., HENDERSON C FAU - ADACHI, Y. & ADACHI, Y. 2001. Phosphorylation and rapid relocalization of 53BP1 to nuclear foci upon DNA damage. *Molecular and Cellular Biology*. 21, 1719-1729
- ASCIERTO, P. A., KIRKWOOD JM FAU - GROB, J.-J., GROB JJ FAU - SIMEONE, E., SIMEONE E FAU - GRIMALDI, A. M., GRIMALDI AM FAU - MAIO, M., MAIO M FAU - PALMIERI, G., PALMIERI G FAU - TESTORI, A., TESTORI A FAU - MARINCOLA, F. M., MARINCOLA FM FAU - MOZZILLO, N. & MOZZILLO, N. 2012. The role of BRAF V600 mutation in melanoma. *Journal of Translational Medicine*. 10, 85.
- BAKKENIST, C. J. & KASTAN, M. B. 2003. DNA damage activates ATM through intermolecular autophosphorylation and dimer dissociation. *Nature*, 421, 499-506.
- BALAJEE, A. S., MAY A FAU - BOHR, V. A. & BOHR, V. A. 1999. DNA repair of pyrimidine dimers and 6-4 photoproducts in the ribosomal DNA. *Nucleic Acids Research*. 27, 2511-2520
- BALL, H. L., MYERS, J. S. & CORTEZ, D. 2005. ATRIP Binding to Replication Protein A-Single-stranded DNA Promotes ATR-ATRIP Localization but Is Dispensable for Chk1 Phosphorylation. *The American Society for Cell Biology*, 16, 2372-2381.
- BANERJEE, S. K., CHRISTENSEN RB FAU - LAWRENCE, C. W., LAWRENCE CW FAU - LECLERC, J. E. & LECLERC, J. E. 1988. Frequency and spectrum of mutations produced by a single cis-syn thymine-thymine cyclobutane dimer in a single-stranded vector. *Proceedings of the National Academy of Sciences of the United States of America*. 85, 8141-8145.
- BARLOW, C., HIROTSUNE, S., PAYLOR, R., LIYANAGE, M., ECKHAUS, M., COLLINS, F., SHILOH, Y., CRAWLEY, J. N., RIED, T., TAGLE, D. & WYNSHAW-BORIS, A. 1996. Atm-deficient mice: a paradigm of ataxia telangiectasia. *Cell*, 86, 159-71.
- BARONE, G., GROOM, A., REIMAN, A., SRINIVASAN, V., BYRD, P. J., MALCOM, A. & TAYLOR, R. 2009. Modeling ATM mutant proteins from missense changes confirms retained kinase activity. *Human Mutation*. 30, 1222-1230.
- BASSET-SEGUIN, N., MOLES, J. P., MILS, V., DEREURE, O. & GUILHOU, J. J. 1994. TP53 tumor suppressor gene and skin carcinogenesis. *J Invest Dermatol*, 103, 102s-106s.
- BECKERMAN, R. & PRIVES, C. 2010. Transcriptional regulation by p53. *Cold Spring Harb Perspect Biol*, 2, a000935.
- BENJAMIN, C. L. & ANANTHASWAMY, H. N. 2007. p53 and the Pathogenesis of Skin Cancer. *Toxicology and applied pharmacology*, 224, 241-248.

- BERG, R. J., VAN KRANEN, H. J., REBEL, H. G., DE VRIES, A., VAN VOLTEN, W. A., VAN KREIJL, C. F., VAN DER LUEN, J. C. & DE GRUIJL, F. R. 1996. Early p53 alterations in mouse skin carcinogenesis by UVB radiation: immunohistochemical detection of mutant p53 protein in clusters of preneoplastic epidermal cells. *Proceedings of the National Academy of Sciences of the United States of America*, 93, 274-278.
- BERNSTEIN, N. K., WILLIAMS RS FAU - RAKOVSKY, M. L., RAKOVSKY ML FAU - CUI, D., CUI D FAU - GREEN, R., GREEN R FAU - KARIMI-BUSHERI, F., KARIMI-BUSHERI F FAU - MANI, R. S., MANI RS FAU - GALICIA, S., GALICIA S FAU - KOCH, C. A., KOCH CA FAU - CASS, C. E., CASS CE FAU - DUROCHER, D., DUROCHER D FAU - WEINFELD, M., WEINFELD M FAU - GLOVER, J. N. M. & GLOVER, J. N. 2005. The molecular architecture of the mammalian DNA repair enzyme, polynucleotide kinase. *Molecular Cell*. 17, 657-670.
- BOGDANOV, K. V., CHUKHLOVIN, A. B., ZARITSKEY, A. Y., FROLOVA, O. I. & AFANASIEV, B. V. 1997. Ultraviolet irradiation induces multiple DNA double-strand breaks and apoptosis in normal granulocytes and chronic myeloid leukaemia blasts. *Br J Haematol*, 98, 869-72.
- BOLSHAKOV, S., WALKER, C. M., STROM, S. S., SELVAN, M. S., CLAYMAN, G. L., EL-NAGGAR, A., S.M, L., KRIPKE, L. M. & ANANTHASWAMY, H. N. 2003. p53 Mutations in Human Aggressive and Nonaggressive Basal and Squamous Cell Carcinomas. *Clinical Cancer Research*, 9, 228-234.
- BONIOL, M., AUTIER, P., BOYLE, P. & GANDINI, S. 2012. Cutaneous melanoma attributable to sunbed use: systematic review and meta-analysis. *BMJ : British Medical Journal*, 345.
- BOUVARD, V., ZAITCHOUK T FAU - VACHER, M., VACHER M FAU - DUTHU, A., DUTHU A FAU - CANIVET, M., CANIVET M FAU - CHOISY-ROSSI, C., CHOISY-ROSSI C FAU - NIERUCHALSKI, M., NIERUCHALSKI M FAU - MAY, E. & MAY, E. 2000. Tissue and cell-specific expression of the p53-target genes: bax, fas, mdm2 and waf1/p21, before and following ionising irradiation in mice. *Oncogene*. 16, 649-660.
- BRASH, D. E. 2015. UV Signature Mutations (). *Photochemistry and photobiology*, 91, 15-26.
- BROERTJES, J. 2015. The Ten Hallmarks of Cancer in Cutaneous Malignant Melanoma. *UNAV Journal for Medical Students*. 1, 6-9.
- BROWN, E. J. & BALTIMORE, D. 2000. ATR disruption leads to chromosomal fragmentation and early embryonic lethality. *Genes and Development*, 14, 397-402.
- BRUGAROLAS, J., MOBERG K FAU - BOYD, S. D., BOYD SD FAU - TAYA, Y., TAYA Y FAU - JACKS, T., JACKS T FAU - LEES, J. A. & LEES, J. A. 1999. Inhibition of cyclin-dependent kinase 2 by p21 is necessary for retinoblastoma protein-mediated G1 arrest after gamma-irradiation. *Proceedings of the National Academy of Sciences of the United States of America*. 96, 1002-1007
- BRUINS, W., ZWART, E., ATTARDI, L. D., IWAKUMA, T., HOOGERVORST, E. M., BEEMS, R. B., MIRANDA, B., VAN OOSTROM, C. T., VAN DEN BERG, J., VAN DEN AARDWEG, G. J., LOZANO, G., VAN STEEG, H., JACKS, T. & DE VRIES, A. 2004. Increased sensitivity to UV radiation in mice with a p53 point mutation at Ser389. *Mol Cell Biol*, 24, 8884-94.
- BUNTING, S. F., CALLEN E FAU - WONG, N., WONG N FAU - CHEN, H.-T., CHEN HT FAU - POLATO, F., POLATO F FAU - GUNN, A., GUNN A FAU - BOTHMER, A., BOTHMER A FAU - FELDHAHN, N., FELDHAHN N FAU - FERNANDEZ-CAPETILLO, O., FERNANDEZ-CAPETILLO O FAU - CAO, L., CAO L FAU - XU, X., XU X FAU - DENG, C.-X., DENG CX FAU - FINKEL, T., FINKEL T FAU - NUSSENZWEIG, M., NUSSENZWEIG M FAU - STARK, J. M., STARK JM FAU - NUSSENZWEIG, A. & NUSSENZWEIG, A. 2010. 53BP1 inhibits homologous recombination in Brca1-deficient cells by blocking resection of DNA breaks. *Cell*. 141, 243-254.
- CAI, Z., CHEHAB NH FAU - PAVLETICH, N. P. & PAVLETICH, N. P. 2009. Structure and activation mechanism of the CHK2 DNA damage checkpoint kinase. *Molecular Cell*. 35, 818-829.
- CANCER RESEARCH UK. 2016. Skin cancer incidence statistics [Online] Available: <http://www.cancerresearchuk.org/health-professional/cancer-statistics/statistics-by-cancer-type/skin-cancer/incidence#heading-Zero> [Assessed 30 Oct 2017]

- CHAPMAN, J R., BARRAL, P., VANNIER, J.-B., BOREL, V., STEGER, M., TOMAS-LOBA, A., SARTORI, ALESSANDRO A., ADAMS, IAN R., BATISTA, FACUNDO D. & BOULTON, SIMON J. 2013. RIF1 Is Essential for 53BP1-Dependent Nonhomologous End Joining and Suppression of DNA Double-Strand Break Resection. *Molecular Cell*, 49, 858-871.
- CHAPPELL, C., HANAKAHI, L. A., KARIMI-BUSHERI, F., WEINFELD, M. & WEST, S. C. 2002. Involvement of human polynucleotide kinase in double-strand break repair by non-homologous end joining. *Embo j*, 21, 2827-32.
- CHEN, J., SAHA, P., KORNBLUTH, S., DYNLACHT, B. D. & DUTTA, A. 1996. Cyclin-binding motifs are essential for the function of p21CIP1. *Molecular and Cellular Biology*, 16, 4673-4682.
- CHENE, P. 2001. The role of tetramerization in p53 function. *Oncogene*. 20, 2611-2617
- CHOI, J.-H., BESARATINIA, A., LEE, D.-H., LEE, C.-S. & P, P. G. 2006. *The role of DNA polymerase  $\iota$  in UV mutational spectra*. Elsevier. 559, 58-65.
- COELHO, S. G. & HEARING, V. J. 2010. UVA tanning is involved in the increased incidence of skin cancers in fair-skinned young women. *Pigment cell and melanoma research*. 23, 57-63
- COLANTONIO, S., BRACKEN, M. B. & BEECKER, J. 2014. The association of indoor tanning and melanoma in adults: systematic review and meta-analysis. *Journal of the American Academy of Dermatology*. 70, 847-857.
- CORTES-GUTIERREZ, E. I., HERNANDEZ-GARZA, F., GARCIA-PEREZ, J. O., DAVILA-RODRIGUEZ, M. I., AGUADO-BARRERA, M. E. & CERDA-FLORES, R. M. 2012. Evaluation of DNA single and double strand breaks in women with cervical neoplasia based on alkaline and neutral comet assay techniques. *J Biomed Biotechnol*, 2012, 385245.
- DANG, C. V. 1999. c-Myc Target Genes Involved in Cell Growth, Apoptosis, and Metabolism. *Mol and Cellular Biol*. 19, 1-11.
- DANIEL, J. A., PELLEGRINI, M., LEE, B. S., GUO, Z., FILSUF, D., BELKINA, N. V., YOU, Z., PAULL, T. T., SLECKMAN, B. P., FEIGENBAUM, L. & NUSSENZWEIG, A. 2012. Loss of ATM kinase activity leads to embryonic lethality in mice. *J Cell Biol*, 198, 295-304.
- DAVIES, H., BIGNELL, G. R., COX, C., STEPHENS, P., EDKINS, S., CLEGG, S., TEAGUE, J., WOFFENDIN, H., GARNETT, M. J., BOTTOMLEY, W., DAVIS, N., DICKS, E., EWING, R., FLOYD, Y., GRAY, K., HALL, S., HAWES, R., HUGHES, J., KOSMIDOU, V., MENZIES, A., MOULD, C., PARKER, A., STEVENS, C., WATT, S., HOOPER, S., WILSON, R., JAYATILAKE, H., GUSTERSON, B. A., COOPER, C., SHIPLEY, J., HARGRAVE, D., PRITCHARD-JONES, K., MAITLAND, N., CHENEVIX-TRENCH, G., RIGGINS, G. J., BIGNER, D. D., PALMIERI, G., COSSU, A., FLANAGAN, A., NICHOLSON, A., HO, J. W., LEUNG, S. Y., YUEN, S. T., WEBER, B. L., SEIGLER, H. F., DARROW, T. L., PATERSON, H., MARAIS, R., MARSHALL, C. J., WOOSTER, R., STRATTON, M. R. & FUTREAL, P. A. 2002. Mutations of the BRAF gene in human cancer. *Nature*, 417, 949-54.
- DAYA-GROSJEAN, L., 2008. Xeroderma pigmentosum and skin cancer. *Advances in experimental medicine and biology*., 637, 19-27.
- DELACROIX, S., WAGNER, J. M., KOBAYASHI, M., YAMAMOTO, K. & KARNITZ, L. M. 2007. The Rad9–Hus1–Rad1 (9–1–1) clamp activates checkpoint signaling via TopBP1. *Genes and Development*, 21, 1472-1477.
- DELPHI, C., HUANG, K.-P., SCOTTO, C., CHAPEL, A., VINCON, M., CHAMBAZ, E., GARIN, J. & BAUDIER, J. 1997. The in Vitro Phosphorylation of P53 by Calcium-Dependent Protein Kinase C. *European Journal of Biochemistry*, 245, 684-692.
- DIFFEY, B. L. A quantitative estimate of melanoma mortality from ultraviolet A sunbed use in the U.K.
- DOIL, C., MAILAND N FAU - BEKKER-JENSEN, S., BEKKER-JENSEN S FAU - MENARD, P., MENARD P FAU - LARSEN, D. H., LARSEN DH FAU - PEPPERKOK, R., PEPPERKOK R FAU - ELLENBERG, J., ELLENBERG J FAU - PANIER, S., PANIER S FAU - DUROCHER, D., DUROCHER D FAU - BARTEK, J., BARTEK J FAU - LUKAS, J., LUKAS J FAU - LUKAS, C. & LUKAS, C. 2009. RNF168 binds and amplifies ubiquitin conjugates on damaged chromosomes to allow accumulation of repair proteins. *Cell*. 136, 435-446.

- ELSON, A., WANG, Y., DAUGHERTY, C. J., MORTON, C. C., ZHOU, F., CAMPOS-TORRES, J. & LEDER, P. 1996. Pleiotropic defects in ataxia-telangiectasia protein-deficient mice. *Proc Natl Acad Sci U S A*, 93, 13084-9.
- ENGELFRIET PM FAU - JANSEN, E. H. J. M., JANSEN EH FAU - PICAVET, H. S. J., PICAVET HS FAU - DOLLE, M. E. T. & DOLLE, M. E. 2013. Biochemical markers of aging for longitudinal studies in humans. *Epidemiologic Reviews*. 35, 132-151.
- ESCRIBANO-DIAZ, C., ORTHWEIN, A., FRADET-TURCOTTE, A., XING, M., YOUNG, J. T., TKAC, J., COOK, M. A., ROSEBROCK, A. P., MUNRO, M., CANNY, M. D., XU, D. & DUROCHER, D. 2013. A cell cycle-dependent regulatory circuit composed of 53BP1-RIF1 and BRCA1-CtIP controls DNA repair pathway choice. *Mol Cell*, 49, 872-83.
- ESPINOSA, J. M. & EMERSON, B. M. 2001. Transcriptional regulation by p53 through intrinsic DNA/chromatin binding and site-directed cofactor recruitment. *Molecular Cell*. 8, 57-69.
- FALCK, J., COATES, J. & JACKSON, S. P. 2005. Conserved modes of recruitment of ATM, ATR and DNA-PKcs to sites of DNA damage. *Nature*, 434, 605-611.
- FALCK, J., MAILAND N FAU - SYLJUASEN, R. G., SYLJUASEN RG FAU - BARTEK, J., BARTEK J FAU - LUKAS, J. & LUKAS, J. 2001. The ATM-Chk2-Cdc25A checkpoint pathway guards against radioresistant DNA synthesis. *Nature*. 410, 842-847.
- FELL, L. J., PAUL, N. D. & MCMILLAN, T. J. 2002. Role for non-homologous end-joining in the repair of UVA-induced DNA damage. *Int J Radiat Biol*, 78, 1023-7.
- FENG, L. & CHEN, J. 2012. The E3 ligase RNF8 regulates KU80 removal and NHEJ repair. *Nature Structural and molecular biology*. 19, 201-206.
- FENG, L., LI, N., LI, Y., WANG, J., GAO, M., WANG, W. & CHEN, J. 2015. Cell cycle-dependent inhibition of 53BP1 signaling by BRCA1. *Cell Discovery*, 1, 15019.
- FOULKES, W. D., FLANDERS, T. Y., POLLOCK, P. M. & HAYWARD, N. K. 1997. The CDKN2A (p16) gene and human cancer. *Molecular Medicine*, 3, 5-20.
- GOLDING, S. E., ROSENBERG, E., VALERIE, N., FRIGERIO, M., COCKROFT, X., CHONG, W., HUMMERSONE, M., RIGOEREAU, L., MENEAR, K. A., O'CONNOR, M., POVIRK, L. F., VAN METER, T. & VALERIE, K. 2009. Improved ATM kinase inhibitor KU-60019 radiosensitizes glioma cells, compromises insulin, AKT and ERK prosurvival signaling, and inhibits migration and invasion. *Molecular Cancer Therapeutics*, 8, 2894-2902.
- GÖTZ, C., SCHOLTES, P., PROWALD, A., SCHUSTER, N., NASTAINCZYK, W. & MONTENARH, M. 1999. Protein kinase CK2 interacts with a multi-protein binding domain of p53. *Molecular and Cellular Biochemistry*, 191, 111-120.
- GRAWUNDER, U., WILM, M., WU, X., KULESZA, P., WILSON, T. E., MANN, M. & LIEBER, M. R. 1997. Activity of DNA ligase IV stimulated by complex formation with XRCC4 protein in mammalian cells. *Nature*, 388, 492-495.
- GREINERT, R., VOLKMER, B., HENNING, S., BREITBART, E. W., GREULICH, K. O., CARDOSO, M. C. & RAPP, A. 2012. UVA-induced DNA double-strand breaks result from the repair of clustered oxidative DNA damages. *Nucleic Acids Res*, 40, 10263-73.
- GREULICH, K. M., UTIKAL, J., PETER, R. U. & KRAHN, G. 2000. c-MYC and nodular malignant melanoma. A case report. *Cancer*. 89, 97-103.
- GU, J., LU, H., TIPPIN, B., SHIMAZAKI, N., GOODMAN, M. F. & LIEBER, M. R. 2007. XRCC4:DNA ligase IV can ligate incompatible DNA ends and can ligate across gaps. *The EMBO Journal*, 26, 1010-1023.
- HA, L., NOONAN, F., DE FABO, E. & MERLINO, G. 2005. *Animal Models of Melanoma*. The journal of investigative dermatology. Symposium proceedings. 10, 86-88.
- HAMARD, P. J., LUKIN DJ FAU - MANFREDI, J. J. & MANFREDI, J. J. 2012. p53 basic C terminus regulates p53 functions through DNA binding modulation of subset of target genes. *Journal of Biological Chemistry*. 287, 22397-22407.
- HANAHAHAN, D. & WEINBERG, R. A. 2000. The hallmarks of cancer. *Cell*. 100, 57-70
- HANAHAHAN, D & WEINBERG, R. A. 2011. Hallmarks of Cancer: The Next Generation. *Cell*. 144, 646-674

- HARRIGAN, J. A., BELOTSEKOVSKAYA, R., COATES, J., DIMITROVA, D. S., POLO, S. E., BRADSHAW, C. R., FRASER, P. & JACKSON S. P. 2011. Replication stress induces 53BP1-containing OPT domains in G1 cells. *Journal of Cell Biology*. 193, 97-108.
- HAYWARD, N. K. 2003. Genetics of melanoma predisposition. *Nature: Oncogene*. 22, 3053-3062.
- HICKSON, I., ZHAO, Y., RICHARDSON, C. J., GREEN, S. J., MARTIN, N. M. B., ORR, A. I., REAPER, P. M., JACKSON, S. P., CURTIN, N. J. & SMITH, G. C. M. 2004. Identification and Characterization of a Novel and Specific Inhibitor of the Ataxia-Telangiectasia Mutated Kinase ATM. *Cancer Research*, 64, 9152.
- HODIS, E., WATSON, I. R., KRYUKOV, G. V., AROLD, S. T., IMIELINSKI, M., THEURILLAT, J.-P., NICKERSON, E., AUCLAIR, D., LI, L., PLACE, C., DICARA, D., RAMOS, A. H., LAWRENCE, M. S., CIBULSKIS, K., SIVACHENKO, A., VOET, D., SAKSENA, G., STRANSKY, N., ONOFRIO, R. C., WINCKLER, W., ARDLIE, K., WAGLE, N., WARGO, J., CHONG, K., MORTON, D. L., STEMKE-HALE, K., CHEN, G., NOBLE, M., MEYERSON, M., LADBURY, J. E., DAVIES, M. A., GERSHENWALD, J. E., WAGNER, S. N., HOON, D. S. B., SCHADENDORF, D., LANDER, E. S., GABRIEL, S. B., GETZ, G., GARRAWAY, L. A. & CHIN, L. 2012. A Landscape of Driver Mutations in Melanoma. *Cell*, 150, 251-263.
- HOWLADER, N., NOONE, A. M., KRAPCHO, M., MILLER, D., BISHOP, K., KOSARY, C. L., YU, M., RUHL, J., TATALOVICH, Z., MARIOTTO, A., LEWIS, D. R., CHEN, H. S., FEUER, E. J., CRONIN, K. A (eds). 2016. SEER Cancer Statistics Review, 1975-2014. National Cancer Institute. [Online] Available: [https://seer.cancer.gov/csr/1975\\_2014/](https://seer.cancer.gov/csr/1975_2014/) [Assessed: 05/02/17].
- HUEN, M. S. & CHEN, J. 2010. Assembly of checkpoint and repair machineries at DNA damage sites. *Trends in Biochemical Sciences*. 35, 101-108.
- IARC. 1992. *IARC Monographs on the Evaluation of Carcinogenic Risks to Humans: Solar and Ultraviolet radiation*. [Online]. Available: <http://monographs.iarc.fr/ENG/Monographs/vol55/mono55.pdf> [Accessed 18 Oct 2016].
- IARC. 2009. *Sunbeds and UV Radiation* [Online]. Available: [https://www.iarc.fr/en/media-centre/iarcnews/2009/sunbeds\\_uvradiation.php](https://www.iarc.fr/en/media-centre/iarcnews/2009/sunbeds_uvradiation.php) [Accessed 2 Oct 2017].
- IKEHATA, H. & ONO, T. 2011. The mechanisms of UV mutagenesis. *The Journal of Radiation Research*. 52, 115-125
- INNOCENTE, S. A., ABRAHAMSON JL FAU - COGSWELL, J. P., COGSWELL JP FAU - LEE, J. M. & LEE, J. M. 1999. p53 regulates a G2 checkpoint through cyclin B1. *Proceedings of the National Academy of Sciences of the United States of America*. 96, 2147-2152.
- JASIN, M. & ROTHSTEIN, R. 2013. Repair of Strand Breaks by Homologous Recombination. *Cold Spring Harbor Perspectives in Biology*, 5, a012740.
- JOWSEY, P. A., DOHERTY, A. J. & ROUSE, J. 2004. Human PTIP Facilitates ATM-mediated Activation of p53 and Promotes Cellular Resistance to Ionizing Radiation. *Journal of Biological Chemistry*, 279, 55562-55569.
- KINNER, A., WU, W., STAUDT, C. & ILIAKIS, G. 2008.  $\gamma$ -H2AX in recognition and signaling of DNA double-strand breaks in the context of chromatin. *Nucleic Acids Research*, 36, 5678-5694.
- KOBAYASHI, J., TAUCHI, H., SAKAMOTO, S., NAKAMURA, K., MATSUURA, T., KOBAYASHI, T., TAMAI, K., TANIMOTO, K. & KOMASTSU, K. 2002. NBS1 localizes to gamma-H2AX foci through interaction with the FHA/BRCT domain. *Current Biology*, 29, 1846-1851.
- KOZLOV, S. V., GRAHAM, M. E., PENG, C., CHEN, P., ROBINSON, P. J. & LAVIN, M. F. 2006. Involvement of novel autophosphorylation sites in ATM activation. *The EMBO Journal*, 25, 3504-3514.
- KROIS, A. S., FERREON, J. C., MARTINEZ-YAMOUT, M. A., DYSON, H. J. A.-O. H. O. O. & WRIGHT, P. E. 2016. Recognition of the disordered p53 transactivation domain by the transcriptional adapter zinc finger domains of CREB-binding protein. *Proceedings of the National Academy of Sciences of the United States of America*. 113, 1853-62.

- KUMAGAI, A. & DUNPHY, W. G. 2000. Claspin, a novel protein required for the activation of Chk1 during a DNA replication checkpoint response in *Xenopus* egg extracts. *Molecular Cell*, 6, 839-49.
- KUMARAVEL, T. S. & JHA, A. N. 2006. Reliable Comet assay measurements for detecting DNA damage induced by ionising radiation and chemicals. *Mutat Res*, 605, 7-16.
- KUCHENBAECKER, K.B., HOPPER, J.L., BARNES, D.R., et al. 2017 Risks of breast, ovarian, and contralateral breast cancer for BRCA1 and BRCA2 mutation carriers. *JAMA*. 317, 2402-2416
- KUO, L. J. & YANG, L. X. 2008. Gamma-H2AX - a novel biomarker for DNA double-strand breaks. *In Vivo*. 22, 305-309.
- KUZU, O. F., NGUYEN, F. D., NOORY, M. A. & SHARMA, A. 2015. Current State of Animal (Mouse) Modeling in Melanoma Research. *Cancer Growth and Metastasis*, 8, 81-94.
- LANKINEN, M. H., VILPO, L. M. & VILPO, J. A. 1996. UV- and gamma-irradiation-induced DNA single-strand breaks and their repair in human blood granulocytes and lymphocytes. *Mutat Res*, 352, 31-8.
- LANS, H., MARTEIJN JA FAU - VERMEULEN, W. & VERMEULEN, W. 2012. ATP-dependent chromatin remodeling in the DNA-damage response. *Epigenetics and chromatin*. 5, 4.
- LAVIN, M. F., SCOTT S FAU - GUEVEN, N., GUEVEN N FAU - KOZLOV, S., KOZLOV S FAU - PENG, C., PENG C FAU - CHEN, P. & CHEN, P. 2004. Functional consequences of sequence alterations in the ATM gene. *DNA repair*. 3, 1197-1205.
- LEE, C. W., MARTINEZ-YAMOUT MA FAU - DYSON, H. J., DYSON HJ FAU - WRIGHT, P. E. & WRIGHT, P. E. 2010. Structure of the p53 transactivation domain in complex with the nuclear receptor coactivator binding domain of CREB binding protein. *Biochemistry*. 49, 9964-9971.
- LEITER, U. & GARBE, C. 2008. Epidemiology of melanoma and nonmelanoma skin cancer--the role of sunlight. *Advances in experimental medicine and biology*. 624, 89-103.
- LEY, R. D. 1997. Ultraviolet Radiation A-induced Precursors of Cutaneous Melanoma in *Monodelphis domestica*. *Cancer Research*, 57, 3682-3684.
- LI, H., XIE B FAU - RAHMEH, A., RAHMEH A FAU - ZHOU, Y., ZHOU Y FAU - LEE, M. Y. W. T. & LEE, M. Y. 2006. Direct interaction of p21 with p50, the small subunit of human DNA polymerase delta. *Cell cycle*. 5, 428-436.
- LI, J. & STERN, D. F. 2005. Regulation of CHK2 by DNA-dependent protein kinase. *J Biol Chem*, 280, 12041-50.
- LI, Y. & YANG, D.-Q. 2010. The ATM Inhibitor KU-55933 Suppresses Cell Proliferation and Induces Apoptosis by Blocking Akt In Cancer Cells with Overactivated Akt. *Molecular Cancer Therapeutics*, 9, 113.
- LIU, G. & CHEN, X. 2006. DNA polymerase eta, the product of the xeroderma pigmentosum variant gene and a target of p53, modulates the DNA damage checkpoint and p53 activation. *Mol Cell Biol*, 26, 1398-413.
- LOUGHERY, J., COX, M., SMITH, L. M. & MEEK, D. W. 2014. Critical role for p53-serine 15 phosphorylation in stimulating transactivation at p53-responsive promoters. *Nucleic Acids Research*, 42, 7666-7680.
- LU, C., ZHU, F., CHO, Y.-Y., TANG, F., ZYKOVA, T., MA, W.-Y., BODE, A. M. & DONG, Z. Cell Apoptosis: Requirement of H2AX in DNA Ladder Formation, but Not for the Activation of Caspase-3. *Molecular Cell*, 23, 121-132.
- MA, Y., PANNICKE U FAU - SCHWARZ, K., SCHWARZ K FAU - LIEBER, M. R. & LIEBER, M. R. 2002. Hairpin opening and overhang processing by an Artemis/DNA-dependent protein kinase complex in nonhomologous end joining and V(D)J recombination. *Cell*. 108, 781-794.
- MARTI, T. M., HEFNER, E., FEENEY, L., NATALE, V. & CLEAVER, J. E. 2006. H2AX phosphorylation within the G1 phase after UV irradiation depends on nucleotide excision repair and not DNA double-strand breaks. *Proceedings of the National Academy of Sciences*. 103, 9891-9896.
- MAO, Z., BOZZELLA, M., SELUANOV, A., GORBUNOVA, V. 2008. DNA repair by nonhomologous end joining and homologous recombination during cell cycle in human cells. *Cell Cycle*. 7, 2902-6

- MARTEIJN, J. A., LANS, H., VERMULEN, W. & J.H.J, H. 2014. Understanding nucleotide excision repair and its roles in cancer and ageing. *Nature Reviews Molecular Cell Biology*, 15, 465-481.
- MATHEWS, C. K., VAN HOLDE, K. E. & AHERN, K. G. 2000. *Biochemistry*, San Fransisco, The Benjamin/Cummings Publishing Company INC.
- MCCULLOCH, S. D., KOKOSKA, R. J., MASUTANI, C., IWAI, S., HANAOKA, F. & KUNKEL, T. A. 2004. Preferential cis-syn thymine dimer bypass by DNA polymerase eta occurs with biased fidelity. *Nature*, 428, 97-100.
- MCKINNEY, K., MATTIA M FAU - GOTTIFREDI, V., GOTTIFREDI V FAU - PRIVES, C. & PRIVES, C. 2004. p53 linear diffusion along DNA requires its C terminus. *Molecular Cell*. 16, 413-424.
- MEDHURST, A. L., WARMERDAM, D. O., AKERMAN, I., VERWAYEN, E. H., KANAAR, R., SMITS, V. A. & LAKIN, N. D. 2008. ATR and Rad17 collaborate in modulating Rad9 localisation at sites of DNA damage. *J Cell Sci*, 121, 3933-40.
- MEREDITH, P. & RIESZ, J. 2004. Radiative relaxation quantum yields for synthetic eumelanin. *Photochemistry and photobiology*. 79, 211-216.
- MEYER, B., VOSS, K., TOBIAS, F., JAKOB, B., DURANTE, M. & TAUCHER-SCHOLZ, G. 2013. Clustered DNA damage induces pan-nuclear H2AX phosphorylation mediated by ATM and DNA-PK. *Nuclei Acid Res*. 41, 6109-6118.
- MITCHELL, D. L., FERNANDEZ, A. A., NAIRN, R. S., GARCIA, R., PANIKER, L., TRONO, D., THAMES, H. D. & GIMENEZ-CONTI, I. 2010. Ultraviolet A does not induce melanomas in a Xiphophorus hybrid fish model. *Proceedings of the National Academy of Sciences*, 107, 9329-9334.
- MOON, A. F., GARCIA-DIAZ, M., BATRA, V. K., BEARD, W. A., BEBENEK, K., KUNKEL, T. A., WILSON, S. H. & PEDERSEN, L. C. 2007. The X Family Portrait: Structural Insights into Biological Functions of X Family Polymerases. *DNA repair*, 6, 1709-1725.
- MOYNAHAN, M.E., CHIU. J.W., KOLLER. B.H. & JASIN, M. 1999. Brca1 Controls Homology-Directed DNA Repair. *Mol Cell*. 4, 511-518.
- MOYNAHAN, M.E., PIERCE. A.J. & JASIN. M. 2001. BRCA2 Is Required for Homology-Directed Repair of Chromosomal Breaks. *Mol. Cell*. 7, 263-272.
- NAGATA, S. & GOLSTEIN, P. 1995. The Fas death factor. *Science*. 267, 1449-1456.
- NCIN. 2013. *Non-melanoma skin cancer in England, Scotland, Northern Ireland, and Ireland* [Online]. Available: <http://www.ncin.org.uk/view?rid=2178> [Accessed 18 Oct 2016].
- NOONAN, F. P., ZAIDI, M. R., WOLNICKA-GLUBISZ, A., ANVER, M. R., BAHN, J., WIELGUS, A., CADET, J., DOUKI, T., MOURET, S., TUCKER, M. A., POPRATILOFF, A., MERLINO, G. & DE FABO, E. C. 2012. Melanoma induction by ultraviolet A but not ultraviolet B radiation requires melanin pigment. *Nature Communications*, 3, 884.
- O'NEILL, P. & WARDMAN, P. 2009. Radiation chemistry comes before radiation biology. *International Journal of Radiation Biology*, 85, 9-25.
- OPENSTAX COLLEGE. 2013. *Anatomy and Physiology*. [Online] Available: <https://cnx.org/contents/FPtK1z mh@6.27:RxywCGkA@5/Layers-of-the-Skin> [Assessed: 30/10/2017]
- ORTHWEIN, A., NOORDERMEER, S. M., WILSON, M. D., LANDRY, S., ENCHEV, R. I., SHERKER, A., MUNRO, M., PINDER, J., SALSMAN, J., DELLAIRE, G., XIA, B., PETER, M. & DUROCHER, D. 2015. A mechanism for the suppression of homologous recombination in G1 cells. *Nature*, 528, 422-426.
- OSIPOV, A. N., SMETANINA, N. M., PUSTOVALOVA, M. V., ARKHANGELSKAYA, E. & KLOKOV, D. 2014. The formation of DNA single-strand breaks and alkali-labile sites in human blood lymphocytes exposed to 365-nm UVA radiation. *Free Radical Biology and Medicine*, 73, 34-40.
- OU, Y.-H., CHUNG, P.-H., SUN, T.-P. & SHIEH, S.-Y. 2005. p53 C-Terminal Phosphorylation by CHK1 and CHK2 Participates in the Regulation of DNA-Damage-induced C-Terminal Acetylation. *Molecular Biology of the Cell*, 16, 1684-1695.

- PANDITA, T. K. & RICHARDSON, C. 2009. Chromatin remodeling finds its place in the DNA double-strand break response. *Nucleic Acids Research*, 37, 1363-1377.
- PANIER, S. & BOULTON, S. J. 2014. Double-strand break repair: 53BP1 comes into focus. *Nature reviews. Molecular cell biology*. 15, 7-18.
- PARKIN, D. M., MESHER D FAU - SASIENI, P. & SASIENI, P. 13. 2011. Cancers attributable to solar (ultraviolet) radiation exposure in the UK in 2010. *British journal of cancer*. 105, 66-69.
- PAULL, T. T. & GELLERT, M. 1998. The 3' to 5' exonuclease activity of Mre 11 facilitates repair of DNA double-strand breaks. *Molecular Cell*. 1, 969-979.
- PEI, H., ZHANG, L., LUO, K., QIN, Y., CHESI, M., FEI, F., BERGSAGEL, P. L., WANG, L., YOU, Z. & LOU, Z. 2011. MMSET regulates histone H4K20 methylation and 53BP1 accumulation at DNA damage sites. *Nature*, 470, 124-128.
- PFEIFER, G. P., YOU, Y.-H. & BESARATINIA, A. 2005. Mutations induced by ultraviolet light. *MUTATION RESEARCH-FUNDAMENTAL AND MOLECULAR MECHANISMS OF MUTAGENESIS*, 571, 19-31.
- PLEASANCE, E. D., CHEETHAM, R. K., STEPHENS, P. J., MCBRIDE, D. J., HUMPHRAY, S. J., GREENMAN, C. D., VARELA, I., LIN, M. L., ORDONEZ, G. R., BIGNELL, G. R., YE, K., ALIPAZ, J., BAUER, M. J., BEARE, D., BUTLER, A., CARTER, R. J., CHEN, L., COX, A. J., EDKINS, S., KOKKO-GONZALES, P. I., GORMLEY, N. A., GROCOCK, R. J., HAUDENSCHILD, C. D., HIMMS, M. M., JAMES, T., JIA, M., KINGSBURY, Z., LEROY, C., MARSHALL, J., MENZIES, A., MUDIE, L. J., NING, Z., ROYCE, T., SCHULZ-TRIEGLAFF, O. B., SPIRIDOU, A., STEBBINGS, L. A., SZAJKOWSKI, L., TEAGUE, J., WILLIAMSON, D., CHIN, L., ROSS, M. T., CAMPBELL, P. J., BENTLEY, D. R., FUTREAL, P. A. & STRATTON, M. R. 2010. A comprehensive catalogue of somatic mutations from a human cancer genome. *Nature*, 463, 191-6.
- PORTER, A. G. & JANICKE, R. U. 1999. Emerging roles of caspase-3 in apoptosis. *Cell death and differentiation*. 6, 99-104.
- PUNTERVOLL, H. E., YANG XR FAU - VETTI, H. H., VETTI HH FAU - BACHMANN, I. M., BACHMANN IM FAU - AVRIL, M. F., AVRIL MF FAU - BENFODDA, M., BENFODDA M FAU - CATRICALA, C., CATRICALA C FAU - DALLE, S., DALLE S FAU - DUVAL-MODESTE, A. B., DUVAL-MODESTE AB FAU - GHIORZO, P., GHIORZO P FAU - GRAMMATICO, P., GRAMMATICO P FAU - HARLAND, M., HARLAND M FAU - HAYWARD, N. K., HAYWARD NK FAU - HU, H.-H., HU HH FAU - JOUARY, T., JOUARY T FAU - MARTIN-DENAVIT, T., MARTIN-DENAVIT T FAU - OZOLA, A., OZOLA A FAU - PALMER, J. M., PALMER JM FAU - PASTORINO, L., PASTORINO L FAU - PJANOVA, D., PJANOVA D FAU - SOUFIR, N., SOUFIR N FAU - STEINE, S. J., STEINE SJ FAU - STRATIGOS, A. J., STRATIGOS AJ FAU - THOMAS, L., THOMAS L FAU - TINAT, J., TINAT J FAU - TSAO, H., TSAO H FAU - VEINALDE, R., VEINALDE R FAU - TUCKER, M. A., TUCKER MA FAU - BRESSAC-DE PAILLERETS, B., BRESSAC-DE PAILLERETS B FAU - NEWTON-BISHOP, J. A., NEWTON-BISHOP JA FAU - GOLDSTEIN, A. M., GOLDSTEIN AM FAU - AKSLEN, L. A., AKSLEN LA FAU - MOLVEN, A. & MOLVEN, A. 2012. Melanoma prone families with CDK4 germline mutation: phenotypic profile and associations with MC1R variants. *Journal of medical genetics*. 50, 264-270.
- RAPP, A. & GREULICH, K. O. 2004. After double-strand break induction by UV-A, homologous recombination and nonhomologous end joining cooperate at the same DSB if both systems are available. *Journal of Cell Science*, 117, 4935.
- RAPPOLD, I., IWABUCHI, K., DATE, T. & CHEN, J. 2001. Tumor Suppressor P53 Binding Protein 1 (53bp1) Is Involved in DNA Damage–Signaling Pathways. *The Journal of Cell Biology*, 153, 613-620.
- REYNOLDS, P., ANDERSON, J. A., HARPER, J. V., HILL, M. A., BOTCHWAY, S. W., PARKER, A. W. & O'NEILL, P. 2012. The dynamics of Ku70/80 and DNA-PKcs at DSBs induced by ionizing radiation is dependent on the complexity of damage. *Nucleic Acids Research*, 40, 10821-10831.

- REZNIKOFF, C. A., YEAGER TR FAU - BELAIR, C. D., BELAIR CD FAU - SAVELIEVA, E., SAVELIEVA E FAU - PUTHENVEETIL, J. A., PUTHENVEETIL JA FAU - STADLER, W. M. & STADLER, W. M. 1996. Elevated p16 at senescence and loss of p16 at immortalization in human papillomavirus 16 E6, but not E7, transformed human uroepithelial cells. *Cancer research*. 56, 2886-2890.
- RIZZO, J. L., DUNN, J., REES, A. & RÜNGER, T. M. 2011. No Formation of DNA Double-Strand Breaks and No Activation of Recombination Repair with UVA. *Journal of Investigative Dermatology*, 131, 1139-1148.
- ROBERT, C., MUEL, B., BENOIT, A., DUBERTRET, L., SARASIN, A. & STRAY, A. 1996. Cell Survival and Shuttle Vector Mutagenesis Induced by Ultraviolet A and Ultraviolet B Radiation in a Human Cell Line. *Journal of Investigative Dermatology*, 106, 721-728.
- ROCCO, J. W. & SIDRANSKY, D. 2001. p16(MTS-1/CDKN2/INK4a) in cancer progression. *Experimental cell research*. 264, 42-55.
- ROCHETTE, P. J., THERRIEN, J.-P., DROUIN, R., PERDIZ, D., BASTIEN, N., DROBETSKY, E. A. & SAGE, E. 2003. UVA-induced cyclobutane pyrimidine dimers form predominantly at thymine–thymine dipyrimidines and correlate with the mutation spectrum in rodent cells. *Nucleic Acids Research*, 31, 2786-2794.
- ROSEN, J. E., PRAHALAD, A. K. & WILLIAMS, G. M. 1996. 8-Oxodeoxyguanosine Formation in the DNA of Cultured Cells After Exposure to H<sub>2</sub>O<sub>2</sub> Alone or with UVB or UVA Irradiation. *Photochemistry and Photobiology*, 64, 117-122.
- ROSS, D. A. & WILSON, G. D. 1998. Expression of c-myc oncoprotein represents a new prognostic marker in cutaneous melanoma. *The British Journal of Surgery*. 85, 46-51.
- SANLORENZO, M., WEHNER, M. R., LINOS, E., KORNAK, J., KAINZ, W., POSCH, C., VUJIC, I., JOHNSTON, K., GHO, D., MONICO, G., MCGRATH, J. T., EE, OSELLA-ABATE, S., QUAGLINO, P., CLEAVER, J. E. & ORTIZ-URDA, S. 2015. The Risk of Melanoma in Airline Pilots and Cabin Crew A Meta-analysis. *JAMA dermatology*, 151, 51-58.
- SANLORENZO, M., VUJIC, I., POSCH, C., CLEAVER, J. E., QUAGLINO, P. & ORTIZ-URDA, S. 2015. The Risk of Melanoma in Pilots and Cabin Crew: UV Measurements in Flying Airplanes. *JAMA dermatology*, 151, 450-452.
- SASSA, A., KANEMARU, Y., KAMOSHITA, N., HONMA, M. & YASUI, M. 2016. Mutagenic consequences of cytosine alterations site-specifically embedded in the human genome. *Genes and Environment*, 38, 17.
- SCHARFFETTER-KOCHANNEK, K., WLASCHEK M FAU - BRIVIBA, K., BRIVIBA K FAU - SIES, H. & SIES, H. 1993. Singlet oxygen induces collagenase expression in human skin fibroblasts. *FEBS letters*. 331, 304-306.
- SCHULTZ, L. B., CHEHAB, N. H., MALIKZAY, A. & HALAZONETIS, T. D. 2000. P53 Binding Protein 1 (53BP1) Is an Early Participant in the Cellular Response to DNA Double-Strand Breaks. *The Journal of Cell Biology*, 151, 1381-1390.
- SCOVASSI, A. I. & PROSPERI, E. 2006. Analysis of proliferating cell nuclear antigen (PCNA) associated with DNA. *Methods in molecular biology*. 314, 457-475.
- SETLOW, R. B., WOODHEAD, A. D. & GRIST, E. 1989. Animal model for ultraviolet radiation-induced melanoma: platyfish-swordtail hybrid. *Proceedings of the National Academy of Sciences of the United States of America*, 86, 8922-8926.
- SHAHID, T., SORAKA, J., KONG, E.H., MALIVERT, L., MCILWRAITH, M.J., PAPE, T., WEST, S.C. & ZHANG, X. 2014. Structure and mechanism of action of the BRCA2 breast cancer tumor suppressor. *Nat struct & Mol Biol*. 21, 962-968.
- SHANG, Z. F., HUANG B FAU - XU, Q.-Z., XU QZ FAU - ZHANG, S.-M., ZHANG SM FAU - FAN, R., FAN R FAU - LIU, X.-D., LIU XD FAU - WANG, Y., WANG Y FAU - ZHOU, P.-K. & ZHOU, P. K. 2010. Inactivation of DNA-dependent protein kinase leads to spindle disruption and mitotic catastrophe with attenuated checkpoint protein 2 Phosphorylation in response to DNA damage. *Cancer research*. 70, 3657-3666.

- SHEN, J., GILMORE, E. C., MARSHALL, C. A., HADDADIN, M., REYNOLDS, J. J., EYALD, W., BODELL, A., BARRY, B., GLEASON, D., ALLEN, K., GANESH, V. S., CHANG, B. S., GRIX, A., HILL, R. S., TOPCU, M., CALDECOTT, K. W., BARKOVICH, A. J. & WALSH, C. A. 2010. Mutations in PNKP cause microcephaly, seizures and defects in DNA repair. *Nat Genet*, 42, 245-249.
- SHERR, C. J. 2006. Divorcing ARF and p53: an unsettled case. *Nat Rev Cancer*, 6, 663-673.
- SHIEH, S. Y., AHN, J., TAMAI, K., TAYA, Y. & PRIVES, C. 2000. The human homologs of checkpoint kinases Chk1 and Cds1 (Chk2) phosphorylate p53 at multiple DNA damage-inducible sites. *Genes Dev*, 14, 289-300.
- SHILOH, Y. & ZIV, Y. 2013. The ATM protein kinase: regulating the cellular response to genotoxic stress, and more. *Nat Rev Mol Cell Biol*, 14, 197-210.
- SKULACHEV, V. P. 1998. Cytochrome c in the apoptotic and antioxidant cascades. *FEBS letters*. 423, 275-280.
- STEEL, H. 2016. Characterising the biological response to ultraviolet radiation', PhD, Lancaster University.
- STIFF, T., O'DRISCOLL, M., RIEF, N., IWABUCHI, K., LÖBRICH, M. & JEGGO, P. A. 2004. ATM and DNA-PK Function Redundantly to Phosphorylate H2AX after Exposure to Ionizing Radiation. *Cancer Research*, 64, 2390.
- TAKASHIMA, Y., SAKURABA, M., KOIZUMI, T., SAKAMOTO, H., HAYASHI, M. & HONMA, M. 2009. Dependence of DNA double strand break repair pathways on cell cycle phase in human lymphoblastoid cells. *Environ Mol Mutagen*, 50, 815-22.
- TAKATA, M., SASAKI, M. S., SONODA, E., MORRISON, C., HASHIMOTO, M., UTSUMI, H., YAMAGUCHI-IWAI, Y., SHINOHARA, A. & TAKEDA, S. 1998. Homologous recombination and non-homologous end-joining pathways of DNA double-strand break repair have overlapping roles in the maintenance of chromosomal integrity in vertebrate cells. *The EMBO Journal*, 17, 5497-5508.
- TAKAYAMA, H., LA ROCHELLE, W. J., ANVER, M., BOCKMAN, D. E. & MERLINO, G. 1996. Scatter factor/hepatocyte growth factor as a regulator of skeletal muscle and neural crest development. *Proceedings of the National Academy of Sciences of the United States of America*, 93, 5866-5871.
- THORNBORROW, E. C., PATEL S FAU - MASTROPIETRO, A. E., MASTROPIETRO AE FAU - SCHWARTZFARB, E. M., SCHWARTZFARB EM FAU - MANFREDI, J. J. & MANFREDI, J. J. 2002. A conserved intronic response element mediates direct p53-dependent transcriptional activation of both the human and murine bax genes. *Oncogene*. 21, 990-999.
- UEMATSU, N., WETERINGS, E., YANO, K.-I., MOROTOMI-YANO, K., JAKOB, B., TAUCHER-SCHOLZ, G., MARI, P.-O., VAN GENT, D. C., CHEN, B. P. C. & CHEN, D. J. 2007. Autophosphorylation of DNA-PK(CS) regulates its dynamics at DNA double-strand breaks. *The Journal of Cell Biology*, 177, 219-229.
- UZIEL, T., LERENTHAL, Y., MOYAL, L., ANDEGEKO, Y., MITTELMAN, L. & SHILOH, Y. 2003. Requirement of the MRN complex for ATM activation by DNA damage. *The EMBO Journal*, 22, 5612-5621.
- VALDIGLESIAS, V., GIUNTA, S., FENECH, M., NERI, M. & BONASSI, S. 2013.  $\gamma$ H2AX as a marker of DNA double strand breaks and genomic instability in human population studies. *Mutation Research/Reviews in Mutation Research*, 753, 24-40.
- VEGRAN, F., REBUCCI M FAU - CHEVRIER, S., CHEVRIER S FAU - CADOUOT, M., CADOUOT M FAU - BOIDOT, R., BOIDOT R FAU - LIZARD-NACOL, S. & LIZARD-NACOL, S. 2013. Only missense mutations affecting the DNA binding domain of p53 influence outcomes in patients with breast carcinoma. *PLoS one*. 8, e55103.
- VENOT, C., MARATRAT, M., DUREUIL, C., CONSEILLER, E., BRACCO, L. & DEBUSSCHE, L. 1998. The requirement for the p53 proline-rich functional domain for mediation of apoptosis is correlated with specific PIG3 gene transactivation and with transcriptional repression. *The EMBO Journal*, 17, 4668-4679.

- VO, N. & GOODMAN, R. H. 2001. CREB-binding protein and p300 in transcriptional regulation. *Journal of biological chemistry*, 276, 13505-13508.
- WANG, H., WANG, M., WANG, H., BOCKER, W. & ILIAKIS, G. 2005. Complex H2AX phosphorylation patterns by multiple kinases including ATM and DNA-PK in human cells exposed to ionizing radiation and treated with kinase inhibitors. *J Cell Physiol*, 202, 492-502.
- WANG, H. & XU, X. 2017. Microhomology-mediated end joining: new players join the team. *Cell & Bioscience*, 7, 6.
- WANG, X. Q., REDPATH, J. L., FAN, S. T. & STANBRIDGE, E. J. 2006. ATR dependent activation of Chk2. *Journal of Cellular Physiology*, 208, 613-619.
- WARD, I. E. & CHEN, J. 2001. Histone H2AX Is Phosphorylated in an ATR-dependent Manner in Response to Replicational Stress. *Journal of Biological Chemistry*, 276, 47759-47762.
- WIKIMEDIA COMMONS. 2014. MAPK pathway. [Online] Available: [https://commons.wikimedia.org/wiki/File:MAPKpathway\\_diagram.svg](https://commons.wikimedia.org/wiki/File:MAPKpathway_diagram.svg) [Assessed 3/10/2017]
- WISCHERMANN, K., POPP, S., MOSHIR, S., SCHARFETTER-KOCHANNEK, K., WLASCHEK, M., DE GRUIJL, F., HARTSCHUH, W., GREINERT, R., VOLKMER, B., FAUST, A., RAPP, A., SCHMEZER, P. & BOUKAMP, P. 2008. UVA radiation causes DNA strand breaks, chromosomal aberrations and tumorigenic transformation in HaCaT skin keratinocytes. *Oncogene*, 27, 4269-4280.
- XU, Y., SHAO, Y., ZHOU, J., VOORHEES, J. J. 2009. Ultraviolet Irradiation-Induces Epidermal Growth Factor Receptor (EGFR) Nuclear Translocation in Human Keratinocytes. *Journal of Cellular Biochemistry*. 107, 873-880.
- XU, Y., VOORHEES JJ FAU - FISHER, G. J. & FISHER, G. J. 2006. Epidermal growth factor receptor is a critical mediator of ultraviolet B irradiation-induced signal transduction in immortalized human keratinocyte HaCaT cells. *The American journal of pathology*. 169, 823-830.
- YAMAMOTO, K., WANG, Y., JIANG, W., LIU, X., DUBOIS, R. L., LIN, C. S., LUDWIG, T., BAKKENIST, C. J. & ZHA, S. 2012. Kinase-dead ATM protein causes genomic instability and early embryonic lethality in mice. *J Cell Biol*, 198, 305-13.
- YOKOYAMA, H. & R., M. 2014. Structural Biology of DNA (6-4) Photoproducts Formed by Ultraviolet Radiation and Interactions with Their Binding Proteins. *International Journal of Molecular Sciences*, 15, 20321-20338.
- YOU, Y.-H., LI, C. & PFEIFER, G. P. 1999. Involvement of 5-methylcytosine in sunlight-induced mutagenesis<sup>11</sup>Edited by J. Karn. *Journal of Molecular Biology*, 293, 493-503.
- YOU, Y. H., SZABO, P. E. & PFEIFER, G. P. 2000. Cyclobutane pyrimidine dimers form preferentially at the major p53 mutational hotspot in UVB-induced mouse skin tumors. *Carcinogenesis*, 21, 2113-7.
- ZANNINI, L., DELIA, D. & BUSCEMI, G. 2014. CHK2 kinase in the DNA damage response and beyond. *Journal of molecular cell biology*. 6, 442-457.
- ZHANG, Y., MA, W.-Y., KAJI, A., BODE, A. M. & DONG, Z. 2002. Requirement of ATM in UVA-induced Signaling and Apoptosis. *Journal of Biological Chemistry*, 277, 3124-3131.
- ZIEGLER, A., JONASON, A., LEFFEL, D., SIMON, J., SHARMA, H., KIMMELMAN, J., REMINGTON, L., JACKS, T. & BRASH, D. 1994. Sunburn and p53 in the onset of skin cancer. *Nature* 372, 773 - 6.
- ZOLNER, A. E., ABDOU, I., YE, R., MANI, R. S., FANTA, M., YU, Y., DOUGLAS, P., TAHBAZ, N., FANG, S., DOBBS, T., WANG, C., MORRICE, N., HENDZEL, M. J., WEINFELD, M. & LEES-MILLER, S. P. 2011. Phosphorylation of polynucleotide kinase/ phosphatase by DNA-dependent protein kinase and ataxia-telangiectasia mutated regulates its association with sites of DNA damage. *Nucleic Acids Research*, 39, 9224-9237.
- ZOU, L. & ELLEDGE, S. J. 2003. Sensing DNA Damage Through ATRIP Recognition of RPA-ssDNA Complexes. *Science* 300, 1542-1548.